UNIVERSITY OF CAPE TOWN
IYUNIVESITHI YASEKAPA • UNIVERSITEIT VAN KAAPSTAD

DEPARTMENT OF MECHANICAL ENGINEERING

Design, Build and Commission a Shock Tube Apparatus for Autoignition Research

Author: Michael Downey

Supervisors: Adj. Prof. Andrew Yates
Trevor Cloete

Dissertation submitted in partial fulfilment of the requirements for the degree of Master of Science in Mechanical Engineering

December 2009

Declaration

I know the meaning of plagiarism and declare that all the work in the document, save for that which is properly acknowledged, is my own.

Signed by candidate

Michael Downey
December 2009

Acknowledgments

The author wishes to express his sincere gratitude to the following people:

- Prof. Andy Yates, for his time and advice throughout the thesis.
- Trevor Cloete, for his valuable insights, ideas and guidance.
- Mark Wattrus, for his assistance with LabVIEW programming and instrumentation.
- The workshop staff, particularly Len Watkins and Glen Newins, who skillfully manufactured the components of the prototype.
- My parents, whose unfailing belief in me was a constant source of encouragement throughout my studies.

This project was supported and sponsored by the Sasol Technology Fuels Research Group, headed by Paul Morgan.

The additional financial assistance of the National Research Foundation (NRF) towards this research is hereby acknowledged. Opinions expressed and conclusions arrived at are those of the author and are not necessarily to be attributed to the NRF.

Synopsis

Background

An integral part of the research conducted at the Sasol Advanced Fuels Laboratory involves the characterisation of fuel combustion properties such as autoignition behaviour. To facilitate autoignition research, the laboratory was equipped with a rapid compression machine capable of measuring ignition delays ranging from 1 to $50ms$ at test temperatures of up to $1000K$. However, the need to access higher test temperatures and shorter ignition delays led to the requirement for a shock tube apparatus.

Conventionally, a shock tube, which is a conceptually simple device, relies on the sudden rupture of a diaphragm separating a chamber of high pressure (driver) gas from a chamber of low pressure (driven) gas to generate the shock wave. Although the device's most direct application is as a test facility for studying the shock wave phenomenon, it has become an indespensible experimental tool in the field of high temperature chemical kinetics and autoignition research. When applied to this field, the shock wave is utilised to transform the test gas almost instantaneously to a high temperature state which can be well over $1000K$.

Objectives

The Sasol Advanced Fuels Laboratory undertook to develop a shock tube facility suitable for conducting autoignition research at test conditions beyond the capability of the rapid compression machine. It was specified that the facility should be capable of accessing test temperatures in the range 1000 to $1500K$ for a test duration of at least $1ms$. Given the repetitive nature of the experimentation, it was required that the facility be capable of performing multiple tests in rapid succession under automated computer control. Due to the scale of the undertaking, its development was split into two phases. The scope of the present project covered the initial phase of the development, which

included the design, manufacture, installation, instrumentation and commissioning of the basic shock tube. The second phase of the development would involve the addition of automation, thermal control and fuel preparation, supply and purging systems to the facility. Although the development of these systems was beyond the scope of this project, provision for their incorporation was to be considered in the design. It was specified that the basic shock tube was to be commissioned by demonstrating its ability to establish appropriate test conditions with a high degree of repeatability.

Test facility design

A novel, diaphragmless type of shock tube was developed. A specially designed, pneumatically operated rapid opening sleeve valve replaced the function of the diaphragm. The valve was a significantly modified version of the two-stage, piston actuated concept upon which several existing diaphragmless installations are based. The primary reason for adopting a diaphragmless configuration was to facilitate the automation of the apparatus. For convenience, the shock tube was designed to operate using compressed air as the driver gas. A high pressure reservoir, consisting of a bank of gas bottles connected in parallel with a SCUBA compressor, was designed and installed to provide the supply of compressed air. To enable the test conditions established in the shock tube to be determined, it was instrumented with a sequence of high frequency, charge output piezoelectric pressure transducers which were set up to record the propagation of the shock wave. Note that in accordance with The University of Cape Town's strict health and safety policy, all aspects of the facility were designed with safety considerations as a requisite priority.

Commissioning

A commissioning programme was undertaken to make the basic shock tube fully operational, investigate its performance and make refinements to improve its performance. The initial tests were conducted at relatively low driver pressures to verify correct, safe operation of the apparatus. Once this had been established, the apparatus was tested at gradually increasing driver pressures all the way up to the maximum rated driver pressure.

By the end of the commissioning and refinement process, the shock tube functioned reliably and consistently over the entire operating range. Starting with both the driver and driven gases at ambient temperature and the driven gas at atmospheric pressure,

it was capable of accessing a maximum test temperature of $973K$ with a repeatability of $\pm 25K$. The test duration at these conditions was $1.3ms$. It was shown that, by incorporating initial pre-heating and driven gas rarefaction in the second phase of the development, a maximum test temperature of over $1500K$ would potentially be attainable.

Concluding remarks

As required by the scope of this project, a potentially automatable shock tube suitable for use as a high temperature autoignition research apparatus was successfully designed, installed and commissioned. The apparatus was capable of accessing useful test conditions with a high degree of repeatability.

In this application the specially developed rapid opening sleeve valve represented a significant improvement to existing diaphragmless shock tube technology. Its design enabled extremely short opening durations, in the region of $0.5ms$, to be attained and also featured a streamlined flow path between the driver and driven sections. Control of the valve operation could easily be automated and, compared to conventional diaphragmed shock tubes, the test turn around time was reduced by the period required to replace a diaphragm.

The following recommendations are made regarding the implementation of the second phase of the development of the facility:

- Incorporate an air-fuel mixture preparation and supply system with the shock tube. The system must ensure accurate air-fuel ratio metering and complete, homogeneous vaporisation of the mixture. It must also perform the function of purging the combusted test gas after each test. Consider integrating the fuel system with a vacuum system to rarefy the driven gas, as this will enable test temperatures in excess of $1500K$ to be accessed.

- Incorporate a system for controlling the initial driver and driven gas temperature. The system must be capable of uniformly raising the gas temperature to $410K$, and should make use of the water cooling jacket which was purposely designed to ensure thermal isolation of the rapid opening sleeve valve.

- Use computer control to automate the test sequence in order to convenience the repetitive nature of fuel characterisation experimentation.

Contents

List of Figures

List of Tables

Nomenclature

Symbols

a	sound speed
A	flange outside diameter
B	flange inside diameter
c	weld leg size
C	bolt circle diameter
C_v	specific heat at constant volume
D	flange raised face diameter
f	frequency
G	o-ring mean diameter
h	specific enthalpy
L	length
L_d	driven tube length
L_D	driver tube length
m	molecular weight, mass
M	Mach number
M_r	reflected shock Mach number
M_s	incident shock Mach number
n	bolt load factor, resonance node
n_f	safety factor against fatigue failure
n_0	safety factor against joint separation
p	pressure
Q_{HV}	fuel heating value
R	gas constant
S_f	maximum allowable material stress
S_H	flange hub stress
S_R	flange radial stress
S_T	flange tangential stress
T	temperature
t	time, flange thickness
v	absolute velocity
v_c	contact surface velocity
v_h	expansion head velocity
v_r	reflected shock velocity
v_s	incident shock velocity
v_w	shock wave velocity
x	distance
γ	specific heat ratio
Δt	test duration
ΔT_c	combustion temperature rise
ρ	density
ϕ	fuel/air equivalence ratio

Subscripts

1	initial driven state
2	behind incident shock
3	behind expansion wave
4	initial driver state
5	behind reflected shock
a	air
f	fuel, final
i	initial

1 Introduction

1.1 Background

The Sasol Advanced Fuels Laboratory (SAFL), based at the University of Cape Town, was established to research the application of synthetic fuels to combustion engine technologies, with the intent to identify potential for the future growth of Sasol. An integral part of this research involves the characterisation of fuel combustion properties such as autoignition behaviour. Autoignition is the process whereby a combustible substance spontaneously ignites due to its thermal energy - there is no external source of ignition such as a spark or a flame. The time taken for a substance to autoignite at a given thermodynamic state is termed the ignition delay. Autoignition is relevant to a wide range of fuel applications, including compression ignition, spark ignition and jet turbine engines.

To facilitate autoignition research, the Laboratory was equipped with a rapid compression machine (RCM). The principle of RCM operation is as follows: a piston rapidly performs a single compression stroke and is held stationery at the top dead center (TDC) position, allowing the ignition delay of the compression heated substance to be measured. The Laboratory's RCM was capable of measuring ignition delays ranging from 1 to $50ms$ at test temperatures of up to $1000K$. However, the need to access higher test temperatures and shorter ignition delays led to the requirement for a shock tube apparatus.

Conventionally, a shock tube, which is a conceptually simple device, relies on the sudden rupture of a diaphragm separating a chamber of high pressure gas from a chamber of low pressure gas to generate the shock wave. Although the shock tube's most direct application is as a test facility for studying the shock wave phenomenon, it has become an indespensible experimental tool in the field of high temperature chemical kinetics and autoignition research. When applied to this field, the shock wave is utilised to transform the test gas - in this case a mixture of fuel and air - almost instantaneously to

a high temperature state which can be well over $1000K$. At such temperatures, ignition delays are generally below about $2ms$.

1.2 Project scope

The Laboratory undertook to develop a complete shock tube facility suitable for conducting autoignition research at temperatures beyond the capability of the rapid compression machine. Given the repetitive nature of the experimentation, it was required that the facility be capable of performing multiple tests in rapid succession under automated computer control. Due to the scale of the undertaking, its development was split into two phases. The scope of the present project covered the initial phase of the development, which included the design, manufacture, installation, instrumentation and commissioning of the basic shock tube. The second phase of the development would involve the addition of automation, thermal control and fuel mixture preparation, supply and purging systems to the facility. Although the development of these systems was beyond the scope of this project, provision for their incorporation was to be considered in the design. Performing actual fuel characterisation experiments was not a requirement of the present project; it was specified that the basic shock tube was to be commissioned by demonstrating its ability to establish appropriate test conditions with a high degree of repeatability. As there was no existing expertise or experience in shock tube technology at the University of Cape Town, a preliminary objective was to develop a sound knowledge base from which to approach the design by researching the topic and studying the underlying shock wave theory.

1.3 Plan of development

The report begins with a review of the literature on shock tube techniques, followed by a theoretical overview of the method. Then, to clarify the design problem, the specifications to be met by the proposed shock tube are identified, and the factors which affect its ability to comply with them are investigated. The installed facility is then introduced, and details of its features, operation and safety considerations are given. The results of the commissioning and testing programme are then presented and discussed against the context of required performance and theoretical behaviour. Finally, conclusions are drawn based on the test results, and recommendations for further development of the facility are made.

Note that throughout the report, stated pressures are absolute.

2 Literature review

2.1 Development of the shock tube

The shock tube is a well described, conceptually simple apparatus for creating shock waves in a controlled environment. The first published work relating to such a device was authored by the Frenchman Paul Vieille in 1899 [1]. His apparatus consisted of a cylindrical tube more than 6m long, partitioned into two sections by a thin membrane made of collodion. The shock wave was created by increasing the air pressure on one side of the membrane until it burst. This fundamental concept remains the basis for shock tube operation.

In subsequent years, the theoretical analysis of the flow processes occurring in a shock tube was developed and refined by combining the work of a number of independent researchers. According to Glass and Hall [2], at around the time of the second world war, G.I. Taylor [3], G.N. Patterson [4] and A.H. Taub [5] independently deduced the principle shock tube equation which relates the initial pressure ratio to the pressure jump across the shock wave. For a detailed description of both shock tube theory and technology, the Handbook of Shock Waves is recommended [6].

2.2 Description of a conventional shock tube

This section is intended to give an overview of the components and working of a basic shock tube setup. Although there is no unique design, in general the apparatus consists of the following elements:

- a high pressure tube, known as the driver tube
- a low pressure tube, known as the driven tube
- a membrane, which is normally a thin metallic disk, known as the diaphragm.

In the most simple case, both tubes are blanked off at one end and have the same constant, circular cross section. They are aligned axially and joined together at their open ends - with the diaphragm forming a seal between them - as shown in Figure 2.1.

The shock tube operates as follows: the driver and driven sections are filled with gas, the type of which depends on the application of the apparatus. The gas pressure in the driver section is increased until the diaphragm bursts. This generates a shock wave, which propagates rightwards into the driven gas, causing a step jump in its thermodynamic state. When the shock wave encounters the endwall of the driven tube, it reflects off it and propagates leftwards, back through the tube, causing another step jump in the state of the driven gas. Figure 2.1 shows the propagation of the various waves created in a shock tube. It also illustrates the pressure and temperature profiles of the gas within the shock tube at a time $t = t_x$ after rupture of the diaphragm.

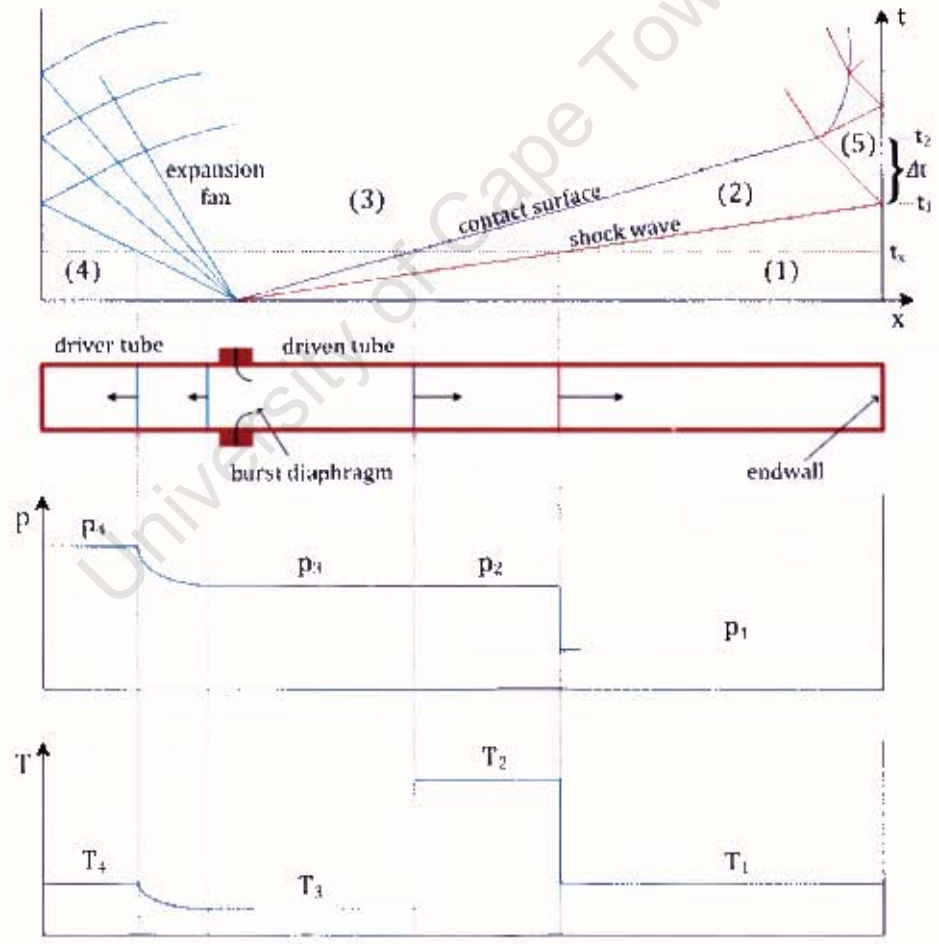

Figure 2.1: Wave propagation and thermodynamic profile in a shock tube (modified from [7])

As illustrated, eventually the reflected shock wave collides with the interface between the driver and driven gases, termed the contact surface, which had been traveling rightwards from the location of the diaphragm at a velocity less than that of the initial shock wave. This collision results in the partial reflection of the shock wave, and thus usually signifies the end of an experiment.

It can also be seen that from the instant of diaphragm rupture, as the shock wave propagates into the driven gas, the high pressure driver gas is being processed by a series of expansion waves, known as the expansion fan, which propagate from the location of the diaphragm, back into the driver gas. The expansion process is isentropic.

Note that the wave fronts shown in Figure 2.1 distinguish the different thermodynamic regions established within the shock tube: region (1) contains driven gas at the initial conditions, region (2) contains shocked driven gas, region (3) contains isentropically expanded driver gas, region (4) contains high pressure driver gas at the initial conditions and region (5) contains driven gas which has been re-shocked by the reflected shock wave. Knowing only the initial conditions in the shock tube, shock wave theory can be used to predict the conditions in each of these regions. This ability of a shock tube to establish a number of distinct, theoretically describable regions of high energy flow makes it a suitable instrument for a diverse range of applications.

Comment:
Although the use of a bursting diaphragm is a simple way to achieve the near instantaneous removal of the separation between the driver and driven sections necessary to generate a shock wave, the method has several practical disadvantages: a new diaphragm must be used for each test, making the method costly, time consuming and inconvenient to automate. It also results in poor repeatability due to the inconsistent rupture of each diaphragm, even when techniques such as cross scratching are employed (see Figure 2.2). Fragments of the burst diaphragm have been known to impact and damage the expensive pressure transducers mounted along the driven tube [8], and can potentially contaminate the test gas. Additionally, when fragmentation occurs it is necessary to at least partially dismantle the shock tube after the test in order to remove the debris. In attempts to overcome these issues, various 'diaphragmless' shock tube configurations have been developed - see Section 2.5.

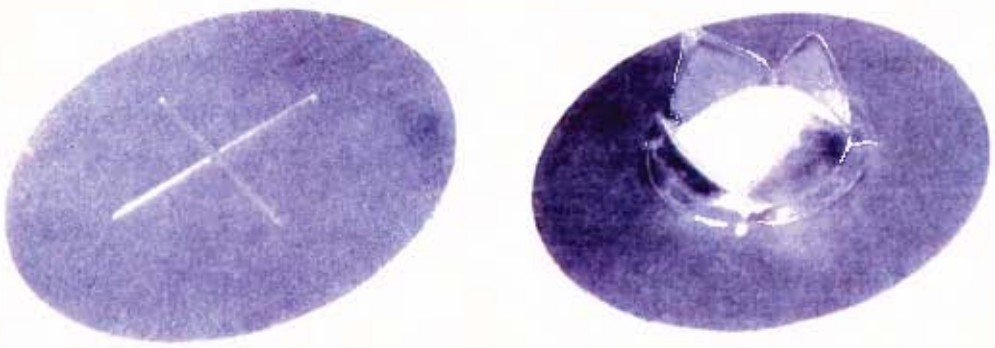

Figure 2.2: Bursting of a cross scratched diaphragm [9]

2.3 Applications of the shock tube

Since its invention about a hundred years ago, the shock tube has found use in a broad spectrum of research areas. Infact its use is so extensive that only some of the more common applications are discussed here. A thorough record of shock tube related research is detailed in the various Proceedings of the Shock Tube Symposium.

As the shock tube is principally a simple device for creating a shock wave in a laboratory environment, its most direct application is as a tool for investigating the shock wave phenomenon. From a gas dynamics perspective, topics studied include shock wave reflection, focusing, bifurcation and transitions through the shock front. From a mechanical design point of view, it has been used to study the shock loading response of structures and materials (see, for example, [10]).

One of the first applications of the shock tube in the U.S.A. was as a device for calibrating piezoelectric blast pressure gauges [5]. Another use is as an aerodynamic test facility capable of producing flows in the subsonic, transonic, supersonic and hypersonic regions, provided that only short flow durations are required [11]. Commercially, an explosives detonator similar in nature to a shock tube is replacing electrical detonators in the mining industry for safety reasons [12].

An important utility of the shock tube at present is as an experimental tool in the field of chemical kinetics research. In this application, it is the ability of a shock tube to almost instantly alter the state of a test gas, from an initial, low energy and unreactive condition, to a comparatively high energy condition at which the chemical reactions of interest are triggered, that makes it so useful. This jump in conditions is achieved across the shock wave. The near instant change in state is required to ensure that any chemical events which occur during the transition do not contribute significantly to the overall reaction

progress. The categories of chemical kinetics where shock tubes have found use are numerous and include reaction rate chemistry, combustion, dissociation and pyrolysis. A review of these experimental methods is given in [13].

2.4 The shock tube for autoignition research

In the combustion branch of chemical kinetics research, autoignition is an important topic. Autoignition is the process whereby a combustible substance spontaneously ignites due to its thermal energy - there is no external source of ignition such as a spark or a flame. It is a topic that is particularly relevant to combustion engine technology. For example, compression ignition (diesel) engines rely on autoignition to ignite the fuel, unlike spark ignition (gasoline) engines, where autoignition can cause the undesirable phenomenon of 'engine knock'. Additionally, autoignition is the principle which underpins flame propagation and is therefore highly relevant to jet turbine engines. The time taken for a substance to autoignite at a given thermodynamic state is termed the ignition delay. In general, the ignition delay decreases with increasing temperature. For a more detailed description of autoignition, see [14].

The aim of this project was to design and build a shock tube for investigating the high temperature autoignition of combustion engine fuels. More specifically the apparatus was intended for characterising fuels by measuring their ignition delay at high temperatures, above $1000K$. For a review of the operation of a shock tube in this mode, see [15]. The basic principle of operation is as follows: as was shown in Section 2.2, the incident shock wave causes a sudden jump in the temperature of the driven gas. The reflected shock wave then causes a further, even greater temperature jump, effectively leaving in its wake a uniform region of stationary, high temperature driven gas referred to as region (5). If a gaseous mixture of fuel and air is used as the driven gas, the initial conditions in the shock tube can be chosen such that the high temperature regime within region (5) triggers the autoignition of the fuel air mixture, whilst the relatively moderate temperature behind the incident shock is below the autoignition threshold.

The ignition delay can be measured by using a fast response pressure transducer to record the pressure history of region (5), as shown in Figure 2.3. Note that this pressure transducer is usually mounted in the endwall of the driven tube, where the shock reflects, as the parcel of gas at that location is the first to be elevated to region (5) conditions and hence will autoignite first. The test conditions can be determined using one dimensional shock wave theory, as shown in Section 3.6.

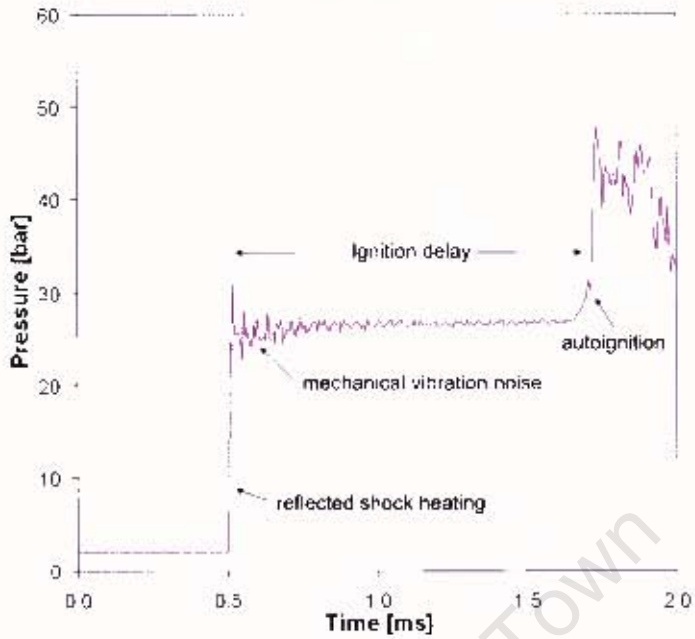

Figure 2.3: Measuring ignition delay from the pressure history at the endwall

The major advantage of using a shock tube for autoignition research is that it offers a simple way of almost instantly preparing a test gas to a very high temperature, quiescent state. The rapidity of the temperature rise, which can be well over 1000K in magnitude, is required so that its duration does not contribute significantly to the ignition delay period. The main drawback is that the test conditions can only be maintained for a very short duration - from the instant the shock reflects to the instant it collides with the contact surface, shown as Δt in Figure 2.1. (If only the gas immediately next to the endwall is of interest the test duration is slightly longer - it lasts until reflections off the contact surface collide with the endwall.) Although the test duration increases with driven tube length, so do the frictional flow losses. Therefore, extremely long tubes are inefficient and cause a severe reduction in shock strength. Typically, existing autoignition facilities have a driven tube length in the range of 5 to $10m$, and are capable of measuring ignition delays no longer than a few milliseconds (see, for example, [16]).

Another practical consideration is that, due to the sudden impact of the shock wave against the endwall, mechanical vibration noise is superimposed on the recorded pressure trace. Techniques such as coupling the driven tube to a large, vibration damping inertial mass have been employed to minimise the severity of the noise (see, for example, [17]).

2.5 Diaphragmless shock tubes

As an alternative to the conventional bursting diaphragm method, various 'diaphragmless' shock tube configurations have been developed whereby the diaphragm is replaced with a quick action valve. Such a configuration is advantageous when highly repeatable test conditions and/or automation are required, as in the present case. As discussed in [18], the longer the diaphragm opening duration the longer the distance required for the shock to attain its peak velocity, hence the primary difficulty with the diaphragmless approach is achieving a sufficiently rapid valve opening time to generate a well formed shock wave in a reasonable tube length.

For a review of some alternative diaphragmless shock tube designs, see [19], however, most are similar in nature to the two-stage, piston actuated concept developed by Oguchi *et al* [20]. A derivative of this concept is shown schematically in Figure 2.4. Note that the driver and driven tubes are arranged in an annular configuration instead of the conventional series arrangement. The valve function is achieved by the motion of two pneumatically operated sliding pistons: the main piston, which replaces the diaphragm at the interface between the tubes, and the auxiliary piston, which operates the outlet ports of the actuating chamber.

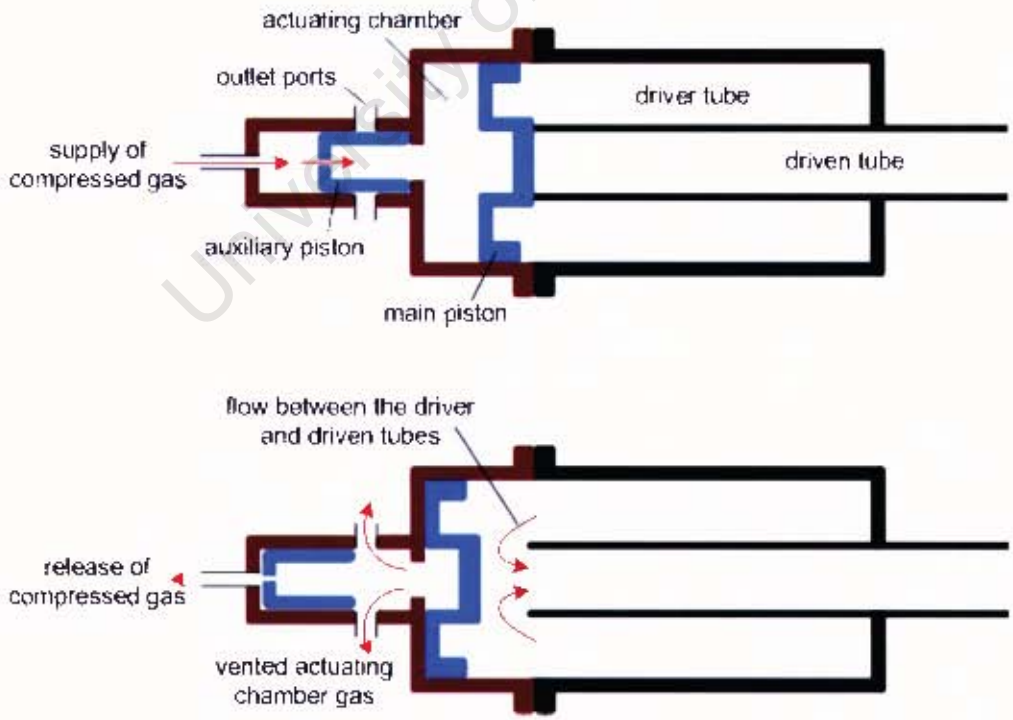

Figure 2.4: The two-stage, piston actuated diaphragmless shock tube concept

With reference to Figure 2.4, the device functions as follows: a backpressure is applied to the auxiliary piston, causing it to slide forward and block the outlet of the actuating chamber. Compressed gas flows through a small orifice in the auxiliary piston, pressurising the actuating chamber and causing the main piston to move forward and block the flow path between the driver and driven tubes. Once the tubes have been charged to the desired conditions, the shock tube is triggered by releasing the backpressure behind the auxiliary piston. The compressed gas in the actuating chamber causes the auxiliary piston to slide backwards and quickly uncover the large outlet ports, out of which the gas rapidly escapes. When the pressure in the actuating chamber drops below a threshold level, the high pressure driver gas propels the main piston backward, opening the flow path between the driver and driven tubes. If the main piston opens sufficiently quickly, a shock wave is generated. Note that the sole purpose of the auxiliary piston is to ensure the rapid evacuation of the actuating chamber so as to maximise the opening acceleration of the main piston.

Comment:
The positioning of the valve at the end of the shock tube enhances its accessibility and servicibility and facilitates its thermal isolation from the potentially heated shock tube. However, the concept does not attempt to streamline the flow path, and thereby minimise the flow losses, where the driver gas is redirected around the 180^o bend. Furthermore, the fact that the main piston begins the opening process from a stationary start is not optimal, as a reduction in opening time would be possible if the piston was already moving at speed as the opening process was begun.

3 Theoretical approach to shock tube flow

3.1 Introduction

The underlying theory upon which shock tube operation is based is described here. To lay a foundation upon which to build the theory, a fundamental understanding of the shock wave is first discussed. Then, a theoretical description of the gas flow in a shock tube is developed, and the principles for determining the test conditions in an autoignition shock tube are covered more specifically. In general, the approach to the theory follows that of the Handbook of Shock Waves [6].

3.2 A fundamental understanding of a shock wave

In a gaseous substance, a shock wave is a jump discontinuity in the state of the gas. In other words, it is a very thin region, of the order of a few mean free paths of the molecules involved, across which there is a sudden change in the state of an otherwise continuous gas. A change in state implies a change in energy, and indeed a shock wave is essentially the means by which a sudden energy release is distributed. The jump discontinuity associated with a shock wave is a result of the fact that a shock wave always travels faster than the speed of sound in the gas into which it is moving. This means that the unshocked gas has no way of anticipating the approach of the shock wave, and is therefore unable to react gradually to any changes caused by the shock to the gas in its wake. Thus the change in the gas' state, from unshocked to shocked, occurs in a sudden jump across the shock wave.

It is also insightful to note that the flow behind the shock wave is subsonic relative to the shock wave. If this was not the case, energy would be unable to propagate up to the shock wave to sustain it.

3.3 Flow across a planar, one-dimensional shock wave

To facilitate the analysis of the flow within a shock tube, a mathematical description of the flow across a shock wave is developed here. Consider the simplest case of a planar shock wave, normal to a uni-directional, inviscid gas flow, as shown in Figure 3.1. Ideally, this is the type of shock wave generated within a shock tube. According to the chosen coordinate system, the shock wave is traveling at an absolute velocity v_w in the positive x direction. Analysing the flow relative to an observer moving along with the shock wave, and noting that the gas flow is also in the x direction, the case can be treated as simple one-dimensional steady state flow, where properties of the gas vary only in the x direction. The passage of the shock wave causes a jump in the absolute velocity, density, pressure and temperature of the gas from v_1, ρ_1, p_1 and T_1 to v_2, ρ_2, p_2 and T_2 respectively.

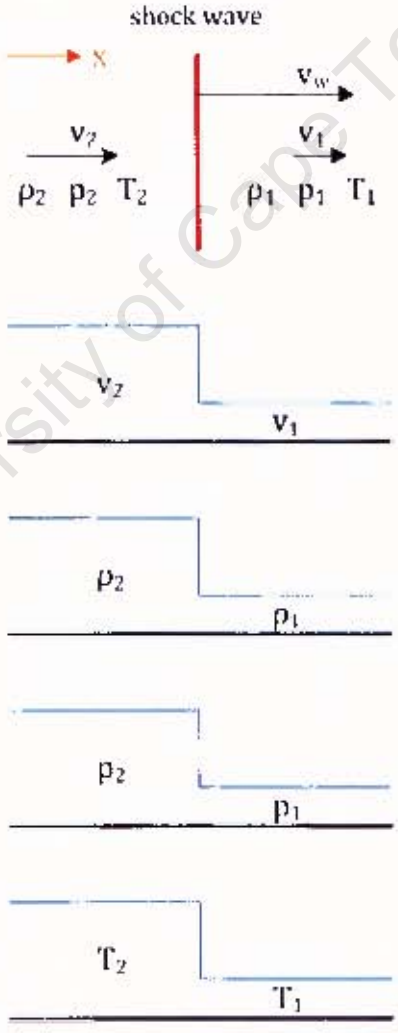

Figure 3.1: Planar shock wave normal to the direction of flow (modified from [21])

The relations governing the flow across the moving shock wave are derived by applying the steady state, one-dimensional versions of the fundamental laws of conservation of mass, momentum and energy:

Conservation of mass

$$\rho_1(v_w - v_1) = \rho_2(v_w - v_2) \tag{3.1}$$

Conservation of momentum

$$\rho_1(v_w - v_1)^2 + p_1 = \rho_2(v_w - v_2)^2 + p_2 \tag{3.2}$$

Conservation of energy

$$h_1 + \frac{(v_w - v_1)^2}{2} = h_2 + \frac{(v_w - v_2)^2}{2} \tag{3.3}$$

where h is the specific enthalpy of the flowing gas, and heat transfer has been assumed to be negligible. To obtain a solvable system of equations, an equation of state is needed. Assuming the gas is ideal and calorifically perfect, then

$$p = \rho RT \quad and \quad h = \frac{\gamma RT}{\gamma - 1} \tag{3.4}$$

where R is the gas constant and γ is the constant ratio of specific heats and both are properties of the gas. At this stage it is convenient to define two terms, namely the speed of sound in a gas and the Mach number, which will be useful in simplifying the subsequent analysis. The speed of sound in a gas, denoted by a, represents the speed at which small pressure disturbances travel in that gas and is given by

$$a = \sqrt{\gamma RT} \tag{3.5}$$

The Mach number of a shock wave, denoted by M, is defined as the ratio of the speed of the shock wave (relative to the unshocked gas into which it is moving) to the speed of sound in the unshocked gas. The Mach number gives an indication of the severity of the shock wave; the greater the Mach number the 'stronger' the shock wave. M is calculated as follows:

$$M = \frac{v_w - v_1}{a_1} \tag{3.6}$$

Equations 3.1 to 3.6 can be combined to yield the relations which describe the steady state, one-dimensional flow across a moving shock in terms of its Mach number [21]:

$$\frac{\rho_2}{\rho_1} = \frac{(\gamma_1 + 1)M^2}{2 + (\gamma_1 - 1)M^2} \tag{3.7}$$

$$v_2 - v_1 = \frac{2a_1}{\gamma_1 + 1}\left(M - \frac{1}{M}\right) \tag{3.8}$$

$$\frac{p_2}{p_1} = 1 + \frac{2\gamma_1}{\gamma_1 + 1}(M^2 - 1) \tag{3.9}$$

$$\frac{T_2}{T_1} = 1 + \frac{2(\gamma_1 - 1)}{(\gamma_1 + 1)^2}\frac{(\gamma_1 M^2 + 1)}{M^2}(M^2 - 1) \tag{3.10}$$

3.4 Ideal analysis of shock tube flow

Consider Section 2.2, in which the operation of a conventional shock tube was described. Figure 2.1 illustrated the various regions established within the shock tube at a time $t = t_x$ after the rupture of the diaphragm. According to the diagram, regions (1) and (4) were at the initial conditions of the driven and driver tubes respectively. If these conditions are known, the flow subsequent to diaphragm rupture can be predicted. In other words, the boundaries and states of regions (2), (3), (5) can be determined with respect to time. The theory of ideal shock tube flow is presented below. Note that throughout the analysis, the properties of region (1) are denoted by the subscript $_1$ and so on. In developing the theory, the following assumptions were made:

1. The flow is inviscid and one-dimensional, and there is no heat transfer.
2. The diaphragm rupture is instantaneous.
3. All gases are ideal and have constant specific heats.

3.4.1 Change in conditions across the incident shock wave

The incident shock wave defines the boundary between regions (1) and (2). It can be shown that the Mach number of the incident shock wave, denoted by M_s, is a function of the initial gas properties and pressure ratio across the diaphragm [22]:

$$\frac{p_4}{p_1} = \left[1 + \frac{2\gamma_1}{\gamma_1 + 1}(M_s^2 - 1)\right]\left[\frac{1}{1 - \frac{\gamma_4 - 1}{\gamma_1 + 1}\frac{a_1}{a_4}\left(M_s - \frac{1}{M_s}\right)}\right]^{\frac{2\gamma_4}{\gamma_4 - 1}} \tag{3.11}$$

The state of region (2) can easily be determined by substituting M_s for M in equations 3.7 to 3.10, which describe the flow across a shock wave. Note that initially the driven and driver gases are stationary, therefore $v_1 = v_4 = 0$.

$$\frac{\rho_2}{\rho_1} = \frac{(\gamma_1 + 1)M_s^2}{2 + (\gamma_1 - 1)M_s^2} \tag{3.12}$$

$$v_2 = \frac{2a_1}{\gamma_1 + 1}\left(M_s - \frac{1}{M_s}\right) \tag{3.13}$$

$$\frac{p_2}{p_1} = 1 + \frac{2\gamma_1}{\gamma_1 + 1}(M_s^2 - 1) \tag{3.14}$$

$$\frac{T_2}{T_1} = 1 + \frac{2(\gamma_1 - 1)}{(\gamma_1 + 1)^2}\frac{(\gamma_1 M_s^2 + 1)}{M_s^2}(M_s^2 - 1) \tag{3.15}$$

3.4.2 Change in conditions across the contact surface

The contact surface defines the boundary between regions (2) and (3), and represents the interface between the driven and driver tube gases. For continuity, the velocity of the contact surface, v_c, is equal to the velocity of the gas in region (2). The density and temperature may vary across the contact surface, however the pressures and velocities immediately adjacent to it must be equal:

$$v_c = v_2 \tag{3.16}$$

$$p_3 = p_2 \tag{3.17}$$

$$v_3 = v_2 \tag{3.18}$$

3.4.3 Change in conditions across the expansion fan

The expansion fan defines the boundary between regions (3) and (4). It consists of a series of expansion waves which isentropically expand the driver gas from the initial pressure of the driver gas to the pressure of the shocked gas. The leading expansion wave in the fan is called the expansion head, and it travels back into the driver tube at a velocity v_h, equal to the speed of sound in region (4):

$$v_h = -a_4 \tag{3.19}$$

As the expansion process is isentropic, the temperature of region (3) can be determined as follows:

$$\frac{T_3}{T_4} = \left(\frac{p_3}{p_4}\right)^{\frac{\gamma_4 - 1}{\gamma_4}} \tag{3.20}$$

Knowing the temperature and pressure of region (3), the density can be calculated from the ideal gas law (see equation 3.4).

3.4.4 Change in conditions across the reflected shock wave

As described in Section 2.2, when the incident shock wave reaches the endwall of the driven tube, it is reflected and propagates back up the tube, effectively re-shocking the gas through which it passes. In Figure 2.1, region (5) consists of the re-shocked driven tube gas. The reflected shock wave defines the boundary between regions (5) and (2). It can be shown that its Mach number, denoted by M_r, is a function of the Mach number of the incident shock wave [23]:

$$M_r = \left[\frac{\gamma_1 M_s^2 - \frac{\gamma_1 - 1}{2}}{1 + \frac{\gamma_1 - 1}{2} M_s^2}\right]^{\frac{1}{2}} \tag{3.21}$$

The conditions in region (5) can be determined by applying equations 3.7 to 3.10 across the reflected shock wave:

$$\frac{\rho_5}{\rho_2} = \frac{(\gamma_1 + 1) M_r^2}{2 + (\gamma_1 - 1) M_r^2} \tag{3.22}$$

$$v_5 = 0 \tag{3.23}$$

$$\frac{p_5}{p_2} = 1 + \frac{2\gamma_1}{\gamma_1 + 1}(M_r^2 - 1) \tag{3.24}$$

$$\frac{T_5}{T_2} = 1 + \frac{2(\gamma_1 - 1)}{(\gamma_1 + 1)^2}\frac{(\gamma_1 M_r^2 + 1)}{M_r^2}(M_r^2 - 1) \tag{3.25}$$

3.4.5 Subsequent processes in the shock tube

When the reflected shock wave collides with the contact surface it is partially reflected. The interaction is complex and the thermodynamic profile within the shock tube is no longer straight forward to analyse, hence this is normally regarded as the instant beyond which the shock tube ceases to maintain useful flow. After this event, the conditions within the shock tube gradually equalise to stagnation values.

However, it should be noted that the initial conditions within the shock tube may be 'tailored' such that the reflected shock wave is completely transmitted through the contact surface such that it leaves the contact surface stationary at the point of collision. This enables the conditions in region (5) to be maintained until the arrival of the reflected expansion fan. A method for determining the tailored condition is described in [24]. Assuming that the same gas is used in the driver and driven sections, tailored operation is obtained when the initial conditions are tuned such that the speed of sound either side of the contact surface is equal:

$$a_3 = a_2 \tag{3.26}$$

Note that within a given range of initial conditions tailoring is not necessarily attainable.

3.5 Non-idealities in real shock tube flow

In reality, all of the assumptions listed in the ideal analysis of shock tube flow above are violated to some degree. As real gases are not inviscid, a boundary layer develops behind the shock wave. This viscous boundary layer results in attenuation of the shock wave, which is seen as a reduction in the shock Mach number with axial distance along the driven tube [25]. The attenuation due to the boundary layer becomes more significant with an increase in shock Mach number, an increase in wall surface roughness and a decrease in driven tube diameter [26].

It has also been shown that an increase in diaphragm rupture time causes an increase in shock formation length. This means that the shock attains its peak velocity at a location further downstream from the diaphragm [27].

Furthermore, real gases have temperature dependent specific heats and can undergo chemical reactions such as dissociation and ionization in the region of elevated temperature behind a shock [28]. All of the above non-idealities result in a reduced shock Mach number compared to the ideal theory prediction. Alpher and White [29]

have shown that the loss in shock strength can be partially offset by using a variable cross section shock tube, whereby the driver tube has a greater cross sectional flow area than the driven tube. As the area ratio approaches infinity, the Mach number may be increased by a factor of up to 1.1 as compared to the constant area case.

For a given initial diaphragm pressure ratio, a measure of the overall efficiency of a particular shock tube is obtained by comparing the actual Mach number with the ideal value as predicted by equation 3.11. Such a comparison is given in Figure 3.2. The shock tube to which it applies was a variation of the piston actuated, diaphragmless type. The driven tube had a diameter of $56mm$, and the driver to driven area ratio was 1.65. Both the driver and driven gases were air at room temperature. For more details of the apparatus, see [19]. Figure 3.2 clearly illustrates that the deviation from ideal theory increases with an increase in shock Mach number [30].

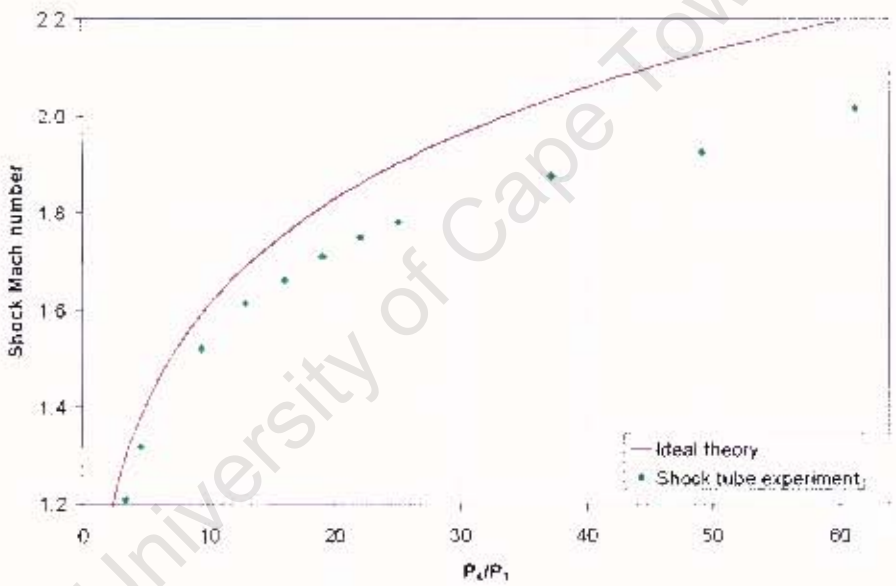

Figure 3.2: Efficiency of a diaphragmless, piston actuated shock tube (adapted from [19])

3.6 Determining the test conditions in an autoignition shock tube

The test conditions, namely the temperature and pressure of region (5), at which a particular ignition delay experiment is to be conducted, are a function of the Mach number of the incident shock wave. If the initial conditions within the shock tube

are known, equation 3.11 can be used to estimate the Mach number, however, due to the non-idealities discussed in Section 3.5, the actual Mach number may be somewhat different.

To ensure accurate determination of the test conditions, the Mach number must be measured. In practice, this can be done by recording the passage of the shock using a series of two or more pressure transducers near the end of the driven tube. Knowing the distance between the transducers and the time interval between the arrival of the shock at each sensors, the velocity and hence Mach number of the shock wave can be calculated.

A comprehensive review describing the effects of non-idealities on the test conditions is given in [26]. However, it can be shown that by manipulating the equations presented in Section 3.4, one can obtain, with reasonable accuracy, the conditions in region (5) as a function of the measured Mach number and the initial conditions of the driven gas [31]:

$$\frac{p_5}{p_1} = \left[\frac{2\gamma_1 M_s^2 - (\gamma_1 - 1)}{\gamma_1 + 1}\right]\left[\frac{-2(\gamma_1 - 1) + M_s^2(3\gamma_1 - 1)}{2 + M_s^2(\gamma_1 - 1)}\right] \tag{3.27}$$

$$\frac{T_5}{T_1} = \frac{[2(\gamma_1 - 1)M_s^2 + 3 - \gamma_1]\,[(3\gamma_1 - 1)M_s^2 - 2(\gamma_1 - 1)]}{(\gamma_1 + 1)^2 M_s^2} \tag{3.28}$$

$$\frac{\rho_5}{\rho_1} = \frac{p_5}{p_1}\frac{T_1}{T_5} \tag{3.29}$$

4 Preliminary investigation of the design problem

4.1 Introduction

Despite the conceptual simplicity of a shock tube, its design presented many technical challenges and required several conflicting requirements to be balanced. To clarify the design problem, the desired specifications to be met by the shock tube were identified, and the factors which affect the device's ability to comply with them were examined.

4.2 Design specifications

The manufacture of the shock tube was undertaken to meet the need for an experimental apparatus capable of characterising the autoignition behavior of fuels at conditions beyond the range of the RCM, which could access a maximum test temperature of $1000K$ and measure ignition delays down to $1ms$. As such, the main criteria to be met by the design were as follows:

1. The apparatus should be capable of accessing test temperatures, i.e T_5, in the range 1000 to $1500K$.

2. The apparatus should be capable of measuring ignition delays of below and up to $1ms$ at such temperatures.

3. The apparatus should be compatible with the use of a fuel-air mixture as the test gas. It was anticipated that the apparatus would primarily be used to test gasoline and jet fuel.

4. The design should facilitate the planned future automation of the apparatus to do multiple tests under computer control.

5. The design should make provision for the incorporation of thermal control and fuel mixture supply and purging systems.

6. The apparatus is to be made cost effectively at UCT's engineering workshop. It should therefore be manufactured using readily available materials and standard fitting and turning equipment.

7. The apparatus should produce valid results with good repeatability.

4.3 Problem clarification

The primary step in the design of the shock tube was to determine the initial conditions and functional dimensions necessary to achieve the desired performance specifications listed above. In this way, the specifications were translated into physical constraints which defined the essential features of, and provided a useful starting point for, the detailed design of the apparatus. The secondary step was to consider the challenges associated with the need for an automatable test sequence and good test repeatability. A summary of the findings of the problem clarification process is given in Table 4.1 at the end of this chapter.

4.3.1 Factors affecting test temperature

4.3.1.1 Initial pressure ratio

An increase in the initial driver/driven pressure ratio causes an increase in the Mach number of the shock wave and hence a greater temperature jump in the driven gas - see equations 3.11 and 3.28. For convenience, the driven (or test) gas, which consists of the fuel-air mixture, was constrained to be at approximately atmospheric pressure:

$$p_1 \approx 1bar \tag{4.1}$$

As will be shown, a suitable driver pressure, p_4, can only be determined once the driver gas type has been selected.

4.3.1.2 Initial gas temperatures

Equation 3.28 indicates that an increase in the initial temperature of the driven gas results in an increase in the final test temperature. Additionally, it was desirable to raise the initial temperature of the test gas to promote vaporisation of the fuel. Jet fuel has a higher boiling range than gasoline and must be heated to about $400K$ to ensure it fully evaporates. Practically, design complexity increases with temperature, hence it was decided to limit the temperature of the driven gas to $410K$ - just sufficiently high to vaporise jet fuel:

$$T_1 \leq 410K \tag{4.2}$$

As will be shown, an increase in the initial driver/driven temperature ratio causes an increase in the Mach number of the shock wave, however, the temperature of the driver gas was also constrained to be below the chosen practical limit of $410K$:

$$T_4 \leq 410K \tag{4.3}$$

4.3.1.3 Driver gas type

According to equation 3.11, an increase in the driver/driven sound speed ratio, which is given by

$$\frac{a_4}{a_1} = \sqrt{\frac{\gamma_4}{\gamma_1}\frac{m_1}{m_4}\frac{T_4}{T_1}} \tag{4.4}$$

where m is the molecular weight, results in an increase in the Mach number of the shock wave and hence a greater jump in the temperature of the test gas [22]. Thus to produce strong shock waves it is desirable to use a high temperature, low molecular weight driver gas, one example of which is Helium. However, this requires pressurised cylinders of Helium to be bought. A more convenient alternative is to use atmospheric air, supplied directly from a compressor, as the driver gas. Although air has a higher molecular weight than Helium, this can be compensated for by compressing it to a higher pressure. The graph over the page compares Helium and air (assuming constant γ values of 1.67 and 1.40 respectively) in terms of the initial driver pressure required to obtain a suitable range of test temperatures. All the other initial conditions are at the limiting values determined above of $p_1 = 1bar$, $T_1 = 410K$ and $T_4 = 410K$.

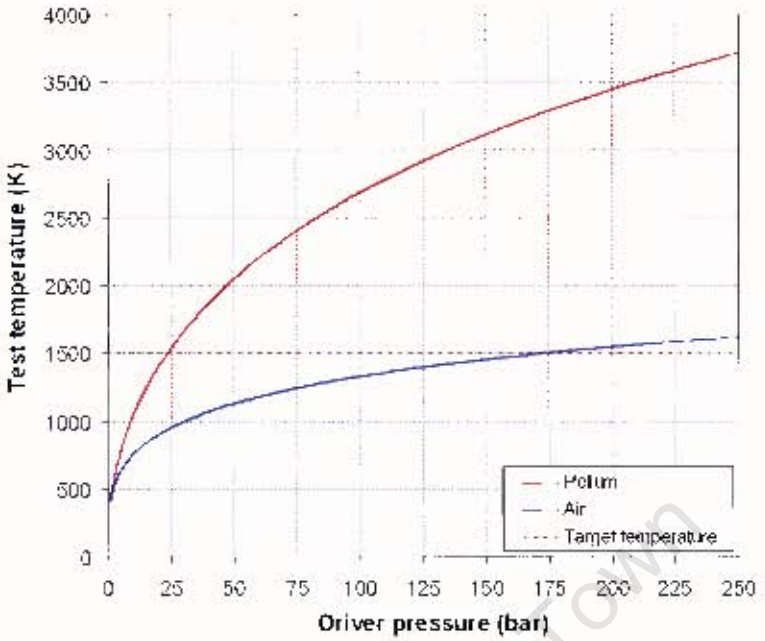

Figure 4.1: Comparison of Helium and air as driver gases

It was decided to use air as the driver gas as the convenience of having an unlimited, free source of driver gas was deemed highly desirable, despite the fact that the shock tube would have to be designed to sustain higher pressures. From Figure 4.1, it can be seen that a driver pressure of nearly $200bar$ is required to obtain test temperatures in the region of $1500K$:

$$p_4 \approx 200bar \tag{4.5}$$

4.3.2 Factors affecting test duration

4.3.2.1 Driven tube length

With reference to Figure 2.1 which shows the propagation of the various waves within a shock tube, the length of the driven tube, L_d, required to give a minimum test duration of Δt, can be estimated as follows:

$$L_d = v_s t_1 \quad and \quad v_c(t_1 - \Delta t) + v_r \Delta t = v_s t_1$$

$$\Rightarrow L_d = \frac{\Delta t v_s (v_c + v_r)}{(v_s \quad v_c)} \tag{4.6}$$

where v_s, v_r and v_c denote the speed of the incident shock, the reflected shock and the contact surface respectively (calculated as per Chapter 3). For a shock tube operating on air at the previously determined initial conditions of $p_1 = 1bar$, $p_4 = 200bar$ and $T_1 = T_4 = 410K$, the wave speeds are as follows:

$$v_s = 1059m/s$$

$$v_r = 457m/s$$

$$v_c = 753m/s$$

Substituting these values into equation 4.6, the driven tube must be more than $4.19m$ long in order to ensure a test duration of at least $1ms$:

$$L_d > 4.19m \tag{4.7}$$

4.3.2.2 Driver tube length

The driver tube must be sufficiently long so that the reflected expansion fan does not overtake the contact surface until the test is complete. This is easily ensured by choosing the length of the driver tube, denoted by L_D, such that the expansion head only reflects after the test is complete. The expansion head travels back into the driver tube at the speed of sound in the driver gas, a_4, hence the minimum driver tube length is given by

$$L_D = a_4(t_1 + \Delta t) \tag{4.8}$$

Noting that $t_1 = \frac{L_d}{v_s}$ and substituting in Δt from equation 4.6, the expression can be re-written as

$$L_D = \frac{L_d a_4}{v_s}\left(\frac{v_s + v_r}{v_c + v_r}\right) \tag{4.9}$$

For the initial conditions above, $a_4 = 406m/s$, hence the driver must be greater than 0.48 times the length of the driven tube:

$$L_D > 0.48L_d \tag{4.10}$$

4.3.3 Factors affecting fuel compatibility

4.3.3.1 Combustion pressure rise

During an experiment in an autoignition shock tube, the reflected shock wave triggers the ignition of the combustible test gas contained within the driven tube. The driven tube must be designed to withstand the resulting combustion pressure rise over and above the pressure rise caused by the shock wave, as well as the increased stagnation pressure. If it is assumed the test gas is a stoichiometric mixture of a typical combustion engine fuel, for example gasoline, and air, representative values of the heating value, Q_{HV}, air to fuel mass ratio, m_a/m_f, and specific heat at constant volume of the mixture, C_v, are as follows [32]:

$$Q_{HV} = 44MJ/kg$$

$$m_a/m_f = 14.6kg/kg$$

$$C_v = 1.1kJ/kg.K$$

For the most severe case in terms of combustion pressure rise, of adiabatic constant volume combustion without dissociation, the temperature rise due to combustion, ΔT_c, can be estimated as follows:

$$m_f Q_{HV} = (m_a + m_f)\, C_v \Delta T_c$$

$$\Rightarrow \Delta T_c = \frac{Q_{HV}}{\left(1 + \frac{m_a}{m_f}\right) C_v} \tag{4.11}$$

Substituting in the above values, $\Delta T_c = 2564K$. For a constant volume heat addition process, the temperature and pressure before and after heat addition, denoted by subscripts $_i$ and $_f$ respectively, are related as follows:

$$\frac{p_i}{R_i T_i} = \frac{p_f}{R_f T_f}$$

$$\Rightarrow p_f = \frac{p_i R_f}{R_i}\left[1 + \frac{T_f - T_i}{T_i}\right] \tag{4.12}$$

For an experiment at the previously determined initial conditions, shock tube theory indicates that the temperature and pressure behind the reflected shock are $T_5 = 1547K$ and $p_5 = 34.6bar$ respectively. Substituting in these values of T_5, p_5 and ΔT_c for T_i, p_i and $(T_f - T_i)$ respectively, and neglecting the change in gas composition due to combustion, the post-combustion pressure in the driven tube (given by p_f in equation 4.12) is about $92bar$. As this is less than the initial driver pressure of $200bar$, the final

pressure in the shock tube will equalise to a value between 92 and $200bar$. Thus it was decided that the design pressure of both the driver and driven tubes would be $200bar$, with an appropriate safety factor.

4.3.3.2 Material selection

All components of the shock tube that come into contact with the fuel-air test gas had to be selected so that they would not chemically react with, or be degraded by, the fuel. It was decided to construct the driven tube from carbon steel, as although stainless steel is less reactive and would be preferred, the cost of using it was prohibitive. Where seals were required, it was decided that Viton® o-rings would be used, as they are compatible with hydrocarbon fuels, can withstand ambient temperatures of over $450K$, and provide a cheap, reliable and simple means of sealing.

4.3.4 Factors affecting shock tube performance

4.3.4.1 Shock tube diameter

It was desired to keep the overall size of the shock tube as compact as possible in order to minimise manufacturing costs and complexity, thus the nominal internal diameter of the driven tube was set at $50mm$, which is the minimum diameter below which boundary layer build up behind the shock wave causes significant deviation from ideal theory [26]. As discussed in Section 3.5, improved performance is obtained if the driver tube is designed to have a larger cross sectional area than the driven tube.

4.3.4.2 Operational concept

As the specifications stipulated that the shock tube was to be automatable and produce highly repeatable results, it was decided that a diaphragmless type of shock tube was most suitable. It was felt that significant improvements could be made to the existing diaphragmless concepts described in Section 2.5. As discussed there, the main challenge in designing a diaphragmless shock tube is to minimise the opening time of the valve which replaces the diaphragm, such that a shock is formed within a reasonable tube length. A rule of thumb suggests that for every millisecond of opening time, the shock requires a length of about 100 tube diameters to form adequately [33]. For a driven tube of diameter $50mm$ and length around $5m$, it was clear that the aim should be to design a rapid opening valve that would open fully in well under $1ms$, thereby ensuring that

the incident shock would be adequately formed well before it reflected off the endwall of the driven tube.

4.3.5 Summary of problem clarification

By investigating the principles of shock tube operation, the design specifications, which define the desired performance of the shock tube, were translated into physical constraints which define the essential features of the required product. The most important of these constraints are the initial conditions at which the shock tube must operate, the functional dimensions of the shock tube and the operational concept . Table 4.1 lists these constraints.

Table 4.1: Shock tube functional requirements

Initial conditions	
Driven tube pressure, p_1	nominally atmospheric
Driver tube pressure, p_4	up to $200bar$
Driven gas temperature, T_1	up to $410K$
Driver gas temperature, T_4	up to $410K$
Driven gas type	fuel-air mixture
Driver gas type	compressed air
Functional dimensions	
Driven tube length, L_d	greater than $4.19m$
Driver tube length, L_D	greater than $0.48L_d$
Driven tube internal diameter	nominally $50mm$
Driver tube cross section	to give larger c/s area than driven tube
Operation	
Principle of operation	diaphragmless valve
Diaphragmless valve opening time	under $1ms$

5 The solution: a diaphragmless, high pressure air driven shock tube facility

5.1 Introduction

As required for this project, a basic shock tube apparatus was designed, built and installed. It will be shown that the working concept for the shock tube possessed some novelty. A number of subsystems were developed and integrated with the shock tube to produce a basic, functioning facility suitable for the intended application of autoignition research. These subsystems included a high pressure air supply, a pneumatic control circuit, a mounting system and a diagnostic and data capture system. Throughout the design, planned future developments of the facility were borne in mind, and provision was made for the incorporation of automation, thermal control and fueling systems. This chapter summarises the components, features and operation of the installed shock tube facility. Details of the subsystems are given in Appendix A. A complete set of manufacturing drawings for the apparatus is contained in Appendix G.

5.2 General description of the facility

A novel, diaphragmless type of shock tube was developed. A rapid opening valve replaced the function of the diaphragm. The primary reason for adopting a diaphragmless configuration was to facilitate the automation of the apparatus. The driver tube was a $2.9m$ long carbon steel tube, of the type commonly used to make high pressure hydraulic cylinders. It had an internal diameter of $110mm$ and an external diameter of $140mm$. The driven tube was $6.1m$ long, was also made from hydraulic cylinder tube and had an internal diameter of $50mm$ and an external diameter of $65mm$. The shock tube was designed to operate at initial driver conditions of up to $200bar$ and $410K$, and initial

driven conditions in the region of $1bar$ and up to $410K$. A pneumatic circuit controlled its operation. Figure 5.1 is a photograph of the shock tube apparatus. It was mounted on a portable frame which allowed for height adjustment. When fully assembled and mounted, the shock tube - excluding all connected subsystems - occupied a space $7m$ long by $0.9m$ wide by $1.4m$ high.

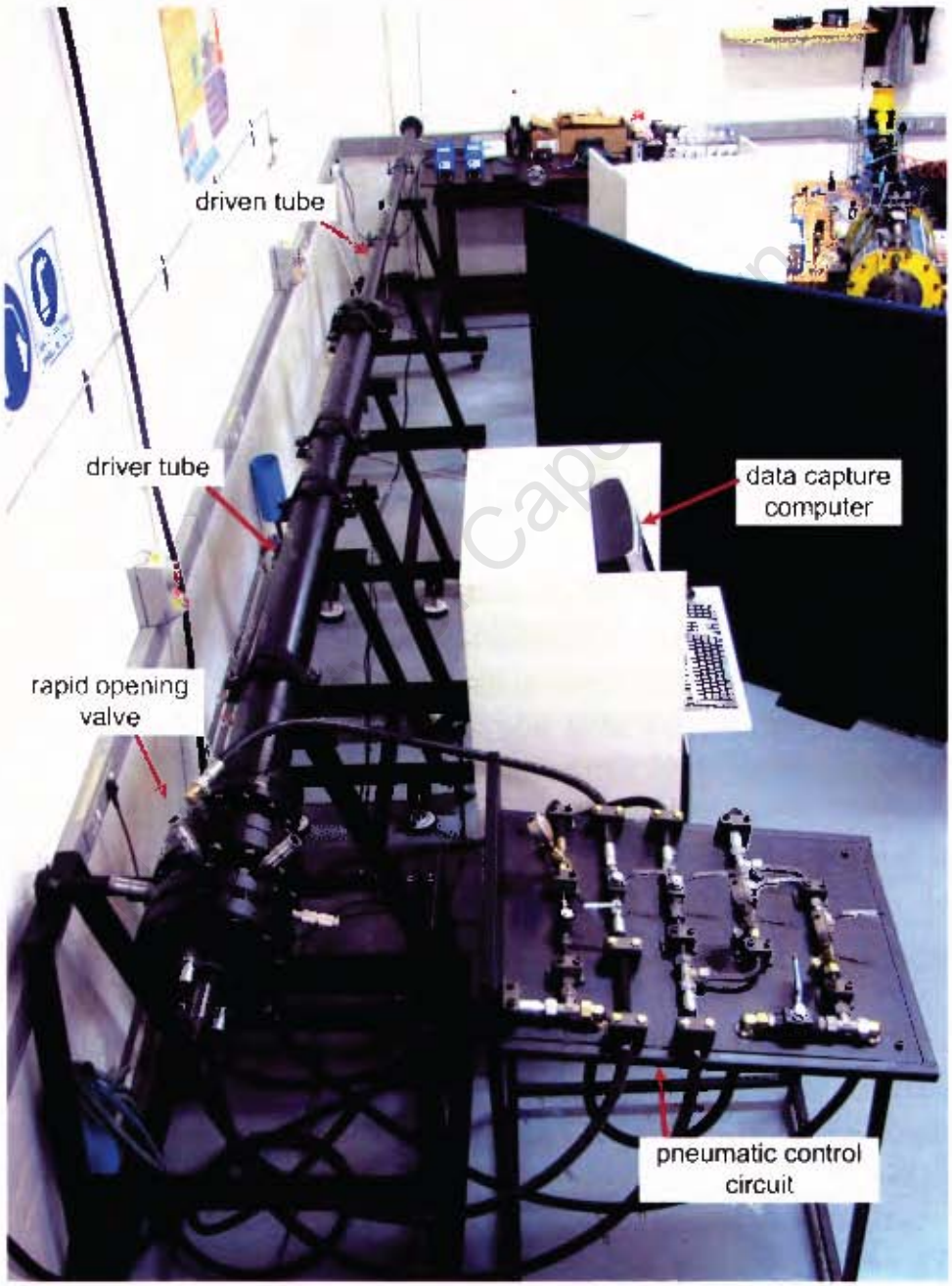

Figure 5.1: Photograph of the shock tube apparatus

The rapid opening valve was a significantly modified version of the two-stage, piston actuated concept described in Section 2.5. It was pneumatically operated and could be reset in under one minute. This gave the facility a greatly reduced test turn-around time compared to conventional diaphragmed shock tubes. The design of the valve is discussed in more detail in Section 5.4.

The shock tube used compressed air as the driver gas. A high pressure reservoir was designed to supply the compressed air. The reservoir consisted of a bank of three $50l$ high pressure gas bottles connected in parallel with a SCUBA compressor. The system was automated to run independently of the shock tube, whereby the compressor switched on when the reservoir pressure dropped below $190bar$ and switched off again when the pressure rose above $200bar$. The compressor pumped air to $200bar$ at a rate of $1.1l/min$. Each shock tube experiment required about $20l$ of air at the driver pressure. Thus each test at a driver pressure of $200bar$ required about 20 minutes of compressor operation. Figure 5.2 is a photograph of the compressed air reservoir.

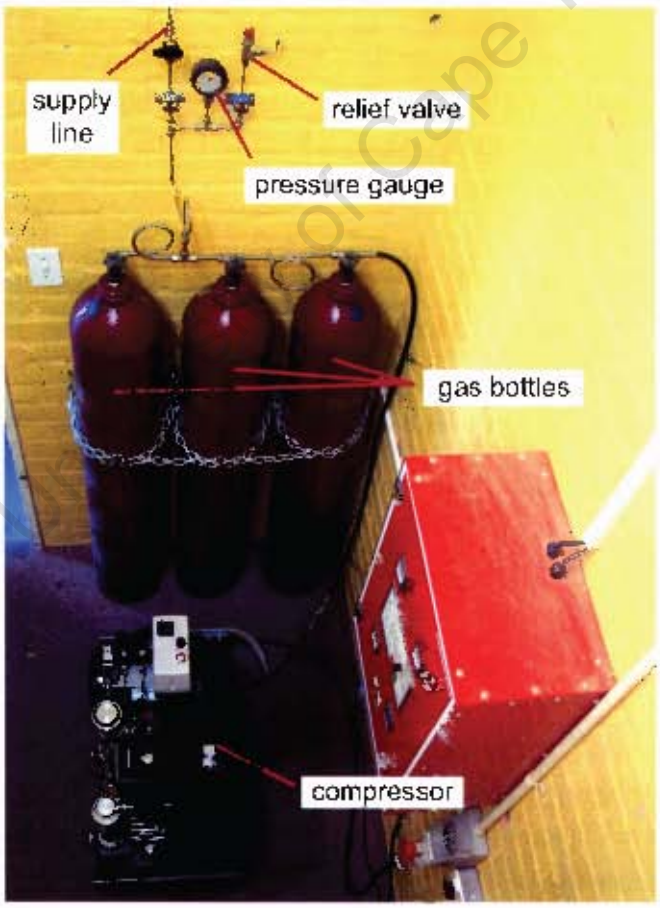

Figure 5.2: Photograph of the compressed air reservoir

A high frequency piezoelectric pressure transducer (Kistler model 603B1) was mounted $1m$ from the endwall of the driven tube, and another was mounted in the endwall itself. The pressure signals from these sensors were sampled simultaneously at 200kHz, giving a time resolution of $5\mu s$. The data was captured on a computer, and was used to determine the speed of the shock wave and the ignition delay for a given experiment.

Table 5.1 gives the rated operating conditions of the shock tube and compressed air reservoir. Also given are the test conditions which were theoretically accessible by the apparatus. Note that the overall fuel-air equivalence ratio, denoted by ϕ, of the driven gas was limited to values lean of stoichiometric. This prevented the possibility of excess fuel combusting with the oxygen in the driver gas and thereby causing overpressurisation of the shock tube. However, it was possible to test fuel-rich mixtures by diluting the test gas with an inert bath gas such as Argon.

Table 5.1: Operational range of the shock tube facility

Shock tube operating conditions	
Driven tube pressure range $[bar]$	$0.5 \leq p_1 \leq 1.5$
Driver tube pressure range $[bar]$	$7 \leq p_4 \leq 200$
Driven tube temperature range $[K]$	$290 \leq T_1 \leq 410$
Driver tube temperature range $[K]$	$290 \leq T_4 \leq 410$
Driven gas type	$0 \leq \phi \leq 1$ fuel-air mixture
Driver gas type	compressed air
Compressed air reservoir	
Maximum reservoir pressure $[bar]$	208
Maximum reservoir temperature $[K]$	300
Reservoir capacity $[l]$	50, 100 or 150
Reservoir gas type	compressed air
Ideal test conditions (assuming $\gamma = 1.40$***)***	
Maximum test temperature $[K]$	$T_5 = 1547$
Maximum test pressure $[bar]$	$p_5 = 34.6$
Test duration at these conditions $[ms]$	$\Delta t = 1.4$

Throughout the development of the shock tube facility, safety was the major priority. Safety issues are discussed in Section 5.5. Furthermore, an evaluation of the operational safety risks associated with the facility, and details of the steps taken to address them, are given in Appendix D.

5.3 Provisions for future development of the facility

As permitted by the scope of this project, the basic shock tube was manually operated with the driver and driven gases initially at ambient temperature. For the purpose of evaluating the performance of the shock tube, it was sufficient to use atmospheric air as the driven gas, because the test conditions achieved in air are similar to those achieved in a lean fuel-air mixture. Furthermore, it was possible to conduct a proof of concept ignition delay experiment by injecting a precise amount of liquid fuel into the driven tube and allowing sufficient time for it to completely evaporate and diffuse. The following provisions were made for incorporating those aspects of the design which were beyond the scope of this project:

- An axial flow inlet valve for the fuel-air mixture was provided - see Figure 5.3. Additionally, Viton® o-ring seals were used throughout the shock tube as they are compatible with fuel vapour.
- The driver and driven tubes can be heated by wrapping insulated electrical heating coils along their length. To thermally isolate the rapid opening valve, a water cooling jacket was incorporated - see Figure 5.3. Heating of the valve was undesirable as thermal expansion could upset the small tolerances between the sliding valve components.
- The use of a rapid opening valve instead of a diaphragm facilitates computerised control of the shock tube. The pneumatic control circuit shown in Figure 5.1 can easily be automated by replacing the manual levers on the two-way ball valves with computer activated quarter-turn solenoids.

Important notes:

1. The two-way ball valves were rated for use up to 350K, therefore when the heating system is installed, these valves need to be replaced if they will be exposed to higher temperatures.
2. It is recommended that before any new development is added to the shock tube facility, a complete risk assessment should be conducted and documented.

5.4 The rapid opening diaphragmless valve

5.4.1 Mode of operation

Developing the rapid opening valve presented the major design challenge of the project. A cross section through the center of the valve is shown in Figure 5.3. As illustrated, the driver tube surrounded a section of the driven tube in an annular arrangement, and the valve acted at their interface, where the flow was redirected through 180°.

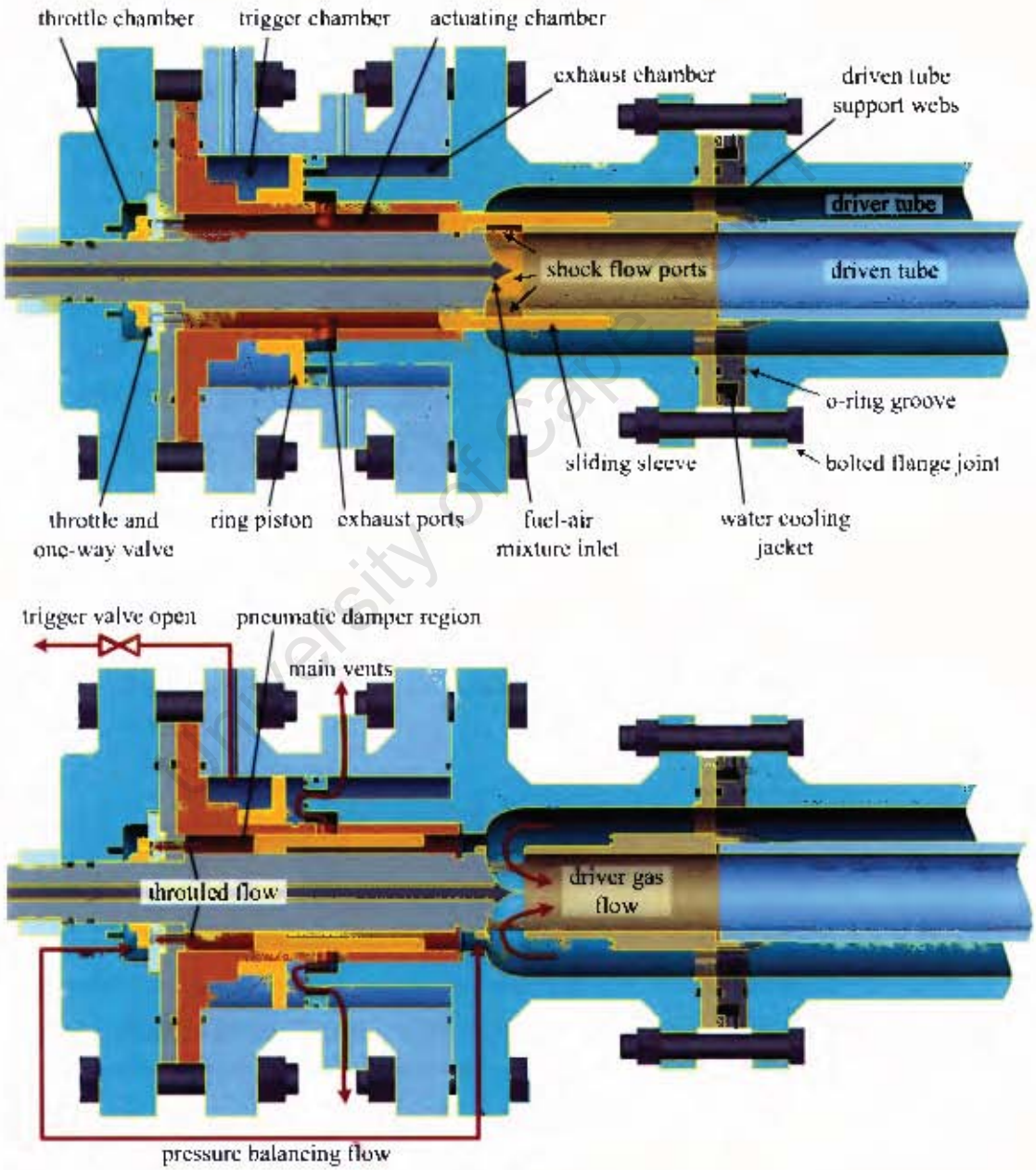

Figure 5.3: The pneumatically operated rapid opening sleeve valve system

With reference to Figure 5.3, the valve mechanism functioned as follows: compressed gas was supplied to the trigger chamber, causing the ring piston to slide forward and close the exhaust ports of the actuating chamber. Compressed gas was then supplied to the actuating chamber through small leakage holes in the one-way valve, causing the sliding sleeve to move forward and block the shock flow ports between the driver and driven tubes. The driver tube was then charged with compressed gas, and the driven tube filled with test gas at the desired conditions. The apparatus was now ready to perform a test.

The test was initiated by opening the trigger valve to release the pressure in the trigger chamber. When the pressure there dropped below a certain threshold, the compressed gas in the actuating chamber forced the ring piston to snap backward, and flowed through the large exhaust ports into the exhaust chamber, which was vented to the atmosphere through several orifices. This caused the pressure in the actuating chamber to drop rapidly. The high pressure gas in the driver tube then propelled the sleeve backward into the actuating chamber, rapidly opening the shock flow ports. The subsequent rush of driver gas through the shock flow ports generated the shock wave.

5.4.2 Design features

The valve mechanism had some novel design features which warrant special mention. Firstly, the valve was designed to operate using compressed gas from the same supply and at the same pressure as the the gas used in the driver tube. This aided convenience and eliminated the need to prevent leakage between the valve and driver through the clearance space around the outside of the sliding sleeve.

Secondly, the mechanism was designed such that when the ring piston was in the closed position, the pressure of the gas in the actuating chamber acted on a smaller area of the piston than the pressure of the gas in the trigger chamber. As these pressures were equal just prior to a test, the pressure in the trigger chamber had to drop below a threshold level before the ring piston would unseat. This allowed time for the trigger valve to be fully opened before the threshold level was reached - in other words the valve action was insensitive to the rate at which the trigger valve was opened. Additionally, as the ring piston unseated it exposed more of its area to the actuating chamber gas and hence was forced open quickly, thereby promoting rapid evacuation of the actuating chamber. Note that a similar area differential technique was used to ensure that the sliding sleeve only started moving once the ring piston had opened fully.

Thirdly, the sliding sleeve was made from high strength aluminium (which is a lightweight metal), and had a 'run-up length' whereby, as it started sliding backward, it had to travel a distance more than twice the length of the shock flow port openings before it actually uncovered them. Thus by the time it did uncover them, the sleeve had been accelerated to a high speed and the opening process was rapid.

Fourthly, the flow path between the driver and driven tubes was sculpted so as to streamline the flow, and therefore minimise the losses, as the avalanche of driver gas was redirected around the 180^o bend.

Fifthly, a self-regulating pneumatic damper was designed to decelerate the sliding sleeve once it uncovered the shock flow ports. A damper was necessary as the sliding sleeve travelled at such a high speed that it would have been be damaged were it stopped by metal on metal impact. The pneumatic damper functioned as follows: at the instant the sleeve fully uncovered the shock flow ports, it also blocked the exhaust ports, trapping the gas still remaining behind the sleeve in the actuating chamber. As the sleeve continued to move backward, it compressed this trapped gas and consequently slowed down. To prevent the sleeve from rebounding excessively, the trapped compressed gas was allowed to escape through a throttle and one-way valve into the throttle chamber. The throttle chamber was maintained at the same pressure as the driver gas propelling the sleeve via a direct connecting gas line. Thus gas could only flow from the actuating chamber into the throttle chamber once the back-pressure in the actuating chamber exceeded the pressure propelling the sleeve - at which stage the sleeve was decelerating. The major feature of the pneumatic damper design was that it was inherently self-regulating in terms of operating pressure. In other words, it was not necessary to make any adjustments to the setup of the damper when different driver tube pressures were used.

Additionally, as the valve contained a number of annular sliding parts, much attention was paid to ensuring good concentricity and accurate location of the various sliding surfaces. The valve components were spigoted so that they would be naturally aligned and located during the assembly process. And finally, o-rings were used to provide seals wherever needed throughout the valve and shock tube. O-rings were chosen as they provide a simple, reliable, reusable and cheap method of sealing.

5.4.3 Valve performance model

During the design of the rapid opening valve, a model for simulating and optimising its performance was developed and programmed into Microsoft Excel®. The main aim of the model was to predict the motion of the sliding sleeve during the opening process. Inputs to the model were the dimensions and masses of the various valve components, volumes of its chambers and the initial conditions such as gas pressure and temperature. Gas dynamics and thermodynamics theory were used to model the gas flow processes within the valve, and basic kinetic theory was used to model the resulting motion of the valve's moving parts.

Some design phase simulations of valve performance are illustrated as follows. Figures 5.4 and 5.5 show the anticipated performance at the maximum rated driver pressure of $p_4 = 200bar$. Then to demonstrate the versatility of the concept, Figures 5.6 and 5.7 show the anticipated performance at the minimum rated driver pressure of $p_4 = 7bar$. In both cases, all other parameters were equal, with $p_1 = 1bar$ and $T_1 = T_4 = 300K$.

The simulation of valve performance at the maximum driver pressure indicated a valve opening time, measured from the first open to the fully open position, of $0.54ms$. Once the valve was fully open, the pressure in the actuating chamber built up, causing the sleeve to decelerate, and then fluctuated as the sleeve rebounded slightly. After a few of these damped oscillations, the sleeve was brought to rest in the fully open position. Note that the sleeve never impacted the end stop, nor did it rebound past the fully open position. The slope of the line indicating sleeve motion gives the velocity of the sleeve. The average sleeve velocity during the opening process was about $46m/s$. The simulation at the minimum driver pressure also indicated correct valve operation. However, in this case the opening time and velocity were slower at $2.7ms$ and $9m/s$ respectively.

As shown in Figure 5.4, the modelled pressure in the actuating chamber built up to about twice the initial driver pressure, hence the components of the actuating chamber were designed to withstand twice the maximum driver pressure, which equates to $400bar$, with an adequate safety factor.

During commissioning of the shock tube, the model was used to check that the valve was functioning properly. This was achieved by recording the pressure in the actuating chamber during testing of the shock tube, and then fine tuning the model parameters until good agreement with the experimental data was obtained. The validated model was then used to provide an indication of the actual motion of the sliding sleeve.

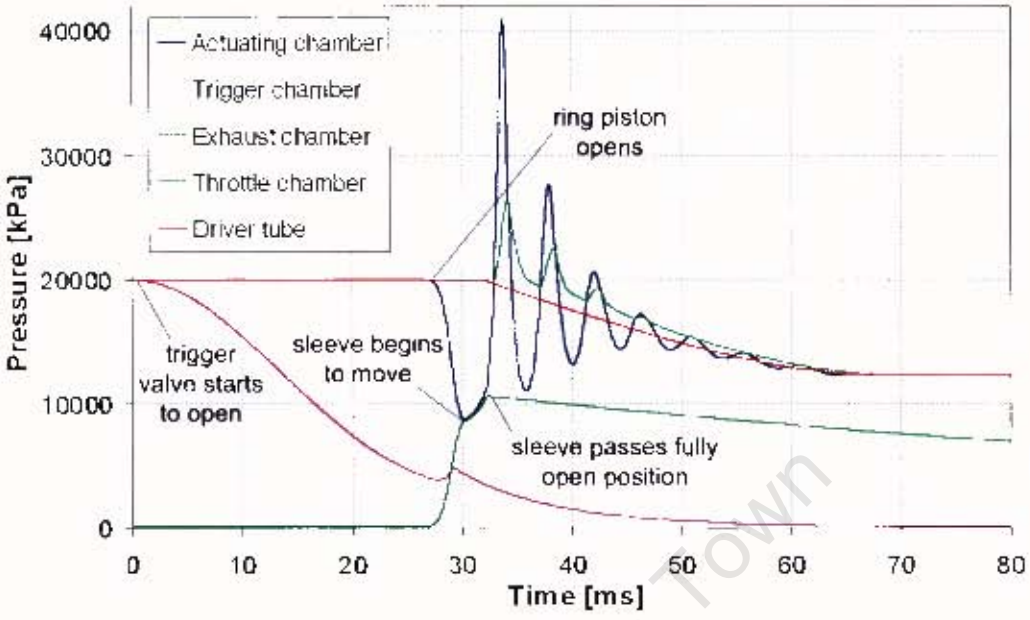

Figure 5.4: Pressures in the various valve chambers at maximum driver pressure

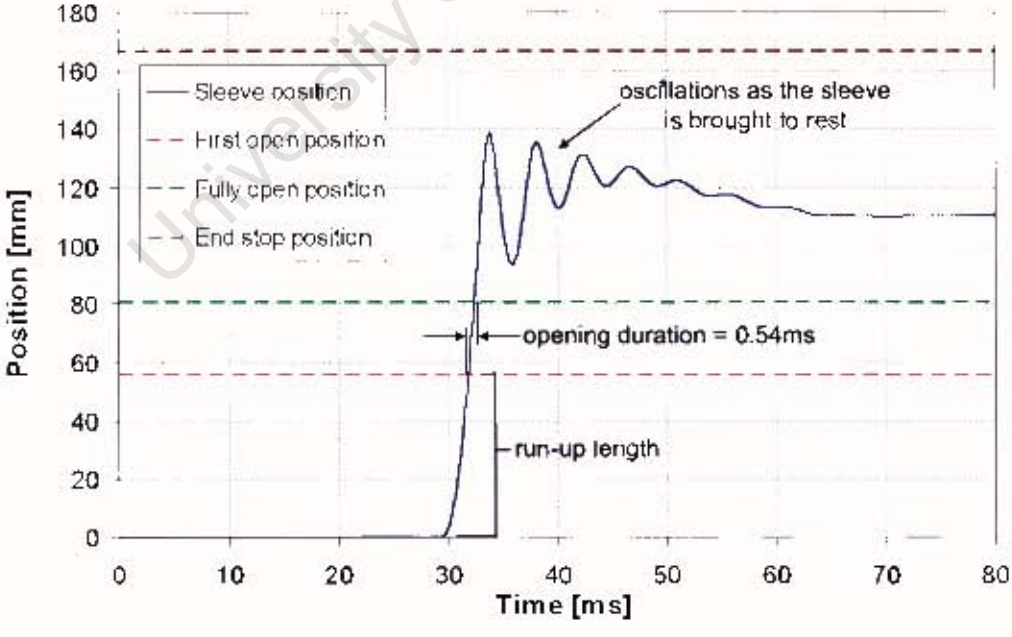

Figure 5.5: Predicted sleeve motion at maximum driver pressure

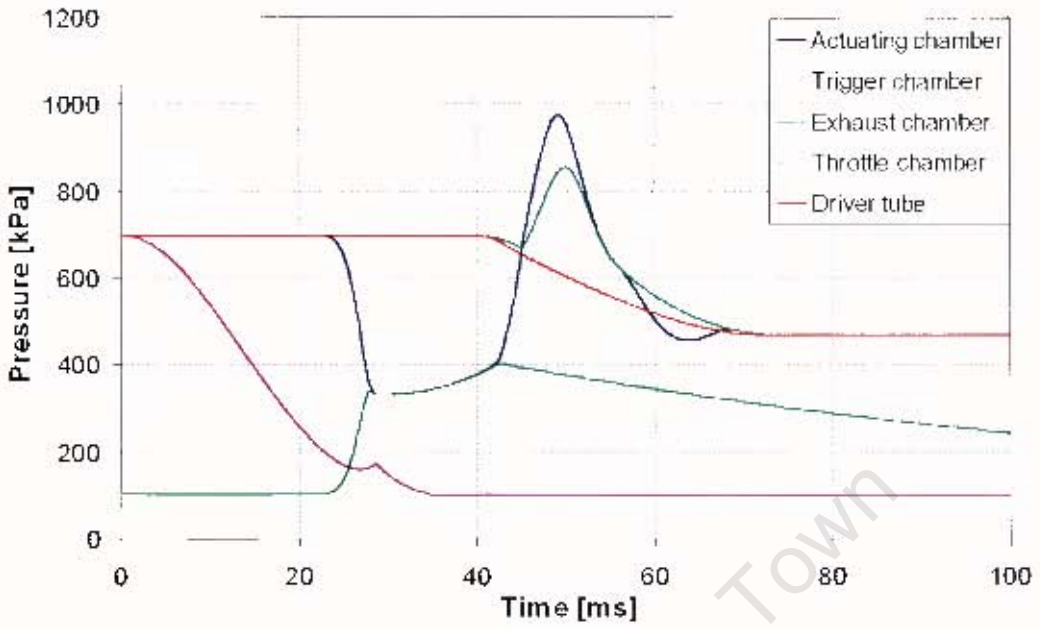

Figure 5.6: Pressures in the various valve chambers at minimum driver pressure

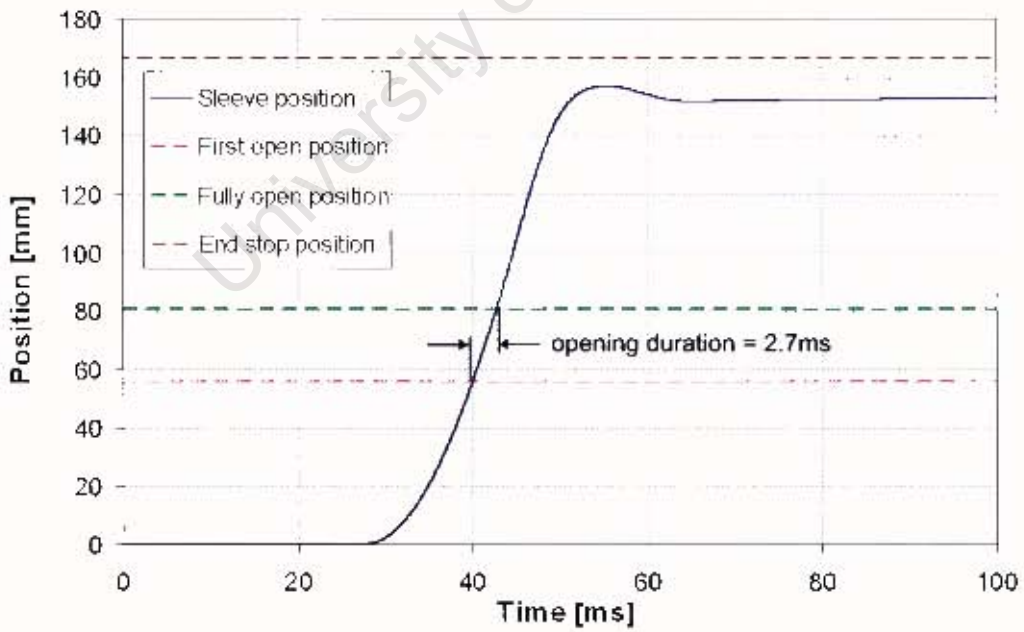

Figure 5.7: Predicted sleeve motion at minimum driver pressure

5.5 Safety considerations

5.5.1 General safety instructions

In accordance with The University of Cape Town's strict health and safety policy, the shock tube facility was designed with safety considerations as a requisite priority. To this end, a risk assessment was conducted to identify and address any potential operational hazards. The results of the risk assessment are presented in Appendix D. To ensure the safety of the operator and those in the vicinity of the facility, the following safety instructions were made mandatory:

- Wear eye and ear protection when operating any part of the facility. If the shock tube is heated, or if handling fuels, also wear gloves. If other people are in the vicinity, also provide them with this equipment and make them aware of potential hazards.
- Adhere strictly to the operating procedures described in Appendix C.
- Never operate the facility outside of the rated conditions listed in Table 5.1.
- Adhere strictly to the assembly, inspection and maintenance instructions described in Appendices A and B.
- Perform and document a thorough risk assessment a) before making any modifications to the facility, and b) before using the facility or any of its components for any purpose other than they were specifically was designed for.

5.5.2 High pressure equipment safety issues

The shock tube assembly included three main pressure containing vessels: the driven tube, the driver tube and the outer cylinder of the rapid opening valve. Each of these vessels was constructed from a section of seamless hydraulic cylinder tube and two boilerplate steel flanges - one welded at each end of the tube. South African law regulates the manufacture of pressure vessels that have a nominal internal diameter over $150mm$ [34], hence the shock tube components, which all had internal diameters under $150mm$, were not subject to this legislation. However, in the design phase careful consideration was given to the fact that during operation the vessels would contain very high pressure gas, which is inherently dangerous, and would undergo cyclic pressurisation, making them susceptible to fatigue. To ensure the safety of the pressure containing vessels, they were designed using the ASME code for pressure vessel design

as a guide [35]. Note that safeguard against fatigue is intrinsically built into the code. In addition, to double check that safe stress levels would not be exceeded during pressurisation, a basic stress analysis of the vessels was carried out using the Abaqus® finite element analysis (FEA) software package. Details of the design calculations are given in Appendix E.

During the manufacture and commissioning of the facility, the following important safety measures were implemented to minimise the potential danger of the high pressure equipment:

- All critical welding of the flanges onto the tube sections was done by certified welders, and was stress relieved and tested for cracks. The welding report is contained in Appendix F.
- The assembled shock tube apparatus, comprising of the driver tube, the driven tube and the rapid opening valve, was hydrostatically pressure tested to 250bar. The test certificate is contained in Appendix F.
- The high pressure gas bottles used as the compressed air reservoir were inspected, hydrostatically pressure tested to $358bar$ and re-certified to their design pressure of $208bar$ by an accredited authority prior to their installation. The test certificate is contained in Appendix F.
- All components of the high pressure pneumatic circuitry, such as valves, air supply lines, seals and fittings were purchased new from reputable OEM suppliers, and were rated for safe operation at the conditions to which they would be exposed during normal shock tube operation.
- Inspection and maintenance schedules, assembly instructions and operational procedures for the subsystems of the facility were compiled. They are contained in the relevant appendices.

Important note: The shock tube apparatus was designed to be a full scale, working prototype. Although every effort was made to ensure high levels of safety, if the prototype is to be put into regular service the dangers associated with the high pressure equipment warrant the extra precaution of having the facility independently evaluated by an experienced professional engineer, particularly with regard to the long term fatigue life of the pressure containing vessels and the safety of the high pressure circuits/systems.

6 Commissioning of the shock tube

6.1 Introduction

The objectives of the commissioning programme were to make the shock tube facility fully operational, investigate its performance and make refinements to improve its performance. The commissioning strategy was to conduct initial tests at relatively low driver pressures to verify correct, safe operation of the facility, and then to test at gradually increasing driver pressures all the way up to the maximum rated driver pressure. Once reliable operation over the complete operating pressure range was obtained, the focus shifted to improving the performance of the shock tube. At the end of the chapter, the final performance of the shock tube is discussed.

As the installation of a heating system and a fuel mixture preparation system were beyond the scope of this project, all commissioning tests were done using air at room temperature and pressure as the driven gas, and compressed air at room temperature as the driver gas. The diagnostic equipment for evaluating the shock tube's performance consisted of three high frequency piezoelectric pressure transducers. Two of these sensors were mounted in the driven tube - one was located in the sidewall of the tube exactly $1m$ from the endwall, the other was mounted in the endwall itself. Both sensors were flush mounted. They provided a means of analysing the propagation, rise time and magnitude of the pressure jump caused by, and indicative of, the shock wave. The third transducer was used to measure the pressure in the actuating chamber of the rapid opening valve for the purpose of validating the valve performance model.

All commissioning tests were conducted according to the following basic procedure:

1. Set the rapid opening valve to the closed position.
2. Fill the driver tube with compressed air at the desired pressure.
3. Normalise the driven tube to atmospheric pressure.

4. Record the initial test conditions (p_1, T_1, p_4 *and* T_4).
5. Ready the data capture system to record the signals from the pressure transducers.
6. Operate the shock tube by triggering the rapid opening valve.
7. Examine the test results to check that the shock tube operated correctly
8. Repeat to perform another test, or discharge and shut down the facility.

6.2 Preliminary low pressure commissioning

For the initial tests, the shock tube was operated at a driver pressure below $10bar$. No difficulties were encountered during these tests. The facility as a whole operated reliably. Most notably, the rapid opening sleeve valve functioned well. When the valve was closed, no leakage occurred between the driver and driven tubes, and when it was triggered, it opened sufficiently quickly for a shock wave to be generated, as evidenced by the recorded driven tube pressure traces. A typical test result is shown in Figure 6.1. Note that the pressure traces were not smoothed or filtered in any way. The initial conditions at which the test was performed are given in Table 6.1.

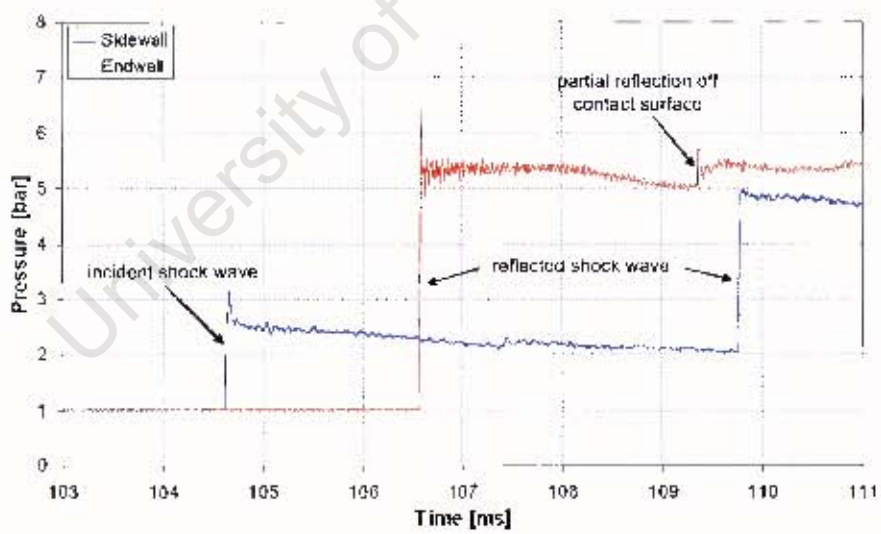

Figure 6.1: Driven tube pressure traces from a typical low pressure test

Figure 6.1 shows that the incident shock wave travelled down the driven tube, passing the sidewall pressure transducer at $t = 104.625ms$. It reached and was reflected off the endwall at $t = 106.580ms$. Thus the endwall pressure transducer experienced a

Table 6.1: Initial conditions for the test result shown in Figure 6.1

Driven gas pressure, $p_1 \pm 0.01\ [bar]$	1.01
Driver gas pressure, $p_4 \pm 0.2\ [bar]$	7.7
Driven gas temperature, $T_1 \pm 5\ [K]$	295
Driver gas temperature, $T_4 \pm 5\ [K]$	295

single pressure jump equal in magnitude to the sum of the incident and reflected shock wave pressure jumps. The reflected shock wave then propagated back up the driven tube, eventually passing the sidewall pressure transducer at $t = 109.760ms$. The small pressure jump trailing the reflected shock wave was a partial reflection of the reflected shock wave off the contact surface. The gradual pressure decay behind the incident shock was attributed to boundary layer growth.

The rapid opening sleeve valve operated reliably and consistently throughout the low pressure commissioning phase. After the testing had been completed, the valve was dismantled and inspected for wear or damage. All components were found to be in good order. There was no evidence of impact between the sliding sleeve and endstop, which indicated that the pneumatic damper was performing its primary function. From the success of the low pressure tests it was concluded that the shock tube was functioning correctly and operating safely. The next step was to commence the high pressure commissioning phase.

6.3 High pressure commissioning

During the high pressure commissioning phase, the shock tube was tested at gradually increasing driver pressures, up to the maximum rating of $200bar$. This section first details the difficulties that were encountered in trying to obtain reliable operation at high pressure and the solutions implemented to address those difficulties. Then, the refinements made to optimise the efficiency of the shock tube in comparison to ideal shock tube flow are described.

6.3.1 Operational difficulties encountered during testing

6.3.1.1 Seal failures

The rapid opening valve operated reliably at driver pressures below $100bar$, and the driven tube pressure traces indicated that the shock tube was consistently generating

a shock wave. However, when the rapid opening valve was reloaded for the next test following the first $100bar$ test, it was discovered that compressed gas was leaking into the driven tube. Disassembly and inspection of the valve revealed that the o-ring which seals between the actuating chamber and the driven tube had been blown from its groove. It was found, broken into three pieces, near the end of the driven tube. Figure 6.2 illustrates the mechanism by which this was thought to have happened. Just after the valve was fired and the sliding sleeve was moving off the o-ring, the pressure in the actuating chamber would still be high relative to the (atmospheric) driven tube pressure. This pressure differential across the o-ring caused it to squeeze out of its groove, between the edges of the groove and the sleeve, and subsequently get blown down the driven tube by the avalanche of driver gas.

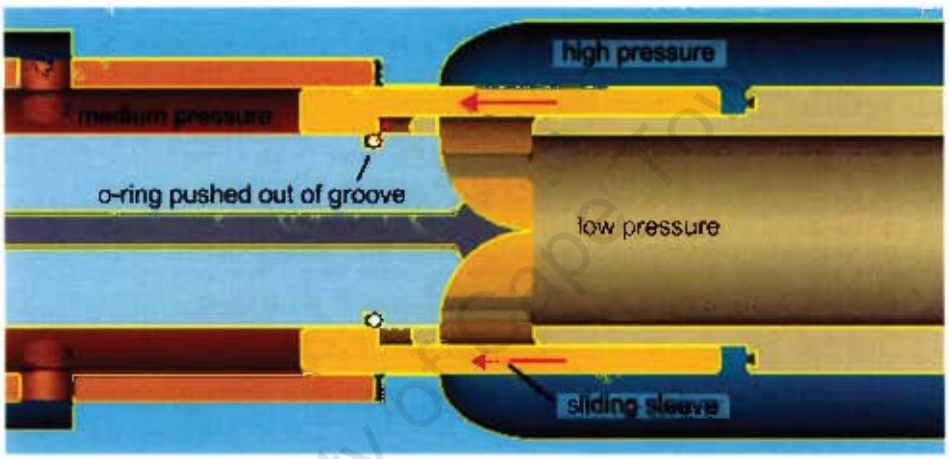

Figure 6.2: Illustration of the process by which the o-ring seal failed

The problem was resolved by replacing the original o-ring with one that had a smaller internal diameter but a greater cross sectional diameter, so that when in its groove the o-ring was significantly stretched and its elasticity held it in place. Table 6.2 compares the dimensions of the original and replacement o-rings.

Table 6.2: Comparison between original and replacement o-rings

Dimension	***Original***	***Replacement***
Internal diameter $[mm]$	43	35
Cross section diameter $[mm]$	4	5

After this modification, the shock tube operated without incident as the driver pressure was increased to just below $200bar$. The first two tests at $200bar$ were successful, and the driven tube pressure traces indicated that the shock tube continued to effectively generate shock waves. However, when the rapid opening valve was reloaded after

the second $200bar$ test, two leaks were noticed. Compressed gas was leaking into the exhaust chamber of the valve, and once again there was leakage of compressed air into the driven tube. Disassembly and inspection of the valve revealed the two o-ring seals indicated in Figure 6.3 to be at fault. Both o-rings had been fitted into dove-tail grooves designed to retain them, however at the extremely high test pressure they had both partially popped out of their grooves.

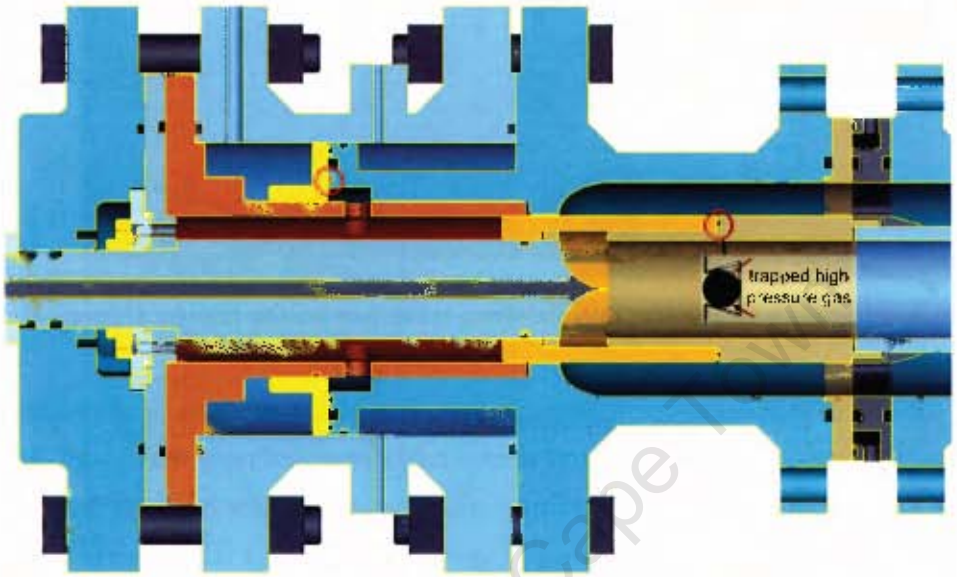

Figure 6.3: Problematic o-ring seals

It was suspected that in both cases this had occurred as follows: when the valve was loaded and pressurised, compressed air was forced into the groove around the o-ring. Then when the valve was triggered, causing the pressure within it to drop suddenly, the o-ring was pushed out of its groove by the expanding gas trapped behind it. The problem was resolved by gluing both o-rings into their grooves using a cyanoacrylate adhesive. Subsequently the rapid opening valve operated reliably.

6.3.1.2 Component wear

When the rapid opening valve was disassembled after the second $200bar$ test to investigate the causes of the leaks, all of its components were inspected for wear. There was no indication of impact between the sliding sleeve and the endstop, however there was some scratching on the outer surface of the sleeve. This was expected given that the sleeve was made from aluminium and slid within a much harder steel cylinder. The scratches were very minor and were easily polished away using a scouring pad and polishing fluid. Figure 6.4 shows a photograph of the scratches on the sleeve.

Figure 6.4: Photograph showing scratches on the sliding sleeve

All of the other valve components were in good condition and showed virtually no signs of wear. Inspection of the driver and driven tubes revealed only one issue: the gasket that sealed between the flanges at the endwall of the driven tube had been burnt through. A photograph of the gasket is shown in Figure 6.5. This was seen as evidence that the shock tube had established a region of very high temperature gas behind the reflected shock wave. The gasket was replaced.

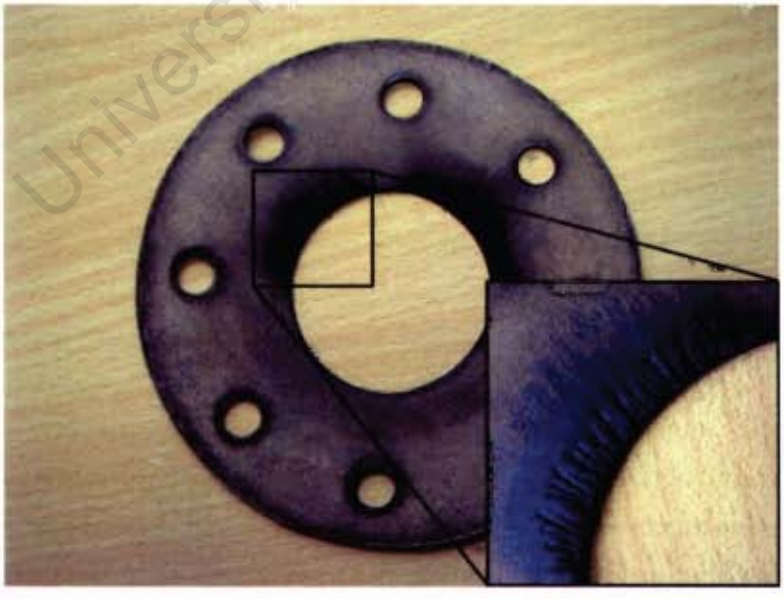

Figure 6.5: Photograph of the burnt endwall gasket

6.3.2 Shock tube performance investigation

Consider Figure 6.6 which shows the driven tube pressure traces from the first two tests nominally at the maximum rated driver pressure of $200bar$. The initial conditions for these tests are given in Table 6.3. The high degree of reproducibility obtained was a feature of all repeated tests, and indicated that the rapid opening valve was operating consistently. For a comparison between the calculated test conditions, see Table 6.4.

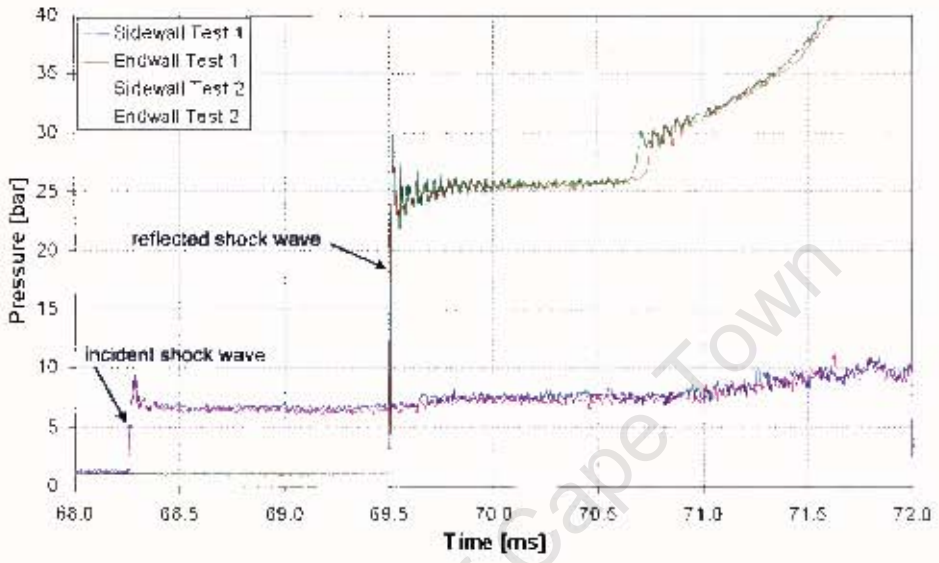

Figure 6.6: Driven tube pressure traces for the first two nominally $200bar$ tests

Table 6.3: Initial conditions for the test results shown in Figure 6.6

Test number	***Test 1***	***Test 2***
Driven gas pressure, $p_1 \pm 0.01$ $[bar]$	1.01	1.01
Driver gas pressure, $p_4 \pm 1$ $[bar]$	203	204
Driven gas temperature, $T_1 \pm 5$ $[K]$	295	295
Driver gas temperature, $T_4 \pm 5$ $[K]$	295	295

The incident and reflected shock waves are indicated on the pressure traces. The incident shock wave had a rise time of under $5\mu s$. The reflected shock wave had a rise time of under $10\mu s$. Note that the recorded signals had a time resolution of $5\mu s$, hence the rise times may in fact have been significantly shorter. The noise on the pressure traces immediately after the passage of the shock waves was most likely due to mechanical vibration of the pressure transducer mountings as they were impacted by the shock wave, and was not actual gas phenomena. This issue has been reported previously, and in some cases has been addressed by coupling the shock tube to a large mass

whose inertia helps minimise vibration [17]. Installing such an inertial mass may be a worthwhile future modification to the facility.

Excluding the noise, the endwall pressure traces indicate a steep pressure rise coinciding with the reflected shock wave, followed by a period of steady, elevated pressure more than $1ms$ in duration. This is exactly the pulse shape required of the apparatus. However, for the given initial driver to driven pressure ratio, ideal shock tube theory predicts a significantly higher shock Mach number, and therefore reflected shock pressure, than that which was actually obtained. The reasons for this inefficiency of the shock tube relative to ideal performance were discussed in Section 3.5. A comparison of the actual and ideal test results is given in Table 6.4.

Table 6.4: Comparison between actual and ideal performance

Test result	***Test 1***	***Test 2***	***Ideal***
Incident shock Mach number, M_s	2.34	2.33	2.61
Incident shock pressure, p_2 $[bar]$	6.3	6.2	7.9
Test pressure, p_5 $[bar]$	25.1	24.7	34.9
Test temperature, T_5 $[K]$	935	929	1113

In Section 4.2 it was specified that the shock tube should be capable of accessing test temperatures of up to $1500K$. Extrapolation from the above results indicated that, assuming both the driver and driven gases were initially heated to $410K$, the shock tube was actually only capable of accessing a maximum test temperature of about $1300K$. Clearly the efficiency of the shock tube would have to be improved if it was to meet the test temperature specification. Considering the non-idealities discussed in Section 3.5, it was evident that improvements could potentially be made by:

- reducing the opening time of the rapid opening valve,
- polishing the inside of the driven tube to reduce its surface roughness and thereby decrease attenuation of the shock wave,
- further streamlining the flow path between the driver and driven tubes to minimise frictional flow losses.

The strategy for improving the efficiency of the shock tube was as follows: firstly, the performance of the rapid opening valve was evaluated to check that it was operating optimally. Then, the driven tube was polished internally to see what gains could be made. Finally, the webs between the driver and driven tubes were streamlined to see

if doing so yielded any further improvement. Note that the shock tube was tested in between polishing and streamlining so that the relative gains from each of these modifications could be assessed.

6.3.2.1 Evaluating the performance of the rapid opening valve

The valve performance model was fine tuned to fit the experimentally recorded actuating chamber pressure history by adjusting the model parameters. Figure 6.7 is a comparison of the recorded and modelled actuating chamber pressure profiles for Test 1 in Table 6.3. The high frequency oscillations on the recorded pressure trace were most likely due to resonance of the air in the connecting passageway between the actuating chamber and the pressure transducer. This is proved as follows: the resonant frequencies, f, of a gas passageway closed at one end are given by the following equation:

$$f = \frac{na}{4L} \tag{6.1}$$

where a is the speed of sound in the gas, L is the length of the passageway and n is an odd, positive integer $(1, 3, 5...)$ representing the resonance node. The speed of sound in air at room temperature is $\approx 340m/s$. The connecting passageway is a straight drilled hole, through the flange on the outer cylinder of the actuating chamber, of length $57mm$. Substituting these values into Equation 6.1 and setting $n = 3$, one obtains a resonant frequency of $4473Hz$. This compares very well to the frequency of $4317Hz$ measured as the gas in the actuating chamber drops back down to the initial valve pressure (see Figure 6.7), at which instant the gas would be at approximately room temperature.

Excluding these oscillations from the comparison, good agreement between the model and experimental data is evident from the instant the sliding sleeve begins to move. The accuracy of the model's calculations for sleeve velocity and opening time was estimated at $\pm 20\%$. The motion of the sleeve according to the validated model is shown in Figure 6.8. It indicates that the sleeve had accelerated to $48m/s$ by the time it opened the shock flow ports. Although the process of decelerating the sleeve was not identical to the motion anticipated in Figure 5.5, the desired function of bringing the sleeve to rest without either impacting the endstop or re-bounding past the fully open position was achieved. Also note that the deceleration process has no effect on shock tube efficiency. The predicted opening time of $0.52ms$ meets the requirement stated in Table 4.1 that for effective shock wave formation, the opening time should be below $1ms$. Hence it was decided that the valve was performing sufficiently well and further attempts to reduce the opening time were unnecessary.

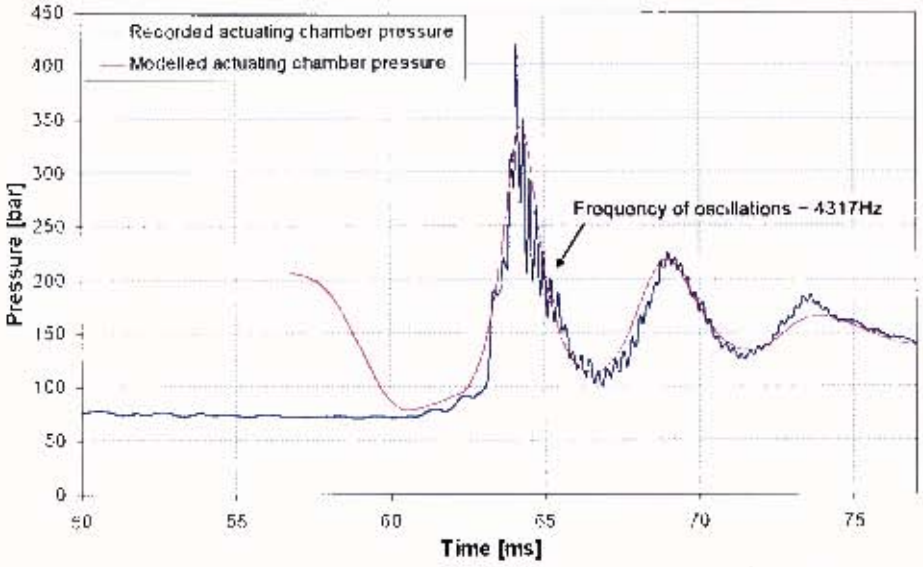

Figure 6.7: Comparison between the actual and modelled actuating chamber pressure

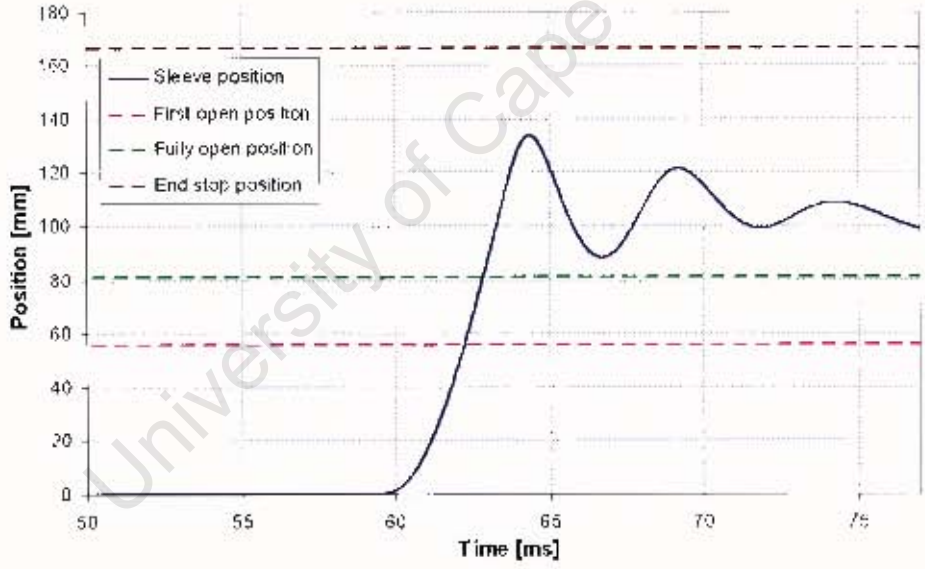

Figure 6.8: Motion of the sliding sleeve according to the validated model

6.3.2.2 Effect of polishing the inside of the driven tube

To reduce the surface roughness of the inside of the driven tube, it was thoroughly polished using a fine grit cylinder hone. The improvement in surface finish this yielded was substantial, as previously the only surface preparation had been to use a sanding flap wheel to remove scale and rust from the as manufactured tube. The shock tube was then tested again at a nominal driver pressure of $200bar$. The results of the test are shown in Figure 6.9. The initial conditions for the test are given in Table 6.5.

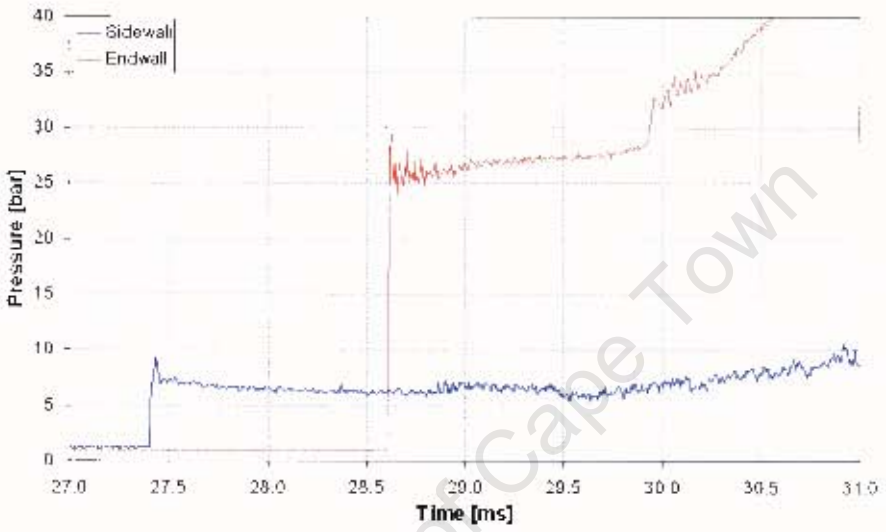

Figure 6.9: Driven tube pressure traces obtained subsequent to polishing

Table 6.5: Initial conditions for the test results shown in Figure 6.9

Driven gas pressure, $p_1 \pm 0.01\ [bar]$	1.01
Driver gas pressure, $p_4 \pm 1\ [bar]$	202
Driven gas temperature, $T_1 \pm 5\ [K]$	295
Driver gas temperature, $T_4 \pm 5\ [K]$	295

Compared to the tests performed prior to polishing the driven tube, a significant improvement in efficiency was evident. The shock Mach number increased from 2.34 to 2.39, and the reflected shock pressure increased by about $2bar$. It was suspected that the slight dip in pressure at the endwall immediately after the reflection of the shock wave was due to leakage past the endwall gasket, which again showed evidence of burn through. It was replaced with a new one made from high temperature gasket material, and the endwall was reattached using extra high tensile bolts (property class 12.9) to increase the clamping force on the gasket.

6.3.2.3 Effect of streamlining the flow path between the driver and driven tubes

The design of the shock tube had incorporated sculpting of the 180° bend between the driver and driven tubes for optimal flow. However, the driven tube support webs indicated in Figure 5.3 had only been rounded at their leading edges. To try reduce the flow losses due to these webs, it was decided to shape them by hand to be as aerodynamically streamlined as possible. The trailing edges were tapered so that the webs had the cross section of an aerofoil, and the web surfaces were polished. The shock tube was then re-assembled and tested once again at a nominal driver pressure of $200bar$. The results of the test are shown in Figure 6.10. The initial conditions at which the test was performed are given in Table 6.6.

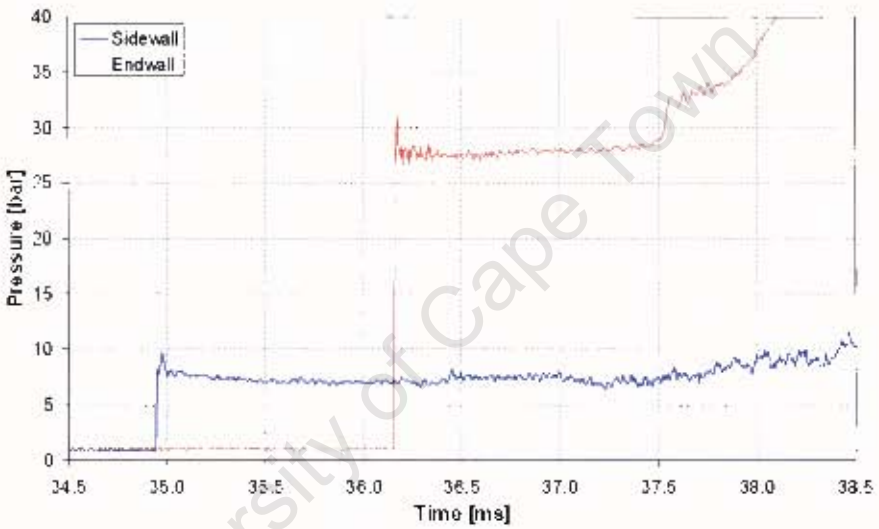

Figure 6.10: Driven tube pressure traces obtained subsequent to streamlining the webs

Table 6.6: Initial conditions for the test results shown in Figure 6.10

Driven gas pressure, $p_1 \pm 0.01$ $[bar]$	1.01
Driver gas pressure, $p_4 \pm 1$ $[bar]$	205
Driven gas temperature, $T_1 \pm 5$ $[K]$	295
Driver gas temperature, $T_4 \pm 5$ $[K]$	295

When compared to Figure 6.9, Figure 6.10 shows that streamlining the flow path resulted in a minor increase in shock tube efficiency over and above the improvement already gained by polishing the driven tube. The shock Mach number increased from 2.39 to 2.40. More significantly the tighter clamping of the new high temperature gasket helped reduce the dip in pressure upon reflection of the shock wave.

6.4 Final test results and discussion

6.4.1 Shock tube performance

To assess the final performance of the shock tube after all modifications had been made, a series of tests were conducted over a range of driver pressures between 10 and 200bar. Note that for all these tests, the driven gas was air at room temperature and pressure (approximately 295K and 1.01bar respectively), and the driver gas was compressed air at room temperature. The incident shock Mach number obtained in each test was measured and used to calculate the test pressure and temperature according to equations 3.27 and 3.28 respectively. The results of these tests are presented and discussed below.

6.4.1.1 Efficiency of the shock tube

Figure 6.11 gives an indication of the efficiency of the shock tube relative to ideal performance. As expected, the deviation from ideal theory increased with the shock Mach number. Real gas effects are a cause of this non-ideal behaviour (see Section 3.5). Comparison with Figure 3.2 shows the shock tube to be more efficient than the similar diaphragmless installation described in Section 3.5. In that case, no attempt had been made to optimise the flow path between the driver and driven tubes. It is likely that further improvements in efficiency can be made by additional polishing and streamlining of all flow surfaces, particularly the inside of the driven tube - whose surface finish was shown to have a significant effect on efficiency, as well as the inside of the driver tube - whose surface finish was not improved from the as manufactured condition.

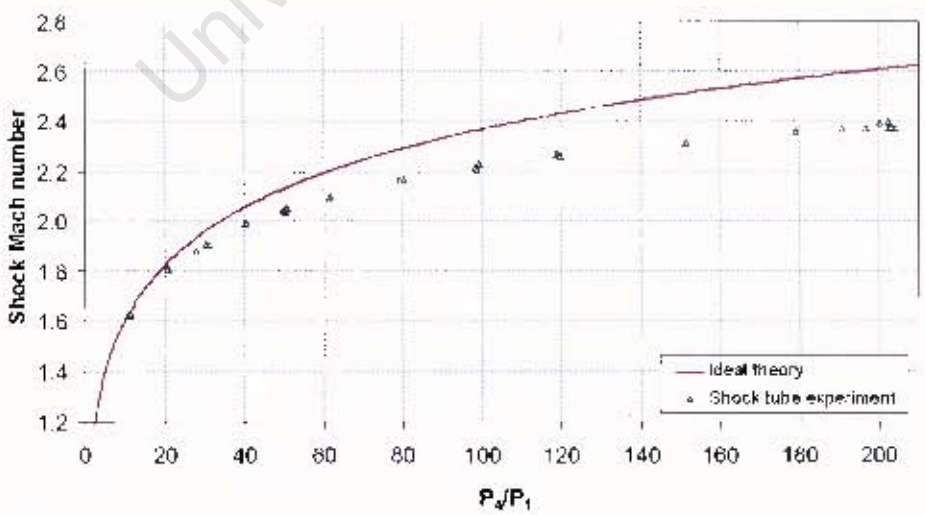

Figure 6.11: Incident shock Mach number as a function of initial pressure ratio

6.4.1.2 Attained test conditions

Figure 6.12 shows the test conditions attained the by shock tube as a function of initial driver pressure. At the maximum driver pressure, where test to test variation was most severe, test temperature was repeatable to within $\pm 25K$, and test pressure was repeatable to within $\pm 1.2bar$. As expected, test temperature increased diminishingly with an increase in pressure ratio. The recorded pressure traces from a test performed at the maximum rated driver pressure are shown in Figure 6.10. Apart from the mechanical vibration noise, the shape of the pressure pulse at the endwall of the driven tube is well suited for the intended application of autoignition research: the pressure rise due to the reflected shock wave has an extremely rapid rise time of under $10\mu s$, and subsequently the elevated pressure in the test section of the driven tube remains approximately steady for the entire test duration of $1.3ms$. The measured Mach number of the incident shock wave was 2.40. The calculated test pressure and temperature were $27.1bar$ and $973K$ respectively. Note that the calculated test pressure agrees well with the recorded test pressure shown in Figure 6.10.

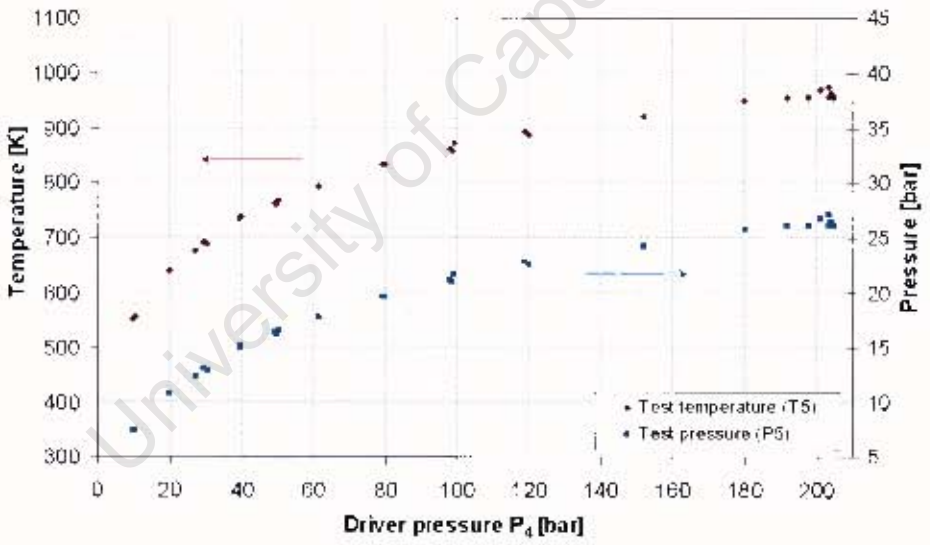

Figure 6.12: Test temperature and pressure as a function of initial driver pressure

6.4.1.3 Maximum accessible test conditions

Extrapolating from the observed shock tube performance, when a heating system is installed to pre-heat the driver and driven gases to an initial temperature of $410K$, the shock tube will be capable of accessing a maximum test temperature of $1353K$. Although this is still below the target test temperature of $1500K$, it was deemed high

enough for the shock tube to be a valuable and useful research apparatus. A further increase in test temperature, beyond the target of $1500K$, could be obtained by operating the shock tube at a driven gas pressure below $0.6bar$. This would necessitate the design of a vacuum system for rarefying the driven gas. The obvious solution is to incorporate the vacuum system into the future development of the fuel mixture preparation system. The potential testing capability of the shock tube is summarised in Table 6.7.

Table 6.7: Maximum testing capability of the shock tube

Parameter	*Tested range*	*Potential ability*
Driven gas pressure, p_1 $[bar]$	1.01	0.60
Driver gas pressure, p_4 $[bar]$	200	200
Driven gas temperature, T_1 $[K]$	295	410
Driver gas temperature, T_4 $[K]$	295	410
Test pressure, p_5 $[bar]$	27.1	20.0
Test temperature, T_5 $[K]$	973	1518
Test duration, Δt $[ms]$	1.3	0.9

6.4.2 Performance of the rapid opening valve

Figure 6.13 shows the valve opening time as a function of driver pressure as calculated by the experimentally validated valve performance model. The other initial conditions were set at p_1 $1bar$ and T_1 T_4 $300K$. Note that for all driver pressures higher than $50bar$ the opening time is under $1.0ms$.

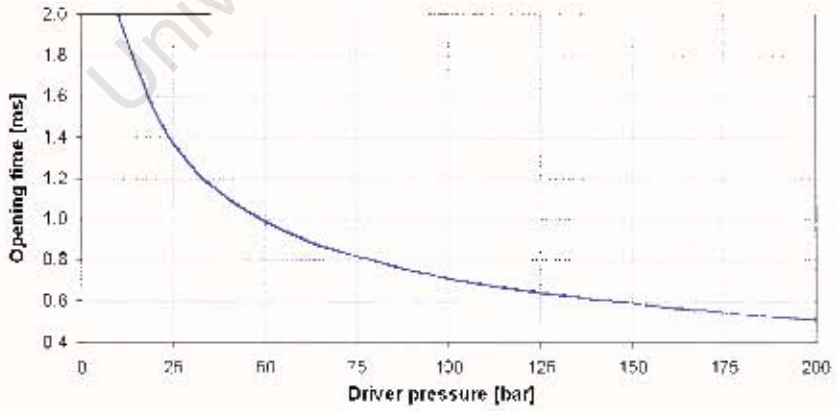

Figure 6.13: Calculated valve opening time as a function of driver pressure

6.4.3 Autoignition experiment

To prove that the shock tube was capable of performing useful autoignition experiments, a final test was conducted using a fuel-air mixture as the driven gas. In the absence of a dedicated mixture preparation system, the test procedure was as follows:

1. Set the rapid opening valve to the closed position. Note this requires at least partial charging of the driver tube.
2. Remove the pressure transducer in the endwall of the driven tube and inject precisely the mass of fuel required to achieve a stoichiometric air-fuel ratio within the driven tube.
3. Replace the pressure transducer and leave the apparatus overnight so that the fuel has time to evaporate and diffuse throughout the driven tube.
4. Charge the driver tube and ready the data capture system.
5. Operate the shock tube by triggering the rapid opening valve.
6. Safely discharge the shock tube.
7. Examine the recorded pressure traces for evidence of autoignition.

The initial conditions at which the test was performed are given in Table 6.8. The fuel tested was n-heptane, as it readily evaporates at room temperature. $1.38cm^3$ of n-heptane was injected into the driven tube; precisely the amount required to give a stoichiometric air-fuel ratio when mixed completely with the driven gas.

Table 6.8: Initial conditions for the autoignition experiment

Fuel tested	n-heptane
Fuel-air equivalence ratio, $\phi \pm 0.05$	1
Driven gas pressure, $p_1 \pm 0.01$ $[bar]$	1.01
Driver gas pressure, $p_4 \pm 1$ $[bar]$	195
Driven gas temperature, $T_1 \pm 5$ $[K]$	295
Driver gas temperature, $T_4 \pm 5$ $[K]$	295

The recorded driven tube pressure traces are shown in Figure 6.14. The onset of autoignition is clearly evident. The Mach number of the incident shock wave was measured and used to determine the test temperature and pressure. The results of the test are summarised in Table 6.9.

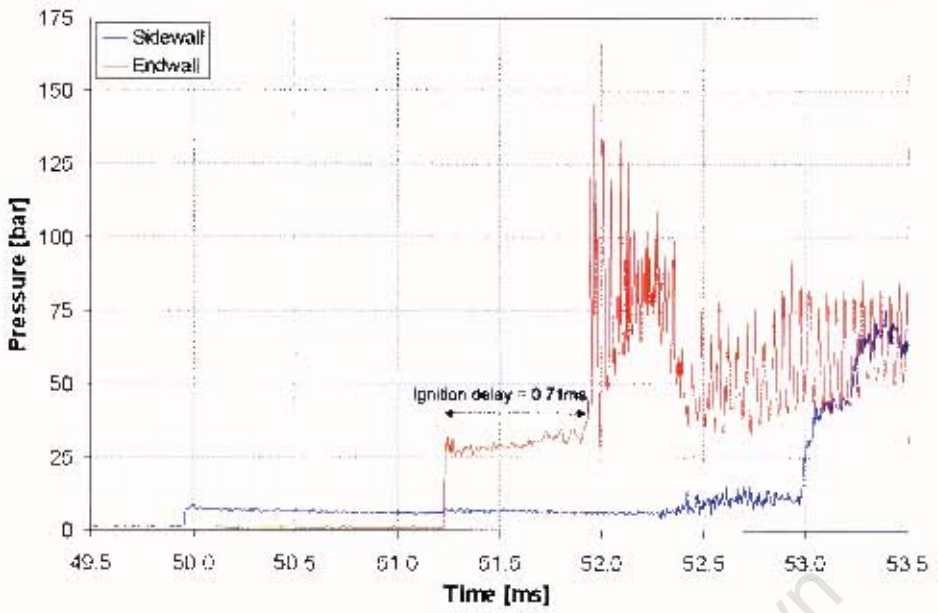

Figure 6.14: Driven tube pressure traces for the autoignition experiment

Table 6.9: Results of the autoignition experiment

Incident shock Mach number, M_s	2.34
Test pressure, p_5 $[bar]$	25.5
Test temperature, T_5 $[K]$	881
Ignition delay, $[ms]$	0.71

The measured ignition delay of $0.71ms$ was shorter than expected. To investigate the accuracy of the result, a chemical kinetic simulation of the test was run using CHEMKIN® software to solve the mechanism developed by Westbrook et al [36]. The simulation predicted an ignition delay of $1.07ms$. The most likely explanation for this discrepancy was that the fuel was not given sufficient time to diffuse completely and evenly throughout the driven gas, resulting in a rich air-fuel ratio at the test section. This explanation was supported by further CHEMKIN simulations, which indicated that a $0.71ms$ ignition delay corresponds to a fuel rich equivalence ratio of $\phi = 1.5$. The test result gave strong evidence of the potential of the of the shock tube as a useful autoignition research apparatus, whilst highlighting the need for a dedicated fuel mixture preparation system to be developed.

7 Concluding remarks

A potentially automatable shock tube facility suitable for high temperature autoignition research was designed, installed and commissioned. The shock tube was capable of establishing useful test conditions with high reproducibility. Upon completion of commissioning, starting with both the driver and driven gases at ambient temperature and the driven gas at atmospheric pressure, it was capable of accessing a maximum test temperature of $973K$ for a duration of $1.3ms$. It was shown that, by incorporating initial pre-heating and driven gas rarefaction in future developments to the facility, a maximum test temperature of over $1500K$ is potentially attainable.

The shock tube used compressed air as the driver gas. A high pressure compressor and reservoir system was installed to supply the compressed air. This setup gave the advantage that, excluding the running costs of the compressor, the supply of driver gas was free, unlimited and non-toxic. The disadvantage was that the shock tube had to operate at significantly higher driver pressures than would have been necessary if a lighter gas, such as Helium, was used.

The specially developed rapid opening sleeve valve was a novel feature of the shock tube facility. It effectively replaced the function of a diaphragm. The valve was a significantly improved version of the two-stage, piston actuated concept of Oguchi *et al* [20]. A model for assessing the performance of the valve was developed and validated with experimental data. It indicated that extremely short opening times, in the region of $0.5ms$, were attained. The short opening time combined with the sculpting and streamlining of the flow path through the valve, between the driver and driven tubes, helped maximise the efficiency of the shock tube. Control of the valve operation could easily be automated and, compared to conventional shock tubes, the test turn around time was reduced by the period required to replace a diaphragm. By the end of the commissioning process, reliable and consistent operation of the valve had been attained.

8 Recommendations

The developed shock tube was essentially a working prototype, and as such, several areas where improvements could be made had been identified upon completion of commissioning. Additionally, the incorporation of automation, thermal control and fuel preparation, supply and purging systems were beyond the scope of this project and should be undertaken in future projects. Note that the provisions made to facilitate the integration of these systems are described in Section 5.3. The recommendations for further development and improvement of the facility are as follows:

- Incorporate an air-fuel mixture preparation and supply system with the shock tube. The system must ensure accurate air-fuel ratio metering and complete, homogeneous vaporisation of the mixture. It must also perform the function of purging the combusted test gas after each test. Consider integrating the fuel system with a vacuum system to rarefy the driven gas, as this will enable test temperatures in excess of $1500K$ to be accessed.

- Incorporate a system for controlling the initial driver and driven gas temperature. The system must be capable of uniformly raising the gas temperature to $410K$, and should make use of the water cooling jacket which was purposely designed to ensure thermal isolation of the rapid opening sleeve valve.

- Use computer control to automate the operation of the facility in order to both reduce the risk of human error and convenience the repetitive nature of fuel characterisation experimentation.

- Couple a large inertial mass to the end of the driven tube to reduce the mechanical vibration noise seen on the endwall pressure trace. Also consider modifying the endwall of the driven tube to the plug design described by Tranter et al [8], as this may eliminate gasket issues and improve the quality of the reflected shock pressure trace.

- Consider further polishing the inside of the driver and driven tubes to improve the efficiency of the shock tube. A preferable alternative would be to chrome plate the tubes internally, as doing so would prevent a deterioration in surface finish due to corrosion.

- Consider mounting additional pressure transducers along the length of the driven tube so that the rate of shock wave attenuation can be measured. This will enable a more accurate calculation of the speed of the shock at the instant it reaches the endwall, which will in turn lead to a more accurate determination of test temperature.

- Investigate to what extent the volume of the driver tube can be reduced without adversely affecting either the operation of the rapid opening valve or the test conditions. Given the time and energy required to compress the driver gas, a reduction in driver volume would be desirable.

- Although every effort was made to ensure high levels of safety, the dangers associated with the high pressure equipment warrant the extra precaution of having the facility independently evaluated by an appropriately qualified, experienced professional engineer, particularly with regard to the long term fatigue life of the pressure containing vessels and the safety of the high pressure pneumatic circuits/systems. It is also important that a thorough risk assessment be performed and documented prior to making any modifications to the facility.

References

[1] P. Vieille. Sur les discontinuites produites par la detente brusque de gas comprimes. *Comptes Rendus de L'Academic des Sciences*, 129:1228, 1899.

[2] Glass, I.I. and Hall, J. Handbook of Supersonic Aerodynamics; Section 18: Shock Tubes. In *Navord Report 1488*, volume 6, 1959.

[3] W. Payman, W.C.F. Sheperd, et al. Explosion waves and shock waves, Part VI: The disturbance produced by bursting diaphragms with compressed air. In *Proc. Roy. Soc.*, volume A186, pages 243–321, 1946.

[4] G.N. Patterson. Theory of the shock tube. *NOL Memorandum 9903*, 1948. White Oak, Md: Naval Ordnance Laboratory.

[5] G.T. Reynolds. A preliminary study of plane shock waves formed by bursting diaphragms in a tube. OSRD No. 1519. Washington Office of Scientific Research and Development, 1943.

[6] Nishida, M. *Chapter 4.1: Shock Tubes and Tunnels.* In: Ben-Dor, G. and Igra, O. and Elperin, T. *Handbook of Shock Waves*, volume 1: Theoretical, Experimental and Numerical Techniques. Academic Press, 2001. Pages: 553 – 585.

[7] Nishida, M. *Chapter 4.1: Shock Tubes and Tunnels.* In: Ben-Dor, G. and Igra, O. and Elperin, T. *Handbook of Shock Waves*, volume 1: Theoretical, Experimental and Numerical Techniques. Academic Press, 2001. Page: 564.

[8] R.S. Tranter, K. Brezinsky, and D. Fulle. Design of a high-pressure single pulse shock tube for chemical kinetic investigations. *Review of Scientific Instruments*, 72:3046–3054, 2001.

[9] Ben-Dor, G. and Igra, O. and Elperin, T. *Handbook of Shock Waves*, volume 1: Theoretical, Experimental and Numerical Techniques. Academic Press, 2001.

[10] B.W Skews, O.E. Kosing, and R.J. Hattingh. Use of a liquid shock tube as a device for the study of material deformation under impulsive loading. In *Proc. Instn Mech. Engrs*, volume 218 Part C, pages 39–51, 2004.

[11] Glass, I.I. and Hall, J. Handbook of Supersonic Aerodynamics; Section 18: Shock Tubes. In *Navord Report 1488*, volume 6, 1959. Pages: 451 – 462.

[12] L.P. Lamprecht and M. Bevan. The safe use of shock-tube and detonating cord systems in shaft sinking: a global trend. *The Journal of The South African Institute of Mining and Metallurgy*, 1999.

[13] K.A. Bhaskaran and P. Roth. The shock tube as a wave reactor for kinetic studies and material systems. *Progress in Energy and Combustion Science*, 28:151–192, 2002.

[14] Heywood, J.B. *Internal Combustion Engine Fundamentals*. McGraw-Hill Companies, 1988. Pages: 450 – 478.

[15] Lifshitz, A. *Chapter 16.5: Ignition Delay Times*. In: Ben-Dor, G. and Igra, O. and Elperin, T. and Lifshitz, A. *Handbook of Shock Waves*, volume 3: Chemical Reactions in Shock Waves and Detonations. Academic Press, 2001. Pages: 211 – 256.

[16] S.S. Vasu, D.F. Davidson, and R.K. Hanson. Jet fuel ignition delay times: shock tube experiments over wide conditions and surrogate model predictions. *Combustion and Flame*, 152:125–143, 2008.

[17] E.L. Petersen. *A shock tube and diagnostics for chemistry measurements at elevated pressures with application to methane ignition*. PhD thesis, Stanford University, 1998. Page: 19.

[18] T.R. Simpson, C.J. Chandler and K.B. Bridgman. Effect on shock trajectory of the opening time of diaphragms in a shock tube. *Phys. Fluids*, 10:1894, 1967.

[19] O.E. Kosing, F.J. Barbosa, and B.W. Skews. A new, friction controlled, piston actuated diaphragmless shock tube driver. *Shock Waves*, 9:69–72, 1999.

[20] H. Oguchi, K. Funabiki, and S. Sato. An experiment on the interaction of shock wave with a multiple-orifice plate by means of a snap action shock tube. In *Proc. 10th Int. Shock Tube Symposium*, pages 386–391, 1975.

[21] Nishida, M. *Chapter 4.1: Shock Tubes and Tunnels*. In: Ben-Dor, G. and Igra, O. and Elperin, T. *Handbook of Shock Waves*, volume 1: Theoretical, Experimental and Numerical Techniques. Academic Press, 2001. Pages: 555 – 556.

[22] Nishida, M. *Chapter 4.1: Shock Tubes and Tunnels*. In: Ben-Dor, G. and Igra, O. and Elperin, T. *Handbook of Shock Waves*, volume 1: Theoretical, Experimental and Numerical Techniques. Academic Press, 2001. Pages: 567 – 568.

[23] Emanuel, G. *Chapter 3.1: Shock Waves in Gases*. In: Ben-Dor, G. and Igra, O. and Elperin, T. *Handbook of Shock Waves*, volume 1: Theoretical, Experimental and Numerical Techniques. Academic Press, 2001. Page: 235.

[24] Nishida, M. *Chapter 4.1: Shock Tubes and Tunnels*. In: Ben-Dor, G. and Igra, O. and Elperin, T. *Handbook of Shock Waves*, volume 1: Theoretical, Experimental and Numerical Techniques. Academic Press, 2001. Page: 581.

[25] E.L. Petersen. *A shock tube and diagnostics for chemistry measurements at elevated pressures with application to methane ignition.* PhD thesis, Stanford University, 1998. Pages: 25 – 33.

[26] E.L. Petersen and R.K. Hanson. Nonideal effects behind reflected shock waves in a high pressure shock tube. *Shock Waves*, 10:405–420, 2001.

[27] D.R. White. Influence of diaphragm opening time on shock tube flows. *J. Fluid Mech.*, 4:585, 1958.

[28] Emanuel, G. *Chapter 3.1: Shock Waves in Gases.* In: Ben-Dor, G. and Igra, O. and Elperin, T. *Handbook of Shock Waves*, volume 1: Theoretical, Experimental and Numerical Techniques. Academic Press, 2001. Page: 211.

[29] R.A. Alpher and D.R. White. Flow in shock tubes with area change at the diaphragm section. *J. Fluid Mech.*, 3:457–470, 1958.

[30] Glass, I.I. and Hall, J. Handbook of Supersonic Aerodynamics; Section 18: Shock Tubes. In *Navord Report 1488*, volume 6, 1959. Pages: 80 – 81.

[31] Nishida, M. *Chapter 4.1: Shock Tubes and Tunnels.* In: Ben-Dor, G. and Igra, O. and Elperin, T. *Handbook of Shock Waves*, volume 1: Theoretical, Experimental and Numerical Techniques. Academic Press, 2001. Page: 572.

[32] Heywood, J.B. *Internal Combustion Engine Fundamentals.* McGraw-Hill Companies, 1988. Page: 915.

[33] Conversation held with members of the Flow Research Unit of the University of the Witwatersrand. Discussion regarding shock tube design, Date 06/06/2008.

[34] Vessels under pressure regulations, 1996. Government notice R:1591, 1996.

[35] Rules for construction of pressure vessels. ASME boiler and pressure vessel code Section VIII Division 1, 2004.

[36] C.K. Westbrook, J. Warnatz, and W.J. Pitz. A detailed chemical kinetic reaction mechanism for the oxidation of iso-octane and n-heptane over an extended temperature range and its application to analysis of engine knock. *Twenty-second symposium (Int.) on combustion, The Combustion Institute*, pages 893–901, 1988.

[37] J.E. Shigley, C.R. Mischke, and R.G. Budynas. *Mechanical Engineering Design.* McGraw-Hill Companies, 7th edition, 2004. Chapter 8.

Appendices

A Subsystem design and maintenance

Contents

Figures

A.1 Overview

In order to give the shock tube functionality, several subsystems were integrated with it: the compressed air reservoir provides the supply of high pressure driver gas, the pneumatic circuit controls the operation of rapid opening valve and the pressurisation of the shock tube, and the data capture system records the test results. This appendix details the design and maintenance of these subsystems. Procedures for operating the shock tube via the subsystems are contained in Appendix C.

A.2 The compressed air reservoir

A.2.1 Design details

A detailed schematic of the compressed air reservoir is shown in Figure A.1. It comprises a three-stage high pressure SCUBA compressor connected in parallel to a bank of three $50l$ gas bottles. Thus the system can be configured to have a capacity of either 50, 100 or $150l$. The maximum pressure rating of the reservoir is $208bar$. A gauge indicates the reservoir pressure, and a relief valve prevents over-pressurisation. The compressor pumps air to $200bar$ at a rate of $1.1l/min$. Each shock tube experiment requires about $20l$ of air at the driver pressure. Therefore each test at a driver pressure of $200bar$ corresponds to about $20min$ of compressor operation.

The compressor is a $L\&W225$ purchased from Orca Industries. It has a built in pressure relief valve which limits the maximum pressure it can supply to $240bar$. The manufacturer's manual contains detailed operating and maintenance instructions and must be read by the operator. Note that the following modifications were made to automate the operation of the compressor:

- The compressor was fitted with an adjustable pressure switch which automatically turns it on when the reservoir pressure drops below $190bar$, and then turns it off when the pressure reaches $205bar$.
- Timer controlled solenoids were fitted to the condensate drains to automate their operation.
- The manufacturer's tank filling valve was removed and the outlet from the compressor was plumbed directly into the reservoir manifold.

The gas bottles were sourced from a compressed natural gas storage facility. To ensure their integrity, they were visually inspected, hydrostatically pressure tested and

re-certified to a test pressure of $358bar$ and an operating pressure of $208bar$ by an accredited authority. The test certificate is contained in Appendix F. The rating of the gas bottles was the limiting factor which determined the maximum reservoir pressure - all other pneumatic fittings were rated for operation at pressures at or above $250bar$.

A.2.2 Maintenance

The manufacturer's manual contains a schedule for maintaining the compressor. It specifies maintenance tasks according to hours of operation . To facilitate adherence to this schedule, the compressor was fitted with an hour counter. Take particular note of the sump oil, air filter cartridge, and air inlet filter replacement intervals. Spares for these consumables were purchased and kept in store. If additional spares are required, or for service support, contact Orca Industries. The high pressure gas bottles must be periodically inspected, pressure tested and re-certified by an approved authority. The company Executive Safety Services provides this service. Control the connections between all pneumatic fittings and check for correct functioning of the pressure relief valve regularly. For maximum safety it is recommended that the compressed air reservoir system be completely overhauled within five year intervals.

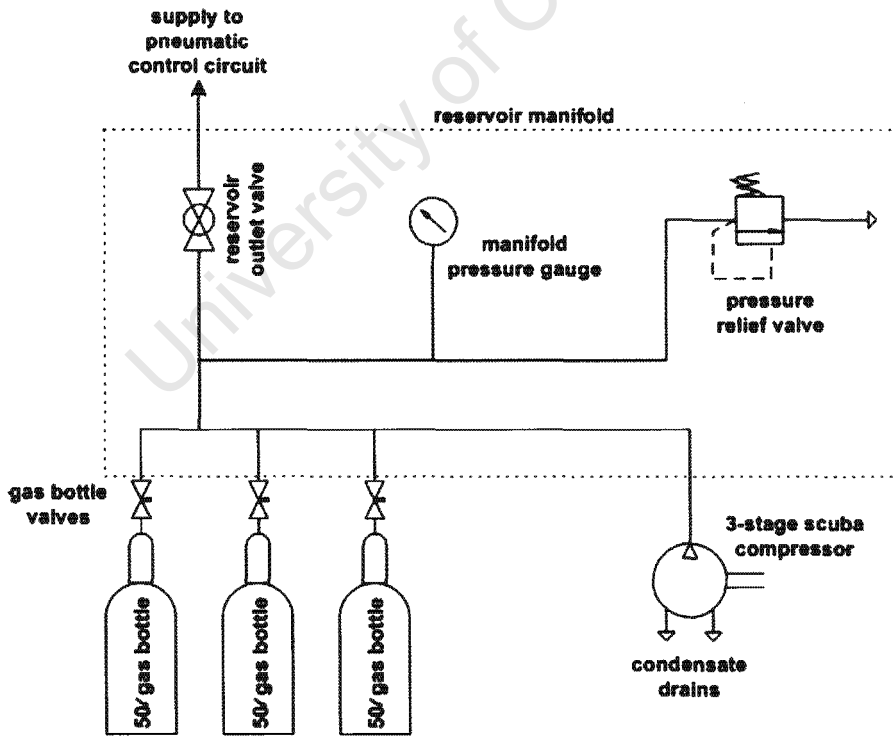

Figure A.1: Schematic of the compressed air reservoir system

A.3 The pneumatic control circuit

A.3.1 Design details

The pneumatic circuit controls the following functions:

- Supply of compressed air from the reservoir to the shock tube.
- Operation of the rapid opening valve and therefore shock tube.
- Depressurisation of both the shock tube and compressed air reservoir manifold.

A detailed schematic of the system is shown in Figure A.2. The adjustable regulator limits the supply pressure from the compressed air reservoir, and the non-return valve prevents backflow to the reservoir. Gauge G1 indicates the trigger chamber pressure, gauge G2 indicates the actuating chamber and driver tube pressure, and gauge G3 indicates the driven tube pressure. The length and flow rating of the lines connected to the rapid opening valve are critical to its performance. The exhaust line was plumbed into a large extraction duct which has an outlet on the roof of the building.

The circuit was assembled from quality OEM high pressure pneumatic and air compatible hydraulic fittings. All pneumatic fittings were sourced from Swagelok, and all hydraulic fittings were supplied by Hyflo. All components have a rated operating pressure of at least $250bar$. The connections between the circuit and the shock tube were made with flexible high pressure hose to allow for recoil of the shock tube as it is triggered.

A.3.2 Maintenance

Prior to operation, ensure that all connections are secure, all line clamps are in place and that no bends in the flexible hydraulic hose violate the minimum bend radius of $180mm$. In the event of a leak, immediately replace the faulty component. Do not interchange the components of the circuit - always make sure to connect a component to the same mating part. Prior to assembling a connection, ensure it is clean and the threads undamaged . The components of the pneumatic circuit have a recommended service life of five years, hence overhaul the system within this interval.

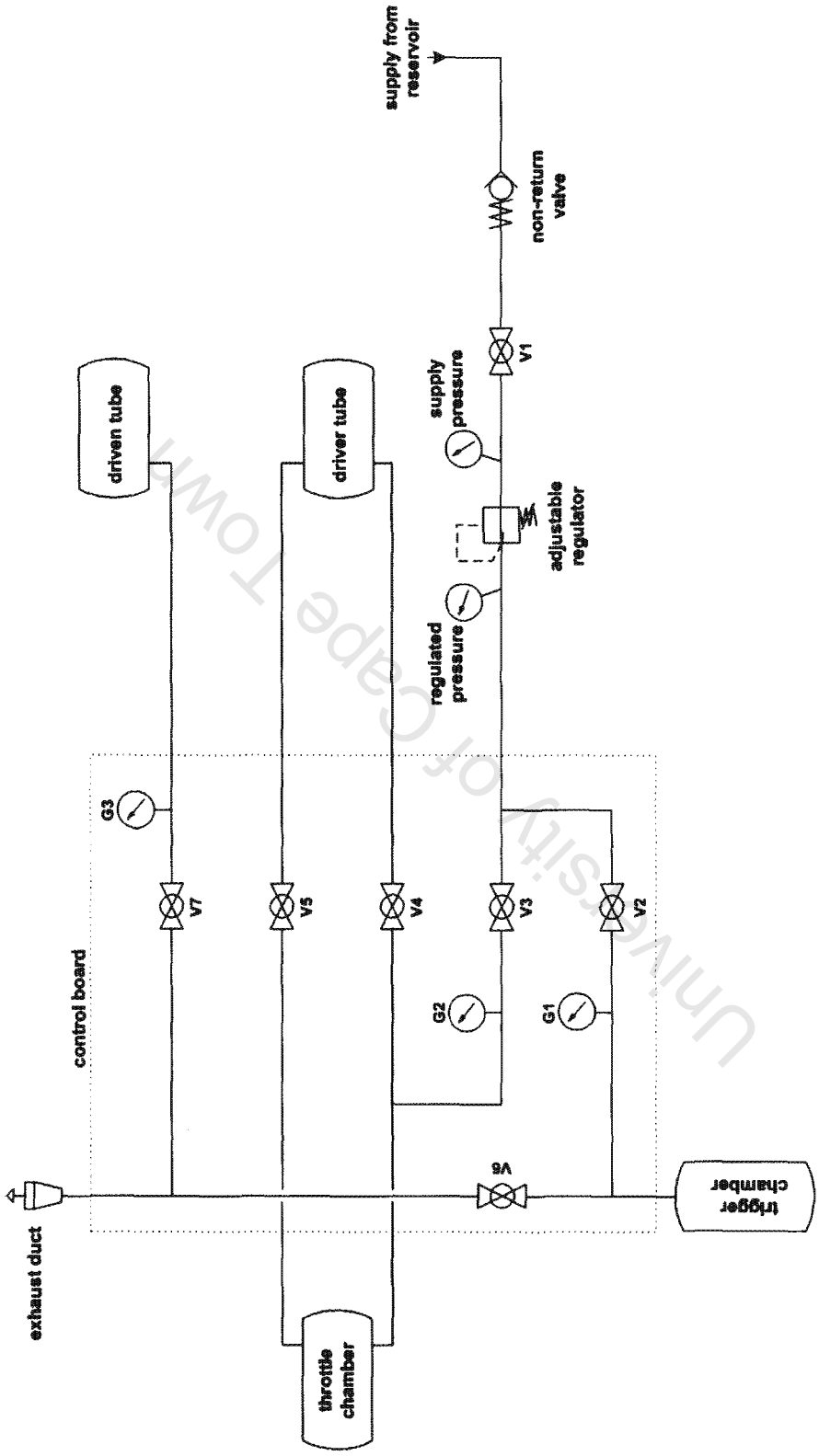

Figure A.2: Schematic of the pneumatic control circuit

A.4 The data capture system

A.4.1 Design details

The primary purpose of the data capture system was to record the propagation of the shock wave along the driven tube. Accurate determination of the incident shock velocity was necessary for calculation of the post shock thermodynamic state. A secondary purpose was to record the pressure in the actuating chamber during a test so that the operation of the rapid opening valve could be verified.

A schematic of the system is shown in Figure A.3. Two high frequency, charge output piezoelectric pressure transducers (Kistler type $603B1$) were mounted in the driven tube - one was located in the sidewall of the tube exactly $1m$ from the endwall, and the other was located in the endwall itself. Both sensors were flush mounted to ensure accurate measurement of the shock rise time. A third, similar transducer (Kistler type $601B1$) was mounted in an air passageway which directly accessed the actuating chamber.

The output from each transducer was connected by a short, low noise signal cable to a charge amplifier (Kistler type $5015A$). The amplifiers output a voltage signal directly proportional to the measured pressure. The voltage signals were connected to the data capture computer, which was equipped with a high speed data card and programmed with a LabVIEW® user interface for controlling the data acquisition. The system is capable of simultaneously sampling each channel at $200kHz$, giving a time resolution of $5\mu s$ per sample, for a duration of $0.5s$. The LabVIEW program triggers sampling from the instant a selected channel crosses a chosen threshold voltage level.

A.4.2 Maintenance

The Kistler pressure transducers and charge amplifiers are valuable equipment. For service support or to repair/replace faulty components, contact the local Kistler agents, Inher SA. To prevent misuse, the operator must read and be familiar with the manufacturer's manuals. Take particular note of the sensor mounting instructions regarding tightening torque and the requirement to keep the cable connections perfectly dry. The sensors are mounted in adapters, a small brass washer forming the seal, and then the adapter is mounted in the shock tube, a special copper washer forming the seal. A supply of spare sealing washers was purchased and kept in store. The manufacturer's calibration sheets for the transducers are kept on file, however to ensure measurement accuracy they should be re-calibrated periodically. Always ensure the equipment is kept in a moisture free environment.

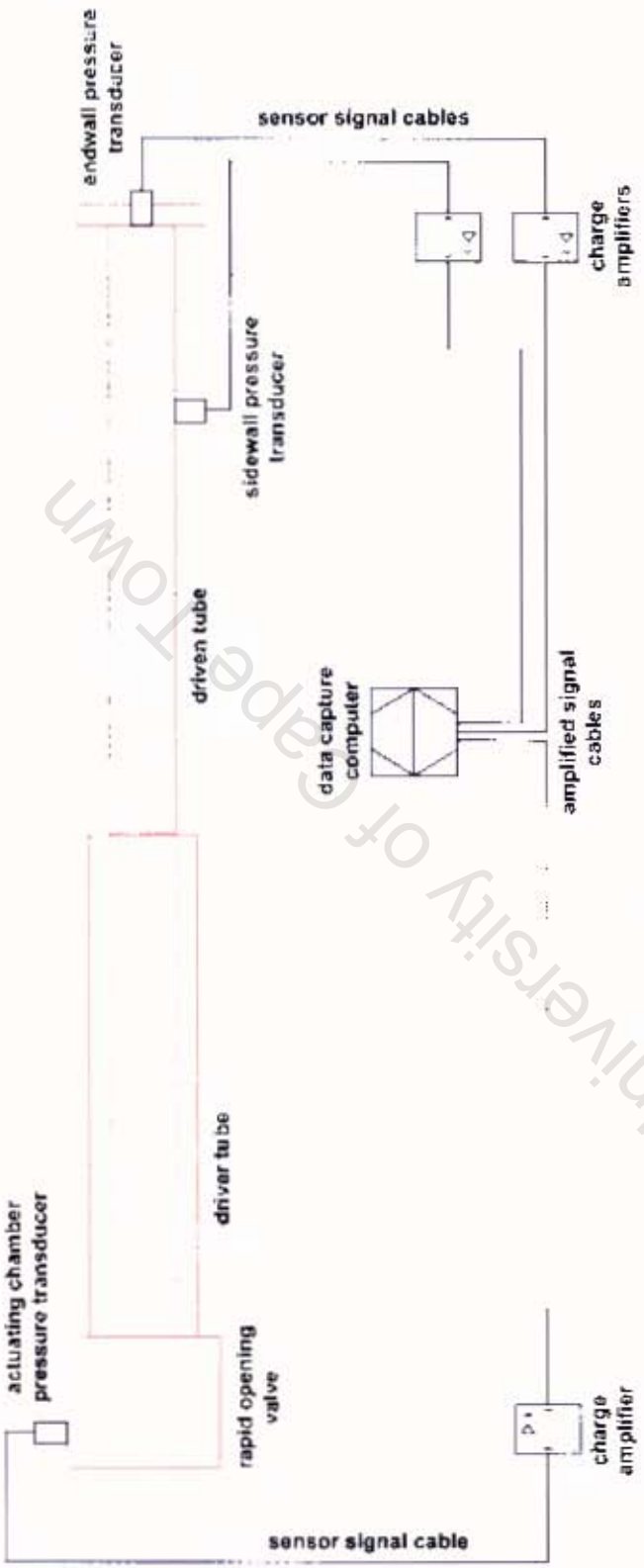

Figure A.3: Schematic of the data capture system

B Assembly, inspection and maintenance of the shock tube

Contents

Figures

B.1 Assembly instructions

B.1.1 General

A detailed assembly drawing of the basic shock tube apparatus (including the rapid opening sleeve valve) is contained in Appendix G. To ensure safe, correct operation, the shock tube must always be assembled according to the arrangement shown therein. Before assembly, inspect all components and replace/repair those which show signs of excessive wear/damage/corrosion. Additionally, all unpainted metallic surfaces must be thoroughly cleaned and then lubricated with a thin oil/grease (suggest $Q20$) in order to both protect against wear and corrosion and reduce friction between the sliding parts. Take great care when dismantling/transporting/assembling components of the apparatus to ensure that the functional surfaces are not damaged in any way. During assembly, never use excessive force - all components were designed and manufactured to fine tolerances and slide easily into place when correctly aligned.

B.1.2 O-ring seals

The shock tube assembly includes a number of o-ring seals. The placement and size of each o-ring is indicated in Figure B.1. During assembly, inspect each o-ring and replace those which are damaged. Coat all o-rings in a thin layer of rubber grease prior to fitting them in place. It is critical for the high temperature and fuel compatibility of the apparatus that Viton® o-rings are used throughout.

B.1.3 Bolt fastening

The shock tube assembly includes several structurally critical bolted flange connections. It is mandatory that these bolts are fastened to the correct torque as indicated in Figure B.1. When either assembling or dismantling a flange connection, use the criss-cross tightening sequence to ensure proper seating and even loading of the joint. Property Class 8.8 high tensile steel bolts and nuts must be used throughout. Assemble each bolt with a true-hardened steel washer under both the bolt head and the nut. The bolts were designed to be re-usable, however it is good practice to replace them after a few re-assemblies. The nuts and washers must be replaced each time the joint is re-assembled for operation.

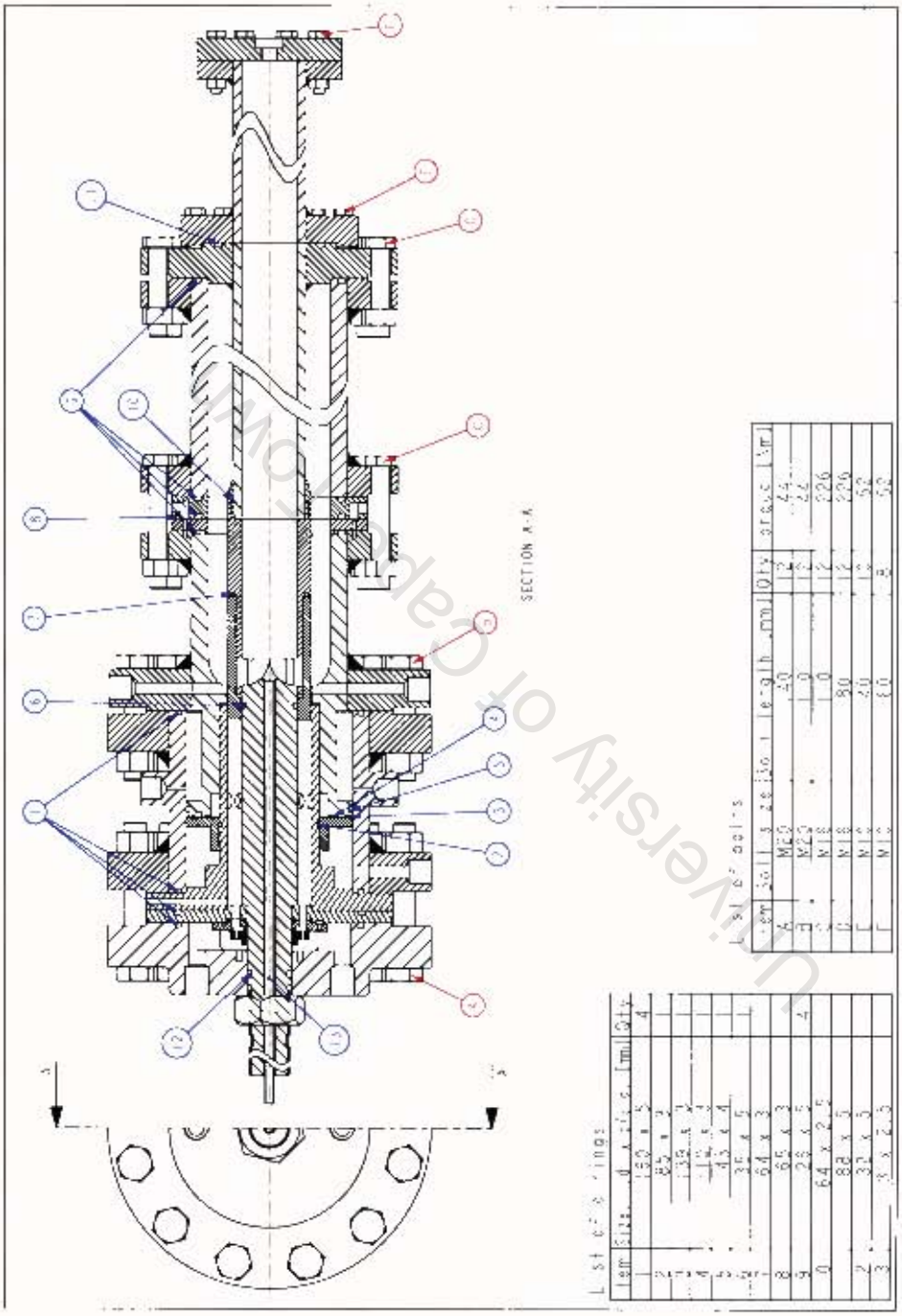

Figure B.1: Standard part specifications: o-rings and bolts

B.2 Inspection and maintenance of the shock tube

It is important that the shock tube apparatus be kept free of corrosion. To this end, it must be kept indoors in a dry environment and its exterior should be repainted when necessary. To establish the long term operational reliability of the shock tube, it should be completely dismantled and visually inspected for internal wear/damage/corrosion after each major round of testing. When this is undertaken, polish off any minor surface corrosion, replace/repair any damaged components and make a note of the maintenance work done. It is recommended that the pressure containing shell be professionally examined for cracks and defects, particularly at the welded flange joints, and hydrostatically pressure tested to $250bar$ after the first year of service and subsequently every two years. Also perform these examinations prior to re-commissioning the shock tube if it has not been used for a long period of time. For maximum safety, a conservative service life of 10 years is recommended, hence the shock tube should either be overhauled or de-commissioned by the year 2019.

C Operational procedures

Contents

C.1 Pre-test checks

The following checks must be completed prior to operating the shock tube or any of its subsystems:

- Ensure that the shock tube has been correctly assembled. In particular, all bolted flange joints must be fastened to the correct torque and all seals must be in place.
- Check that the shock tube is longitudinally aligned, horizontally level and securely fastened to the mounting frame, which must be resting stably on its floor mounts.
- Check that all pneumatic connections are in place and are secure.
- Check that all flexible hose lines are not sharply bent, twisted or damaged in any way.
- Ensure that all pressure transducers are securely in place.
- Check that all the signal cables from the pressure transducers to the data capture computer are connected, untwisted and have some slack to allow for recoil of the shock tube.
- The first test of the day should always be conducted at a low driver pressure ($\approx 10bar$), so that any leaks and/or malfunction can be identified and repaired prior to operating the shock tube at high pressure.
- It is recommended that the operator read through all the procedures herein before operating the shock tube. Doing so will clarify the interaction between the subsystems.
- Note that ear and eye protection must be worn by the operator and those in the immediate vicinity of the system.

C.2 Shock tube testing

The operation of the shock tube relies on the pressurisation of the driver and driven tubes and the action of the rapid opening valve. These functions are controlled by the pneumatic control circuit. With reference to Figure A.2, follow the steps listed below to conduct shock tube experiments.

1. First charge the compressed air reservoir according to the procedure described in Section C.3.
2. Close all valves V1 to V7 and completely unscrew the regulator so that it prevents flow.
3. Open the reservoir outlet valve.
4. Open valve V1 and set the regulator to the desired driver pressure.
5. Slowly open valve V2. This causes the ring piston to move forward and block the outlet from the actuating chamber. Wait until gauge G1 indicates complete pressurisation of the trigger chamber.
6. Slowly open valve V3. This causes the sliding sleeve to move forward and close off the flow ports between the driver and driven tubes. A metallic sound will be heard when the sleeve reaches the closed position.
7. Open valve V4 and then V5. This fills the driver tube and equalises the throttle chamber to the driver pressure.
8. Very slowly, and only partially, open valve V7. Ensure the driven tube is fully depressurised and there is no leakage flow into it.
9. Close valve V7 to seal off the driven tube exhaust line.
10. Monitor gauge G2 which indicates the driver pressure. Once the regulator pressure is reached, close valves V2 and V3 in sequence to isolate the shock tube from the air supply.
11. Fill the driven tube with the chosen test gas.
12. Note and record the initial test conditions: driver gas pressure and temperature, and driven gas pressure and temperature.
13. Operate the data capture system according to the procedure described in Section C.5.

14. Fire the rapid opening valve, and thereby shock tube, by quickly opening valve V6.

15. A few seconds after the shock tube is fired, close valve V6 and then open valve V2. This resets the ring piston and prevents the shock tube from discharging completely through the exhaust chamber.

16. Save the captured test data.

17. To perform another test at the same or higher driver pressure, close valves V5 and V4 in sequence, then repeat from step 6. If testing is complete, follow the remaining steps to depressurise the system.

18. Close valve V1 and V2.

19. Very slowly, and only partially, open valve V7 to depressurise the shock tube.

20. Open valve V6 to discharge the trigger chamber.

21. Slowly open Valve V2 and screw in the regulator to depressurise the supply line.

22. Slowly open valve V3 to ensure the driver tube and rapid opening valve are fully depressurised.

23. Close all valves V2 to V7 and unscrew the regulator to the blocked flow position.

24. Shut down the compressor and depressurise the reservoir manifold according to the procedure described in Section C.4.

C.3 Compressed air reservoir operation

With reference to Figure A.1, follow the steps listed below to operate the compressed air reservoir. In the event of a malfunction, immediately switch off the compressor, close the gas bottles and depressurise the system. It is again stressed that the operator must first be familiar with the compressor manufacturer's manual.

1. Check the compressor sump oil level.
2. Manually switch on the compressor room extraction fan.
3. Close the reservoir outlet valve. This shuts off the supply line leading to the shock tube.
4. Close all gas bottles.
5. Open the two manual condensate drain valves at the base of the compressor to ensure it is fully depressurised. **Once ensured, close both drain valves.**
6. Switch on the compressor and ensure the fan rotates in the correct direction.
7. Observe the reservoir manifold pressure gauge. After 20 to 30 seconds, the gauge will indicate a steady rise in pressure. Check that the compressor turns off when the pressure reaches approximately $205bar$.
8. Slowly open either one, two or all three gas bottles, depending on the desired reservoir capacity. As the pressure drops below $190bar$, the compressor will automatically switch on. Note that the automatic condensate drains were set to open for 10 seconds immediately as the compressor starts, and thereafter at approximately 10 minute intervals.
9. Leave the door of the compressor room open as the gas bottles are filled to ensure good ventilation.
10. During the filling process, monitor the system at approximately 10 minute intervals to check that the pressure is indeed rising and that the automatic condensate drains are functioning.
11. Check that the compressor switches off when the pressure reaches about $205bar$.
12. Perform the shock tube tests according to the procedure described in Section C.2.
13. Upon completion of the day's testing, shut down the compressor and depressurise the reservoir manifold according to the procedure described in Section C.4 below.

C.4 Compressed air reservoir shut down and depressurisation

1. Ensure the shock tube is depressurised, all valves V1 to V7 are closed and the regulator is completely unscrewed to the blocked position.
2. Switch off the compressor.
3. Close all the gas bottles.
4. Open, and leave open, the manual condensate drains to ensure depressurisation of the compressor.
5. Open the the reservoir outlet valve if it is not already open.
6. Open valves V6 and V2.
7. Open valve V1 and slowly screw in the regulator to depressurise the manifold.
8. Once depressurised, close all valves, including the reservoir outlet valve, and unscrew the regulator to the blocked position.

C.5 Set up of the data capture system

With reference to Figure A.3, follow the steps listed below to set up the data capture system to record the results of a shock tube test. Note that the charge amplifiers should be turned on and allowed to warm up for at least half an hour prior to testing. Also note that to save time during testing, the system can be preset up to step 9 before commencing the shock tube testing procedure.

1. Verify that the charge amplifiers and computer are switched on.
2. Verify that the charge amplifiers are set to the correct sensor sensitivity:

Sensor location	**Serial number**	**Manufacturer's calibration**
Sidewall	2067751	$-5.501pC/bar$
Endwall	2067752	$-5.559pC/bar$
Actuating chamber	$C193578$	$-16.25pC/bar$

3. Set the maximum output range of each charge amplifier to the same value. As a guide, the value should be about twice the driver pressure.
4. Check that the charge amplifiers are set to the 'DC long' and 'LP filter off' modes.
5. Note the sensitivity, in bar/V of the charge amplifier output as indicated on the amplifier screen.
6. On the computer, double click on the desktop icon entitled 'Shock Tube'. This opens the LabVIEW user interface.
7. Enter the sensitivity (bar/V) of the charge amplifier output.
8. Set up the data capture trigger. It is suggested that the system is set to trigger when the actuating chamber signal (channel $A2$) drops lower than $-1bar$.
9. Verify that the sample rate and duration are set to $200kHz$ and $0.5s$ respectively.
10. When ready to fire the shock tube, press the 'Meas' button on all amplifiers to activate their output signals. A green led on the amplifier front panel will light up.
11. Click the Capture button on the LabVIEW user interface. The data capture system is now ready, and will begin sampling as soon as the shock tube is fired and the trigger channel crosses the threshold voltage.

12. Remember to save the recorded data after each test. This is done by clicking the save button on the LabVIEW user interface.

13. After the days testing is complete, remember to switch off the amplifiers (switch is at the back panel) and shut down the computer.

D Operational safety assessment

Contents

D.1 Risk assessment

Throughout the development of the shock tube facility, ensuring a high level of safety was the priority. To minimise the operational hazards associated with the facility, a risk assessment was conducted. The following safety concerns were identified and addressed.

D.1.1 System over-pressurisation

The shock tube was rated to operate at a maximum driver pressure of $200bar$. To enable it to be quickly pressurised to this limit, the compressed air reservoir was designed to provide a slightly higher maximum supply pressure of $208bar$. The compressor was equipped with an automatic pressure switch which turns it off once this pressure is reached. A regulator between the reservoir and shock tube closes the supply line when the shock tube pressure reaches $200bar$. Over-pressurisation of either system beyond its upper limit would reduce the design safety factors guarding against their structural failure. Structural failure of these systems could cause a number of hazards. Ranging in severity from minor to extremely dangerous, they include: leaks, system malfunction, damage to equipment, high velocity gas jets and projectiles, and in the worst case bursting of the pressure containing vessels.

Potential modes of over-pressurisation of the compressed air reservoir that were identified included failure of the compressor to turn off at the upper pressure limit and overheating of the reservoir. The following measures were implemented to address these hazards:

- The reservoir was fitted with a pressure relief valve set to blow off if the pressure exceeded safe levels.
- The compressor was equipped with its own pressure relief valve for redundancy.
- The compressor was fitted with a easily accessible manual shut down switch for turning it off should the automatic pressure switch malfunction. The reservoir pressure is indicated by a pressure gauge for monitoring purposes.
- The gas bottles in which the compressed air is stored were inspected, hydrostatically pressure tested and re-certified to a test pressure of $358bar$ and an operating pressure of $208bar$ at room temperature by an accredited authority prior to their installation. The test certificate is contained in Appendix F.

- Instructions for depressurising the reservoir manifold were included in the operating procedure lists.
- The reservoir was installed in an uninhabited, brick wall enclosed room to minimise the consequences of a structural failure.
- The enclosed room is ventilated by an extraction fan to prevent overheating. Mandatory operation of the fan is included in the operating instructions for the system.

Potential modes of over-pressurisation of the shock tube that were identified included failure or incorrect operation of the pressure regulator, and overheating of the shock tube. The following measures were implemented to address these hazards:

- The assembled shock tube was hydrostatically pressure tested to $250bar$ to ensure its structural integrity if the regulator failed and it was subjected to the maximum reservoir pressure of $208bar$. The test certificate is contained in Appendix F.
- The pressure in all sections of the shock tube is indicated by pressure gauges. If the pressure regulator failed to close the supply line when the maximum pressure was reached, a manually operated valve for doing so was provided.
- Instructions for a) operating the regulator and b) depressurising the shock tube were included in the operating procedure lists.
- Recommendation was made that if any modifications are to be made to the facility, such as the installation of a heating system, a thorough risk assessment must first be conducted and documented.

D.1.2 Missassembly of the shock tube

The shock tube comprises three main elements: the driven tube, the driver tube and the rapid opening valve. These elements are assembled together by means of o-ring sealed, bolted flange joints. Additionally, the rapid opening valve is itself assembled from a number of individual parts. Missassembly of the apparatus could result in:

- Malfunction of the rapid opening valve.
- Structural failure and the associated hazards described in Section D.1.1.

Potential modes of failure include missassembly due to incorrect arrangement of components, misalignment of components, left out components, damage caused by forced assembly, use of unsuitable standard components (e.g. wrong size bolts or o-rings), under/over tightened bolts and incorrect lubrication. The following measures were implemented to address these hazards:

- Assembly instructions were compiled.
- Mandatory control of bolt torque was included in the assembly instructions.
- All standard components were specified in the assembly instructions.

D.1.3 High pressure pneumatic circuitry

The shock tube is operated by a high pressure pneumatic circuit which controls the following functions:

- Supply of compressed air from the reservoir to the shock tube.
- Action of the rapid opening valve.
- Discharge of the shock tube and reservoir manifold.

Incorrect operation of this system could damage the shock tube or cause it to malfunction. In addition, breakage of any of the components of the pneumatic circuit could cause dangerous safety hazards such as high velocity gas jets and projectiles, loud noises and lashing pressure hoses.

Potential modes of failure include the use of defective components, missassembly of the components, over-pressurisation of the system, incorrect operation of the system and relative motion between the circuit and shock tube due to shock tube recoil. The following measures were implemented to address these potential safety hazards:

- All pneumatic fittings were purchased new from reputable OEM suppliers, and were rated for safe operation at the conditions to which they would be exposed during normal shock tube operation.
- All pneumatic fittings were assembled strictly according to the manufacturers' recommendations.
- Pressure gauges were included in the circuit so that the pressure in all separated sections could be independently monitored.

- Flexible hose was used to make all connections between the pneumatic circuit and the shock tube to allow for relative motion.
- Wherever practical, pressure hoses and tubes were securely clamped down.
- Operation and maintenance instructions for the system were compiled.
- Mandatory use of eye and ear protection was included in the operating procedures.

D.1.4 Malfunction of the rapid opening valve

The rapid opening valve controls the flow between the driver and driven tubes. It is operated pneumatically by the compressed driver gas. Malfunction of valve could damage its internal components, make the shock tube perform poorly or make it completely inoperable, and trap compressed air within the shock tube.

Potential modes of failure include malfunction due to worn or damaged valve components, broken seals, missassembly of the valve and incorrect valve operation. The following measures were implemented to address these potential hazards:

- All separate chambers of the shock tube were connected to a discharge line to enable complete depressurisation in any valve configuration.
- Pressure gauges connected to the various chambers indicate leakage past seals.
- All the valve's moving parts are contained internally and therefore do not endanger the operator.
- Assembly, operation and maintenance procedures were compiled.

E Pressure vessel design calculations

Contents

Figures

Tables

E.1 Introduction

The pressure containing shell of the shock tube consisted of three main vessels: the outer cylinder of the rapid opening valve, the driver tube and the driven tube extension. Each vessel was constructed from a section of hydraulic cylinder tube and two boilerplate steel flanges - one welded at each end of the tube. The vessels were joined by bolting together the mating flanges. The shell was designed for a maximum internal operating pressure of $200bar$. South African law regulates the manufacture of pressure vessels that have a nominal internal diameter over $150mm$ [34], hence the components of the shell, which all had internal diameters under $150mm$, were not subject to this legislation. However, during the design phase careful consideration was given to the fact that during operation the vessels would contain very high pressure gas, which is inherently dangerous, and would undergo cyclic pressurisation, making them susceptible to fatigue.

To illustrate the method by which these vessels were designed, the calculations involved in the design of the driver tube are described in this appendix. Reference is made to Figure E.1, which shows the elements of the driver tube vessel.

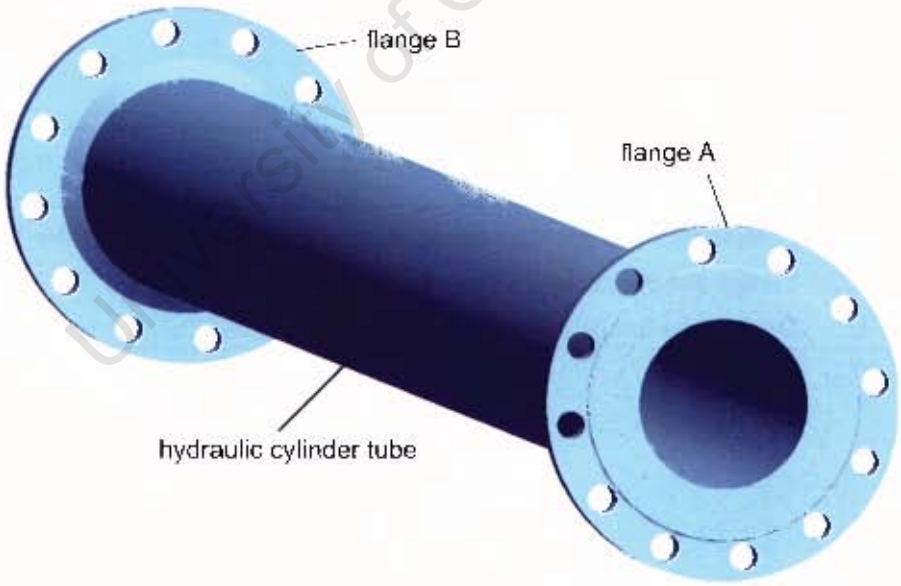

Figure E.1: Driver tube pressure containing vessel

E.2 Pressure containing tube

The basic element of the vessel was a single length of thick walled seamless $ST52$-3 hydraulic tube, of the type commonly used in the construction of large, high pressure hydraulic cylinders. $ST52$-3 steel has a minimum yield strength of $355MPa$. The tube was purchased new from the hydraulic supplies company HYFLO SA (Pty) Ltd. Table E.1 lists the dimensions and manufacturer specified pressure rating of the tube section. Note that the tube was rated for pressures well above $200bar$.

Table E.1: Dimensions and pressure rating of the pressure containing tube

Length [mm]	2760
Internal diameter [mm]	110
Wall thickness [mm]	15
Pressure rating [bar]	520

E.3 Flange design

Figure E.2 shows a schematic of the driver tube flange attachments. The flanges were machined from $ASTM\ A516\ Gr70$ boilerplate steel, which is a commonly used flange metal due to its excellent weldability and stringently controlled mechanical strength properties. It has a minimum yield strength of $262Mpa$. Sealing between each pair of adjoining flanges was by means of a Viton® o-ring.

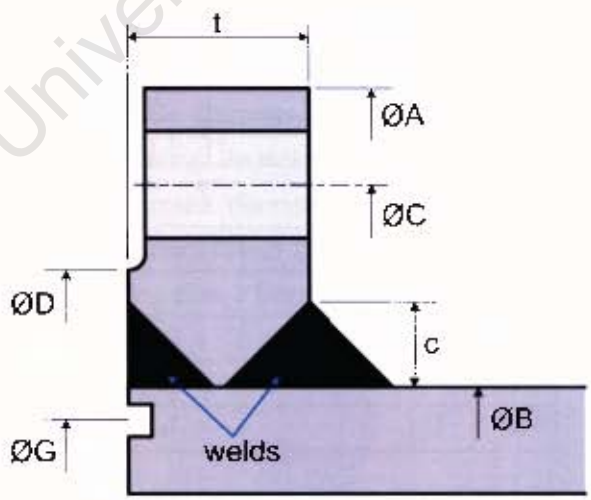

Figure E.2: Driver tube flange schematic

E.3.1 Flange bolting

Adjoining flanges were bolted together using Property Class 8.8 high tensile steel bolts preloaded to 75% of their proof strength. For each joint, the size of the bolts and the number of bolts to use were calculated according to the method for designing fatigue loaded tension joints with preload as detailed in [37]. The method specifies formulae for calculating the following safety factors:

- The bolt load factor, n, defined as the multiple of the tensile load on the joint that would cause bolt yielding.
- The safety factor guarding against fatigue failure, n_f, defined as the ratio of the alternating load strength to the alternating stress in the bolt.
- The safety factor guarding against joint separation, n_0, defined as the ratio of the tensile load which would cause joint separation to the tensile load on the joint.

The results of the flange bolting design calculations are summarised in Table E.2 below.

Table E.2: Flange bolting design

Flange joint	***A***	***B***
Tensile load on joint [kN]	270	270
Bolt size	$M16$	$M16$
Number of bolts	12	12
Bolt grip length [mm]	84	54
Preload torque [Nm]	226	226
n	7.3	5.3
n_f	5.0	3.6
n_0	3.7	3.9

E.3.2 Flange size and welding

The flanges at each end of the driver tube were identical. They were designed using the ASME Boiler and Pressure Vessel Design Code [35] as a guide. Note that safeguard against fatigue failure is intrinsically built into the code. The flanges were double bevel butt welded onto the tube ends (see Figure E.2). To ensure good weld penetration, the flanges were weld prepared by machining large 45^o bevels to a narrow root at the inside diameter. All welding was done by certified welders, and was subsequently stress relieved by heat treatment and tested for cracks using the magnetic particle inspection (MPI) technique. The ASME code specifies maximum safe limits, in terms of the material strength value S_f, for the hub stress, S_H, radial stress, S_R, and tangential stress, S_T, in the welded flange as calculated by formulas specified in the code. The stress limits are as follows:

$$S_H \leq 1.5 S_f$$

$$S_R \leq S_f \quad and \quad (S_H + S_R)/2 \leq S_f$$

$$S_T \leq S_f \quad and \quad (S_H + S_T)/2 \leq S_f$$

For $ASTM\ A516\ Gr70$ boilerplate, $S_f = 138MPa$. The results of the flange design calculations are summarised in Table E.3.

Table E.3: Driver tube flange design

Flange outside diameter, A [mm]	230
Bolt circle diameter, C [mm]	200
Raise face diameter, D [mm]	176
O-ring mean diameter, G [mm]	131
Flange inside diameter, B [mm]	140
Flange thickness, t [mm]	27
Weld leg size, c [mm]	12.5
S_H [MPa]	133
S_R [MPa]	120
S_T [MPa]	65

E.3.3 Finite element analysis of the vessel

To double check that safe stress limits would not be exceeded upon pressurisation of the vessel, a basic analysis of the stresses in the vessel at the maximum rated internal pressure of $200bar$ was carried out using the Abaqus finite element analysis (FEA) software package. The analysis accounted for the internal pressure on the vessel and the external tensile load (due to the internal pressure) on the flange attachments. Figure E.3 illustrates the von Mises stress profile through a cross section of the vessel at the critical flange attachments. As shown, the maximum stress through the section did not exceed $120MPa$, which is below the safe upper stress limit of $138MPa$ specified for the flange metal in the ASME code.

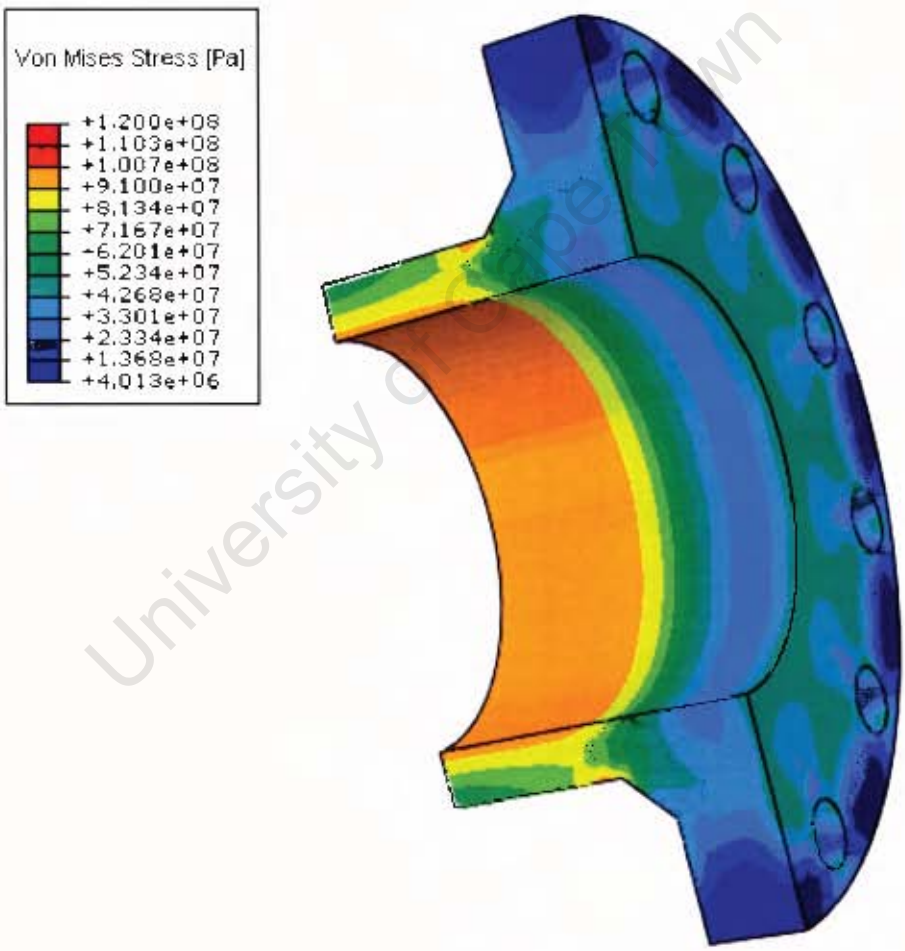

Figure E.3: Stress profile through the flange cross section

F Hydrostatic pressure test and weld quality control certificates

Contents

F.1 Shock tube hydrostatic pressure test certificate

UCT
SHOCK TUBE APPARATUS

HYDRAULIC SYSTEM PRESSURE TEST CERTIFICATE No: 32523

NAME OF TEST COMPANY:	DATE OF TEST: 02 JULY 2009 TEST LOCATION: UCT CAMPUS
HYFLO Southern Africa (Pty) Ltd. Reg. 66/02231/07 PO Box 240, Paarden Eiland, 7420, South Africa 50 Neptune Street, Paarden Eiland Tel. (021) 514 3000 Fax. (021) 511-7877 VAT Reg.4330205479 E-mail: rcw@hyflo.co.za	INSPECTION APPROVAL: N/A
JOB No.: CT 32523	ORDER No.: N/A

SYSTEM DETAIL

DRAWING #: n/a	DESCRIPTION: Shock Tube Apparatus	MANUFACTURER: UCT
SYSTEM TYPE: CLOSED		HOSE USED: ½"
FITTING 1: 16S		FITTING 2: 16S

PRESSURE DETAILS

WORKING PRESSURE:	TEST PRESSURE:	TEST HOLD TIME	TEST FLUID
N/A	25 MPa	15 min.	WATER

TEST REPORT: ACCEPTED, NO LEAKS

TEST GAUGE DETAILS

SERIAL No.:	CALIBRATION DATE:	RECALL DATE:
TEST ENGINEER: RANDOLL WILLIAMS	GL APPROVAL: N/A	CUSTOMER : MICHAEL DOWNEY
SIGN:	STAMP:	SIGN:

HYFLO SOUTHERN AFRICA (PTY) LTD
CAPE TOWN BRANCH
PO. BOX 240
PAARDEN EILAND 7420
PHONE: (021) 514 3000
FAX: (021) 511 7677
VAT: 4330205479

F.2 Gas bottle inspection and hydrostatic pressure test certificate

Independent Pressure Test Station

Bros Park, 29 Scheckter Road
Killarney Gardens
7441
Tel/fax. 021 556 5741
www.ipts.co.za
ipts@telkomsa.net

TEST CERTIFICATE

JOB NO : 6378

DATE ISSUED 09/07/2009

PAGE 1 OF 1

CUSTOMER : U C T
CARE OF : EXECUTIVE SAFETY SERVICES
CONTACT No. : (021) 510 4726

DATE TESTED	CYLINDER ID. NUMBER	CYLINDER TYPE	FILLING MEDIUM	WATER CAPACITY	GIVEN TARE	GIVEN WP	MANUFACTURING SPEC	MANUFACTURING DATE	TEST PROC	EXTERNAL EXAM	INTERNAL EXAM	THREAD EXAM	ACTUAL TARE	TARE LOSS %	HYDRO TP	REMARKS
09/07/2009	97A184/011	50.0 Ltr fe	GAS	50.30 Ltr	69.10 kg	20800 kPa	BS5045/1	5/97	023	ACCEPT	ACCEPT	ACCEPT	69.00 kg	0%	35800 kPa	TEST PASSED
09/07/2009	97A184/018	50.0 Ltr fe	GAS	50.30 Ltr	69.00 kg	20800 kPa	BS5045/1	5/97	023	ACCEPT	ACCEPT	ACCEPT	69.00 kg	0%	35800 kPa	TEST PASSED
09/07/2009	97A184/018	50.0 Ltr fe	GAS	50.10 Ltr	68.60 kg	20800 kPa	BS5045/1	5/97	023	ACCEPT	ACCEPT	ACCEPT	68.65 kg	0%	35800 kPa	TEST PASSED
09/07/2009	97A184/010	50.0 Ltr fe	GAS	50.30 Ltr	69.10 kg	20800 kPa	BS5045/1	5/97	023	ACCEPT	ACCEPT	ACCEPT	69.10 kg	0%	35800 kPa	TEST PASSED
09/07/2009	97A184/015	50.0 Ltr fe	GAS	50.10 Ltr	68.70 kg	20800 kPa	BS5045/1	5/97	023	ACCEPT	ACCEPT	ACCEPT	68.65 kg	0%	35800 kPa	TEST PASSED
09/07/2009	97A184/012	50.0 Ltr fe	GAS	50.30 Ltr	68.80 kg	20800 kPa	BS5045/1	5/97	023	ACCEPT	ACCEPT	ACCEPT	68.75 kg	0%	35800 kPa	TEST PASSED
09/07/2009	97A184/013	50.0 Ltr fe	GAS	50.30 Ltr	69.10 kg	20800 kPa	BS5045/1	5/97	023	ACCEPT	ACCEPT	ACCEPT	69.05 kg	0%	35800 kPa	TEST PASSED
09/07/2009	97A184/014	50.0 Ltr fe	GAS	50.40 Ltr	69.00 kg	20800 kPa	BS5045/1	5/97	023	ACCEPT	ACCEPT	ACCEPT	68.85 kg	0%	35800 kPa	TEST PASSED
09/07/2009	97A184/017	50.0 Ltr fe	GAS	50.20 Ltr	68.70 kg	20800 kPa	BS5045/1	5/97	023	ACCEPT	ACCEPT	ACCEPT	68.80 kg	0%	35800 kPa	TEST PASSED

RECOMMENDED NEXT TEST DATE : #VALUE!

SANAS APPROVED SIGNATORY : J GARBER :

ONLY CYLINDERS PASSING THE ABOVE TESTS WILL BE STAMPED WITH THE IPTS MARK AND DATED / TERMS AND CONDITIONS APPLY AND WILL BE AVAILABLE ON REQUEST

These cylinders have been tested in accordance with SABS ISO 6406 and SABS 019, this certificate should be retained by the client as it may be required by a cylinder filler before refilling

sanas SANAS Accredited Facility

Company Reg. No. 2003/031949/07

Registered Stamp

F-6

F.3 Weld quality control certification

F.3.1 Hand over certificate

Allweld Marine & Industrial

2 Diesel Road, Ndabeni • PO Box 145, Howard Place, 7450 Cape Town, South Africa
Tel. +27 (0)21 511 7473 • Fax. +27 (0)21 511 9409 • Website. www.allweld.co.za • Email: info@allweld.co.za
Vat No: 4800172290 • CK No: 1998/000005/23

Hand Over Certificate

Client: Chevron			
Client's Order Number:	994793	**Description:**	Manufacture 5 x Spool Pieces.
Job Number:	17040		

Scope of Work

Spool Pieces As Per Drawing No: (STW001, STW002, STW003, STW004 & STW005)

- Cut all material and prep.
- Fit and tack material together.
- Fit-Up inspection and dimensional check prior to welding.
- Weld as per welding procedure AW017.
- Clean welding by means of grinding
- In-House MPI prior to PWHT.
- PWHT as per welding procedure AW017
- Machine gasket faces.
- 100% MPI after PWHT
- Final Inspection
- Release.

This is to certify that Allweld Marine and Industrial CC has completed the works or section/s thereof as detailed in the scope of work to the full satisfaction as per your requirement.

Client's Representative:	Allweld Representative: B. Franken
Signature	Signature: ALLWELD QC
Date:	Date: 03/04/2009

F.3.2 Welding procedure specifications

WELDING PROCEDURE SPECIFICATION (WPS) QW-482
ASME BPV Section IX 2004
WPS No. AW017 rev 0

Company Name: Allweld
Welding Procedure Spec. No: AW017
Revision No: 0

By: AMW Badenhorst
Supporting PQR No(s): AV05-0806
Date: 31 Aug 05

Welding Process(es): GTAW and SMAW

Types: Manual

JOINTS (QW-402)

Joint Design: Single V, double bevel
Backing (Yes/No): no
Backing Material: n/a
Joint Preparation: machine and grind

Groove angle: 35-40 degrees
Root gap: 3-5mm
Landing: 0-2mm
Base metal thickness: 4.8mm to 44mm

Joint sketch/details

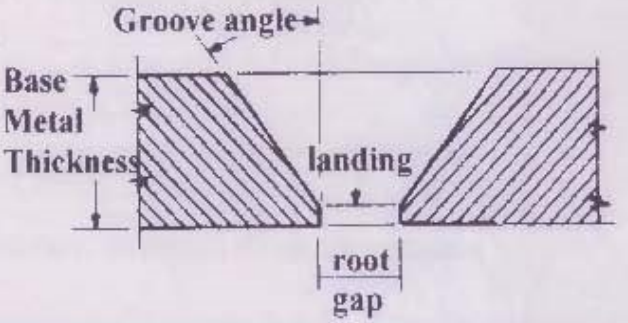

BASE METALS (QW-403)

ASME designation

P No: 1 Group No: 1 to P No: 1 Group No 1

Specification type and grade

ASTM A106 Grade B (and other P No 1 metals) to ASTM A106 Grade B (and other P No 1 metals)

Thickness Range

Base Metal:	Butt:	4.8mm to 44mm	Fillet:	all thickness
Weld Metal:	Butt:	44mm maximum	Fillet:	all sizes

Pipe Diameter Range: all

FILLER METALS (QW-404)

PROCESS	GTAW	SMAW	
SFA No	5.18	5.1	
AWS No	ER70S-6	E7018-1	
F-No	6	4	
A-No	1	1	
Size	1.6mm and 2.4mm	2.5mm, 3.15mm, 4.0mm	
Other	none	none	
Thickness Range			
Butt	12mm maximum	32mm maximum	
Fillet	all	all	
Elec.-Flux (class)	n/a	n/a	
Flux Tradename	n/a	n/a	
Consumable Insert	none	none	
Other			

ALLWELD

WELDING PROCEDURE SPECIFICATION (WPS) QW-482 (reverse side)

WPS Number: AW017 **Revision:0**

POSITIONS (QW-402)

Position(s) of butt: all
Weld Progression: uphill/forwards
Position(s) of fillet: all

POSTWELD HEAT TREATMENT (QW-407)

Temperature Range: 595 - 620 degees Celsius
Time Range: 1 hour per 25mm
Heating/Cooling Rate: 110 C/hr maximum
Notes: Heating/cooling above/below 300C is uncontroled

PREHEAT (QW-406)

Preheat Temp. (min) 20 degrees Celsius
Interpass Temp (max) 200 degrees Celsius
Preheat Maintenance: none
Preheat method: n/a
Other: Min Ambient Temp 10 degrees Celsius

GAS (QW-408)

	Gas(es)	% Comp. (mix)	Flow Rate)
Shielding	Argon	99.997	15-20 lpm
Backing	none	n/a	n/a
Trailing	none	n/a	n/a

ELECTRICAL CHARACTERISTICS (QW-409)

Current AC or DC: DC Polarity - (GTAW) / + (SMAW)
Amperage Range: see below Voltage Range: see below
Tungsten Electrode Size and Type: 2.4mm - 2% Thonated
Mode of Metal Transfer GMAW: n/a
Electrode Wire Feed Speed: n/a

TECHNIQUE (QW-410)

String or Weave Bead: stringer and weave beads
Orifice or Gas Cup Size: 8-12mm
Initial & Interpass Cleaning: grind and wire brush
Method of Back Gouging: none
Oscillation: none
Contact Tube to Work Distance: n/a
Multiple or Single Pass (per side): two passes minimum
Multiple or Single Electrodes: single
Travel Speed (Range): manual
Peening: none

Weld Layer	Process	Filler Metal Classification	Size	F No	A No	Current Type	Pol.	Amp Range	Volt Range	Travel Speed mm/min	notes
root	GTAW	ER70S-6	2.4mm	6	1	DC	-	110 to 135	9-12	45 to 55	3
h/ pass	GTAW	ER70S-6	2.4mm	6	1	DC	-	135 to 175	9-12	90 to 100	3
fill	GTAW	ER70S-6	2.4mm	6	1	DC	-	155 to 175	9-12	70 to 80	3
or	SMAW	E7018-1	2.5mm	4	1	DC	+	90 to 145	21-28	70 to 180	1-3
cap	GTAW	ER70S-6	2.4mm	6	1	DC	-	155 to 175	9-12	85 to 100	3
or	SMAW	E7018-1	2.5mm	4	1	DC	+	90 to 110	21-28	135 to 150	1-3

Notes: 1. Electrodes to be baked as per manufacturer's instructions and kept in a baking oven, on site, to be kept in a hotbox at 80 degrees Celsius minimum.
2. 3.15mm and 4.0mm elecrodes size may also be used.
3 Heat Input (if impact testing a requirement) to be in the range 1 to 3 kJ/mm

ALLWELD

Atlantic Verification Cape (Pty) Ltd
Government Approved Inspection Authority
LVUP061
15 Station Road, Montague Gardens, 7441
www.avcape.com
Tel: 021 552 8728

PROCEDURE QUALIFICATION RECORD

ASME BPV Section IX

Company Name: Allweld Marine

PQR No: AV05-0606

WPS No: AW017 rev 0 **Date:** 27 September 2005

Welding Processes: GTAW and SMAW

Types (Manual, Auto, Semi-Auto): Manual

JOINTS (QW-402)

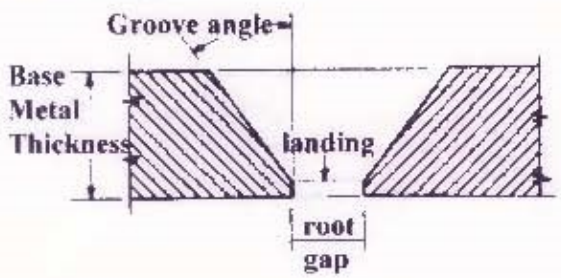

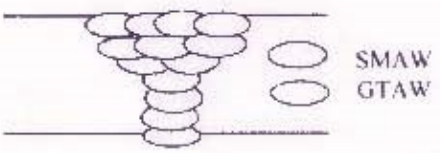

Groove angle (a): 30-40 degrees
Root gap (R): 4mm
Landing (f): 1.5mm

BASE METAL (QW-403)

Material Spec: ASTM A106 to same
Type or Grade: B to same
P No 1 Group No 1 to same
Thickness of test coupon: 22mm to same
Diameter of test coupon: 6"NB to same
Retainers: no

POSTWELD HEAT TREATMENT (QW-407)

Temperature: Soak at 605 degrees Celsius for 1 hr
Heating rate: 220 C/hr from 300 C
Cooling rate: 100 C/hr down to 300C then air cool

GAS (QW-408)

	Type	Mixture	Flow Rate
Shielding	Argon	99.997%	14 lpm
Backing:	n/a	n/a	n/a
Trailing:	n/a	n/a	n/a

FILLER METALS (QW-404)

Process	GTAW	SMAW
SFA No:	5.18	5.1
AWS Class:	ER70S-6	E7018-1
Filler Metal F No:	6	4
Weld Metal A No:	1	1
Filler Metal Size	2.4mm	2.5/3.15mm
Other		
Deposited Weld Metal	6mm	16mm

Other:

ELECTRICAL CHARACTERISTICS (QW-409)

Current: DC
Polarity: - (GTAW) / + SMAW
Amps: 95-164 Volts: 9-28
Tungsten Electrode Size: 2.4mm - 2% Thoriated
Other:

POSITION (QW-405)

Position of groove: 6G
Weld Progression: upwards

TECHNIQUE (QW-410)

Travel Speed.
String or weave bead: weave max. 3x filler OD
Oscillation: none
Multiple/Single Electrodes: single
Multiple/Single Pass: multiple
Other:

ALLWELD

PREHEAT (QW-406)

Preheat Temperature: 56 degrees Celsius
Interpass Temperature: 175 degrees Celsius max.
Other:

PQR No. AV05-0606

MECHANICAL TEST RESULTS

TENSILE TEST Results (QW-150) IMP Labs Report No 05-2652-1

Spec no	Test Type	Dimensions (mm) width	thick	X-SECTION AREA mm 2	TENSILE STRENGTH kN	UTS act.	UTS requ.	Location nature of fracture
TP1	XW	20.1	18.5	372	180	483 MPa	415 MPa	Ductile in parent metal - acceptable
TP2	XW	20.1	19.0	382	187	490 MPa	415 MPa	Ductile in parent metal - acceptable

Note. XW = Transverse cross weld tensile test AW = All weld tensile test

GUIDE BEND TEST Results (QW-160) IMP Labs Report No 05-2652-1

Spec. no.	Test Type	Loc-ation	Bend Angle	Specimen Thickness	Former Diameter	Fracture appearance and remarks
1	SBW	XW	180	10 mm	40 mm	no defects visible - satisfactory
2	SBW	XW	180	10 mm	40 mm	no defects visible - satisfactory
3	SBW	XW	180	10 mm	40 mm	no defects visible - satisfactory
4	SBW	XW	180	10 mm	40 mm	no defects visible - satisfactory

Note SBW = side bend weld test FBW face bend weld test RBW = root bend weld test XW = transverse cross weld

TOUGHNESS TEST Results (QW-170) IMP Labs Report No 05-2652-1

Spec. no.'s	Dimensions (mm) width	thick.	length	Notch Loc.	Test Temp.	Energy absorbed (J) @ test temperature			Act Values ave.	min.	Requ Values ave.	min	Lateral Expansion Results (mm)			% Shear Results		
1-3	10	10	55	WM	-20C	82	118	112	104	82	27	19	-	-	-	-	-	-
1-3	10	10	55	HAZ	-20C	146	120	96	121	96	27	19	-	-	-	-	-	-
1-3	10	10	55	PM	-20C	90	120	114	108	90	27	19	-	-	-	-	-	-

Note: WM = Weld Metal HAZ = Heat Affected Zone PM = Parent Metal

WELD RUN INFORMATION

Weld Layer	Process	Classification	Diameter (mm)	Current Type	Amps	Volts	wfs m/min	Travel Speed mm/min	Heat Input kJ/mm
1	GTAW	ER70S-6	2.4mm	DC-	127	9-10	n/a	50	1.52
2-4	GTAW	ER70S-6	2.4mm	DC-	144-164	9-10	n/a	72-95	1.03-1.37
5-8	SMAW	E7018-1	2.5 / 3.15mm	DC+	95-135	21-28	n/a	71-170	1.10-2.85
9 (cap)	SMAW	E7018-1	2.5mm	DC+	98	21-28	n/a	144	1.02

HARDNESS SURVEY & MACRO IMP Labs Report No 05-2652-2

Notes: Hardness locations in accordance with bs en 288 Part 3 at 6 o clock position

Results of macro exemination: acceptable

LOCATION	cap					
PM	154	160	160	175	170	179
HAZ	203	186	192	230	196	192
WM	245	224	243			

LOCATION	root					
PM	162	173	171	175	175	173
HAZ	198	198	193	186	187	186
WM	205	213	213			

FILLET WELD TESTS (QW-180) none

Results: n/a Penetration into Parent Metal (Yes/No): n/a

Welder's Name: M Higgins I.D. No: 7111125252088

Radiography Performed by: Raysonics Report No: 1721 Results: acceptable

We certify that the statements on this certificate are correct and that the test welds were prepared, welded and tested in accordance with the requirements of ASME BPV Code Section IX : 2004

ALLWELD

For: AVCAPE (Pty) Ltd

A. M. W. BADENHORST PrEng 9-917 IWE6800182 SAQCC IPE 375 CP/PV/6* AVCAPE (PTY) LTD

For: Lloyd's Register

T E A SKELAND IPE 095 CP/PV 213 CP/B 034 Cape Town Lloyd's Register EMEA

Lloyds Register

F.3.3 Welding consumable certification

24 mm 70S/6

AMALGAMATED WELDING & CUTTING

MATERIAL INSPECTION CERTIFICATE (EN 10204: 2004 type 3.1)

PRODUCT: TIGSTEEL ER 70S-6 **DATE:** 2008-08-28

DIAMETER: 2.40 mm

BATCH NUMBER: 1Z403

ELECTRODE MARKING: -

CLASSIFICATION: ASME/AWS-SFA A5.18: ER 70S-6

1. CHEMICAL COMPOSITION (ACTUAL)

% C	% Si	% Mn	% S	% P	% Cu
0.09	0.83	1.43	0.010	0.010	0.053

2. MECHANICAL PROPERTIES (ACTUAL - AS WELDED)

TENSILE STRENGTH (MPa)	YIELD STRENGTH (MPa)	% ELONGATION	HARDNESS	IMPACT STRENGTH (CHARPY-V-NOTCH)	
				TEST TEMP. (°C)	JOULES
593	470	33	-	- 46	**AVE: 167** 127, 221, 154

3. RADIOGRAPHY

Acceptable

This confirms that the product TIGSTEEL ER 70S-6, batch no. 1Z403, has been tested and manufactured in accordance with ASME/AWS SFA 5.01-92. Class S2, Schedule I, and complies with the requirements of ASME/AWS SFA 5.18-93.

THIS CERTIFICATE IS GENERATED ELECTRONICALLY & REQUIRES NO SIGNATURE.

ALLWELD

VALIDATED BY: S. SOOBRAMONEY
QUALITY CONTROLLER
OESA (PTY) LTD

OERLIKON HARRIS ESAB

Amalgamated Welding & Cutting (Pty) Ltd • Registration No: 1967/012686/07
Directors: W.D. Coetzee • H.R. Harris • C. van Zyl
Fitter Road, Spartan, Kempton Park • P.O. Box 273, Kempton Park, 1620 • tel (+27) (0) 11 975 0328 (+27) (0) 11 394 2343/4/5 • fax (+27) (0) 11 975 9120

F.3.4 Welder qualifications

sanas
South African National Accreditation System
LVUP062

[redacted]
Raysonics Inspection, Test & Certification

WELDER QUALIFICATION CERTIFICATE

WELDER NAME: T.ARENDSE	STAMP NO: ST129	
WELDERS I.D: 7408155250081	MANUFACTURER: ALL WELD	
USING WPS NO: AW026	REV No: 0	DATE : 17/02/2009

THE ABOVE WELDER IS QUALIFIED FOR THE FOLLOWING RANGES:

VARIABLES	ACTUAL VALUES	RANGE QUALIFIED
PROCESS: PROCESS TYPE:	GTAW SMAW MANUAL MANUAL	GTAW SMAW MANUAL MANUAL
JOINTS BACKING (metal,weld metal, flux, etc.)	SINGLE V GROOVE ARGON 99.99% WELD METAL	ALL WITH/WITHOUT WITH ONLY
BASE METAL MATERIAL SPECIFICATIONS TO MATERIAL SPECIFICATION TEST COUPON THICKNESS TOTAL PIPE DIAMETER	P1 – P1 ASTM A 106 GR B ASTM A 106 GR B 3.73 mm 21.3 mm	P1 to P11, P34, P41 to P49 & UNASSIGNED METALS OF SIMILAR CHEMICAL COMPOSITION UNLIMITED 21.3 mm TO UNLIMITED
FILLER METAL S.F.A. NO F. NO. CONSUMABLE INSERTS (GTAW,PAW)	ER80S-B8 5.28 F6 NONE	WITHIN F No LIMITS WITHIN F No LIMITS F6
WELD DEPOSIT THICKNESS	3.73mm	7.46mm
POSITION WELD POSITION WELD PROGRESSION	 6G UPHILL	 ALL POSITIONS ALL EXCEPT VERTICAL DOWN
GAS BACKING GAS (GTAW,PAW,GMAW) SHIELDING GAS	 ARGON 99.9% ARGON 99.9%	 ARGON 99.9% ARGON 99.9%
ELECTRICAL CHARACTERISTICS CURRENT POLARITY	 DC E-NEG	 DC E-NEG ONLY

TEST RESULTS

TYPE AND NUMBER: RADIOGRAPHY	ACCEPTABLE (YES/NO) YES
VISUAL EXAMINATION RESULTS: ACCEPTABLE RADIOGRAPHIC TEST RESULTS: ACCEPTABLE REPORT No: 11854	
FILLET WELD - FRACTURE TEST: N/A DEFECTS: NONE FILLET LEG SIZE: N/A mm	LENGTH AND PERCENT MACRO TEST FUSION: CONCAVITY/CONVEXITY N/A mm
WELDING TEST CONDUCTED BY: RITC (Pty) Ltd	
MECHANICAL TESTS CONDUCTED BY: N/A	
WE CERTIFY THAT THE STATEMENTS IN THIS RECORD ARE CORRECT AND THAT THE TEST COUPONS WERE PREPARED, WELDED, AND TESTED IN ACCORDANCE WITH THE REQUIREMENTS OF THE LATEST EDITION AND ADDENDA OF SECTION IX OF THE ASME CODE.	
DATE: 17/02/2009	CLIENT: RITC (PTY) LTD SIGN:

ALLWELD
Marine & Industrial
Base Road, Ndabeni P. O. Box 146, Howard Place
Cape Town, South Africa
Tel +27 (0)21 511 7473 Fax +27 (0)21 511 9409
Website www.allweld.co.za Email: info@allweld.co.za
VAT No 4600172798 CK No 1998/000905/23

RITC (PTY) Ltd

F.3.5 Non-destructive examination reports

R.I.T.C.

NON-DESTRUCTIVE TESTING

SURFACE CRACK TEST REPORT

Report No: 3904

Sheet 1 OF 1

Date: 26/03/2009

COMPONENT / WELD DETAIL	Contractor:	ALLWELD MARINE & INDUSTRIAL	Job No:	17040
	Client:	JCT	System Location:	ALLWELD WSHOP
	ITEM: Drawing No:	SPOOL PIECES STW001	Material:	CARBON STEEL
	Surface: Preparation:	AS WELDED/CLEANED	Thickness:	VARIOUS

TECHNICAL DETAIL	MAGNETIC PARTICLE TEST	PENETRANT FLUID TEST	CONSUMABLE BATCHES
	Testing Apparatus: MAGNAFLUX Y6 YOKE	Penetrant developer: N/A	BATCH No.
	Medium for Testing: ARDROX 5903W / 800-3 BLACK	Removal Method: N/A	5903W: 060308
	Technique (Wet/Dry): WET	Dwell Time (Penenetrant) N/A	800 - 3: 052809
	LIFTING POWER: 4.5KG - AC	Dwell Time (Developer) N/A	
	Acceptance Criteria: ASME B31.3	Acceptance Criteria: N/A	
	PROCEDURE: RITC-P-MT-001 REV 0	PROCEDURE: N/A	

Weld No :	INTERPRETATION	Acc	Rej
SAW01	100% MPI AFTER WELDING AFTER PWHT ON 5X SPOOL PIECES	Acc	
SAW02			
SAW03	C. ARENDSE : ST129		
SAW04			
	NO RECORDABLE INDICATIONS FOUND AT TIME OF TEST.		

Technician			Inspection Authority	Client
Name: F.LOTTERING	Qual: SNT-TC 1A L[illegible]		Sign:	Sign:
Date: 26/03/2009	Sign:		Date:	Date:

ALLWELD

R.I.T.C.

NON-DESTRUCTIVE TESTING

SURFACE CRACK TEST REPORT

Report No: 3905

Sheet 1 OF 1

Date: 26/03/2009

COMPONENT / WELD DETAIL	Contractor:	ALLWELD MARINE & INDUSTRIAL	Job No:	7040
	Client:	UCT	System Location:	ALLWELD W.SHOP
	ITEM: Drawing No:	SPOOL PIECES STW002	Material:	CARBON STEEL
	Surface: Preparation:	AS WELDED/CLEANED	Thickness:	VARIOUS

TECHNICAL DETAIL	MAGNETIC PARTICLE TEST	PENETRANT FLUID TEST	CONSUMABLE BATCHES
	Testing Apparatus: MAGNAFLUX Y6 YOKE	Penetrant developer: N/A	BATCH No.
	Medium for Testing: ARDROX 8903W / 800-3 BLACK	Removal Method: N/A	8903W : 060308
	Technique (Wet/Dry): WET	Dwell Time (Penenetrant) N/A	800 - 3 : 052808
	LIFTING POWER: 4.5KG - AC	Dwell Time (Developer) N/A	
	Acceptance Criteria: ASME B31.3	Acceptance Criteria: N/A	
	PROCEDURE: RITC-P-MT-001 REV 0	PROCEDURE: N/A	

Weld No :	INTERPRETATION	Acc.	Rej.
SAW01	100% MPI AFTER WELDING AFTER PWHT ON 5X SPOOL PIECES	Acc	
SAW02			
SAW03	C. ARENDSE : ST129		
SAW04			
	NO RECORDABLE INDICATIONS FOUND AT TIME OF TEST.		

Technician			Inspection Authority	
Name: F.LOTTERING	Qual: SNT-TC 1A L II		Sign:	Sign:
Date: 26/03/2009	Sign:		Date:	Date:

R.I.T.C.

NON-DESTRUCTIVE TESTING

SURFACE CRACK TEST REPORT

Report No: 3908

Sheet 1 OF 1

Date: 26/03/2009

COMPONENT / WELD DETAIL	Contractor:	ALLWELD MARINE & INDUSTRIAL	Job No.	17040
	Client:	UCT	System Location:	ALLWELD W.SHOP
	ITEM: Drawing No:	SPOOL PIECES STW003STF003	Material:	CARBON STEEL
	Surface Preparation:	AS WELDED/CLEANED	Thickness:	VARIOUS

TECHNICAL DETAIL	MAGNETIC PARTICLE TEST	PENETRANT FLUID TEST	CONSUMABLE BATCHES
	Testing Apparatus: MAGNAFLUX Y6 YOKE	Penetrant developer: N/A	BATCH No.
	Medium for Testing: ARDROX 8903W / 800-3 BLACK	Removal Method: N/A	8903W : 060308
	Technique (Wet/Dry): WET	Dwell Time (Penenetrant) N/A	800 - 3 : 052808
	LIFTING POWER: 4.5KG - AC	Dwell Time (Developer) N/A	
	Acceptance Criteria: ASME B31.3	Acceptance Criteria: N/A	
	PROCEDURE: RITC-P-MT-001 REv 0	PROCEDURE: N/A	

Weld No :	INTERPRETATION	Acc.	Rej.
SAW01	100% MPI AFTER WELDING / AFTER PWHT ON 5X SPOOL PIECES	Acc	
SAW02			
SAW03	C. ARENDSE : ST129		
SAW04			
	NO RECORDABLE INDICATIONS FOUND AT TIME OF TEST.		

Technician		Inspection Authority	
Name: F.LOTTERING	Qual: SNT-TC 1A L/II	Sign:	Sign:
Date: 26/03/2009	Sign:	Date:	Date:

R.I.T.C.

NON-DESTRUCTIVE TESTING

SURFACE CRACK TEST REPORT

Report No: 3906

Sheet 1 OF 1

Date: 26/03/2009

COMPONENT / WELD DETAIL	Contractor:	ALLWELD MARINE & INDUSTRIAL	Job No:	17040
	Client:	UCT	System Location:	ALLWELD W.SHOP
	ITEM: Drawing No:	SPOOL PIECES STW004	Material:	CARBON STEEL
	Surface: Preparation:	AS WELDED/CLEANED	Thickness:	VARIOUS

TECHNICAL DETAIL	MAGNETIC PARTICLE TEST	PENETRANT FLUID TEST	CONSUMABLE BATCHES
	Testing Apparatus: MAGNAFLUX Y8 YOKE	Penetrant developer: N/A	BATCH No.
	Medium for Testing: ARDROX 8903W / 800-3 BLACK	Removal Method: N/A	8903W : 060308
	Technique (Wet/Dry): WET	Dwell Time (Penenetrant) N/A	800 - 3 : 052808
	LIFTING POWER: 4.5KG - AC	Dwell Time (Developer) N/A	
	Acceptance Criteria: ASME B31.3	Acceptance Criteria: N/A	
	PROCEDURE: RITC-P-MT-001 REV 0	PROCEDURE: N/A	

Weld No :	INTERPRETATION	Acc.	Rej.
SAW01	100% MPI AFTER WELDING / AFTER PWHT ON 5X SPOOL PIECES	Acc	
SAW02			
	C. ARENDSE : ST129		
	NO RECORDABLE INDICATIONS FOUND AT TIME OF TEST.		

Technician			Inspection Authority	
Name: F.LOTTERING	Qual: SNT-TC 1A L II		Sign:	Sign: ALLWELD
Date: 26/03/2009	Sign:		Date:	Date:

R.I.T.C.

NON-DESTRUCTIVE TESTING

SURFACE CRACK TEST REPORT

Report No: 3907

Sheet 1 OF 1

Date: 26/03/2009

COMPONENT / WELD DETAIL	Contractor:	ALLWELD MARINE & INDUSTRIAL	Job No:	17040
	Client:	UCT	System Location:	ALLWELD W.SHOP
	ITEM Drawing No:	SPOOL PIECES STW005STF005	Material:	CARBON STEEL
	Surface Preparation:	AS WELDED/CLEANED	Thickness:	VARIOUS

TECHNICAL DETAIL	MAGNETIC PARTICLE TEST	PENETRANT FLUID TEST	CONSUMABLE BATCHES
	Testing Apparatus: MAGNAFLUX Y6 YOKE	Penetrant developer: N/A	BATCH No.
	Medium for Testing: ARDROX 8903W / 800-3 BLACK	Removal Method: N/A	8903W : 060308
	Technique (Wet/Dry): WET	Dwell Time (Penenetrant) N/A	800 - 3 : 052808
	LIFTING POWER: 4.5KG AC	Dwell Time (Developer) N/A	
	Acceptance Criteria: ASME B31.3	Acceptance Criteria: N/A	
	PROCEDURE: RITC-P-MT-001 REV 0	PROCEDURE: N/A	

Weld No :	INTERPRETATION	Acc.	Rej
SAW01	100% MPI AFTER WELDING / AFTER PWHT ON 5X SPOOL PIECES	Acc	
SAW02			
SAW03	C. ARENDSE : ST129		
SAW04			
	NO RECORDABLE INDICATIONS FOUND AT TIME OF TEST.		

Technician			Inspection Authority	Client
Name F.LOTTERING	Qual: SNT-TC 1A L II		Sign:	Sign:
Date: 26/03/2009	Sign:		Date:	Date:

G Detailed manufacturing drawings

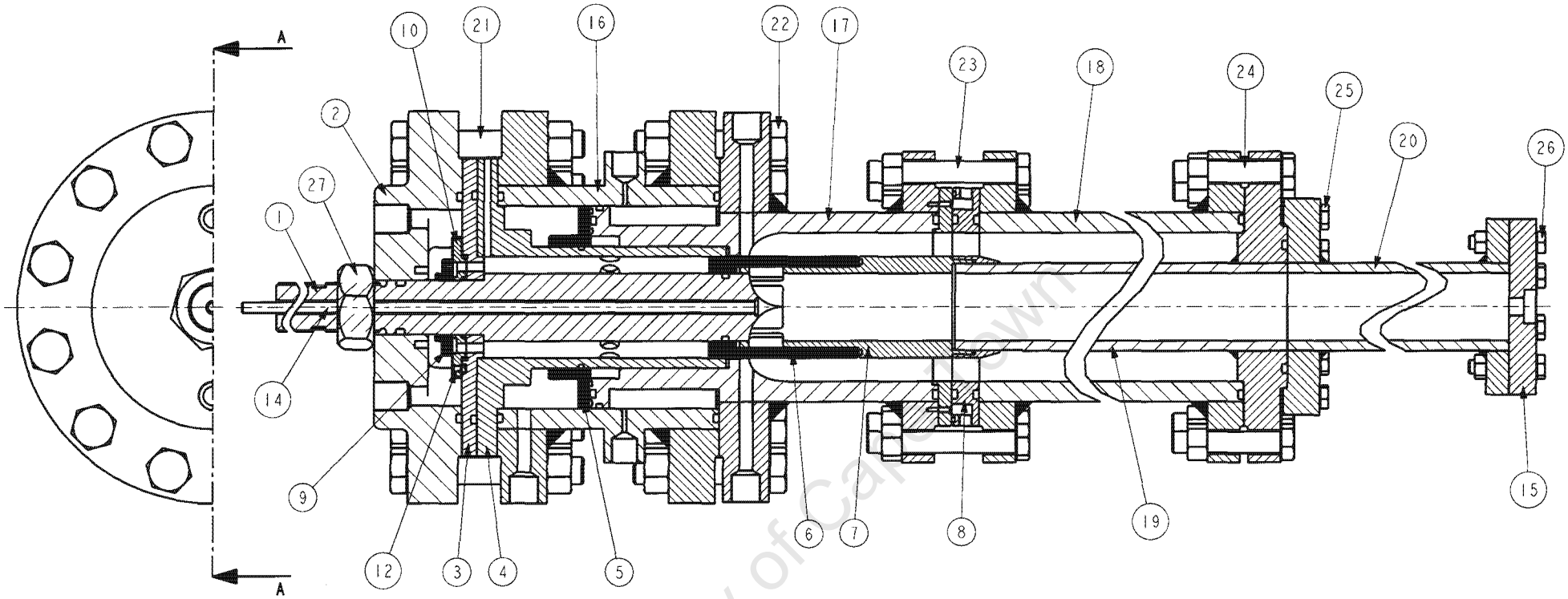

SECTION A-A

Parts list

Item	Part Name	Qty	Material	Remark
1	shaft	1	Mild steel	
2	head plate	1	50C steel	
3	shaft flange	1	Mild steel	
4	guide cylinder	1	EN9	Condition N
5	ring piston	1	Bronze	
6	sliding sleeve	1	Aluminium 7075	Condition T6
7	driven connector	1	EN9	Condition N
8	sliding coupler	1	EN9	Condition N
9	oneway ring	1	Bronze	
10	throttle plate gear	1	As supplied	Module 1
11	gear pinion	1	As supplied	Not shown
12	gear align pin	1	Mild steel	
13	teflon bush	1	Teflon	Not shown

Continued

14	inlet rod	1	Mild steel	Ball seat
15	endwall	1	ASTM A516 Grade70	Boilerplate
16	valve cylinder asm	1		Weld assembly
17	driver connector asm	1		Weld assembly
18	driver tube asm	1		Weld assembly
19	driven tube inn asm	1		Weld assembly
20	driven tube ext asm	1		Weld assembly
21	M20 by 140mm bolt	12	Class 8.8	Std. part
22	M20 by 110mm bolt	12	Class 8.8	Std. part
23	M16 by 110mm bolt	12	Class 8.8	Std. part
24	M16 by 80mm bolt	12	Class 8.8	Std. part
25	M10 by 40mm bolt	10	Class 8.8	Std. part
26	M10 by 60mm bolt	8	Class 8.8	Std. part
27	M36x2.0 nut	1	Class 8.8	Std. part

University of Cape Town
Department of Mechanical Engineering

Title: Shock Tube Assembly

Dimensions in mm Tolerance U.O.S.	Scale	Date	Sheet	of
0.1	0.333	09.02.2009	1	45
	Drawn By: Michael Downey		Drawing Number: STASM001	

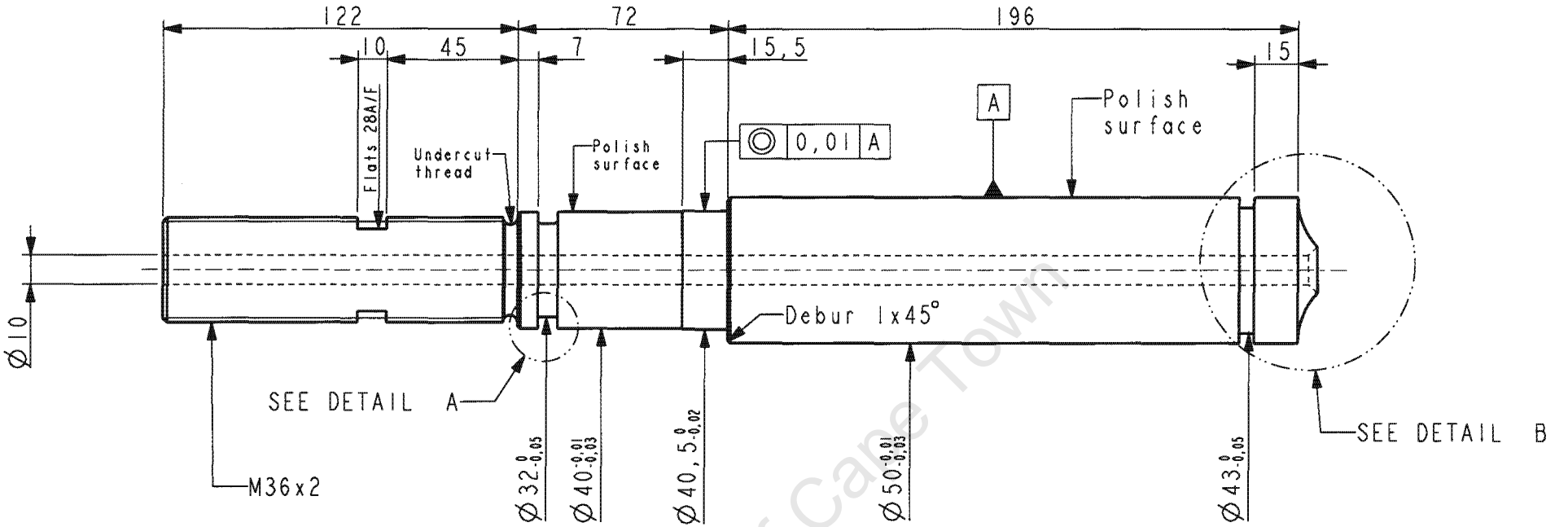

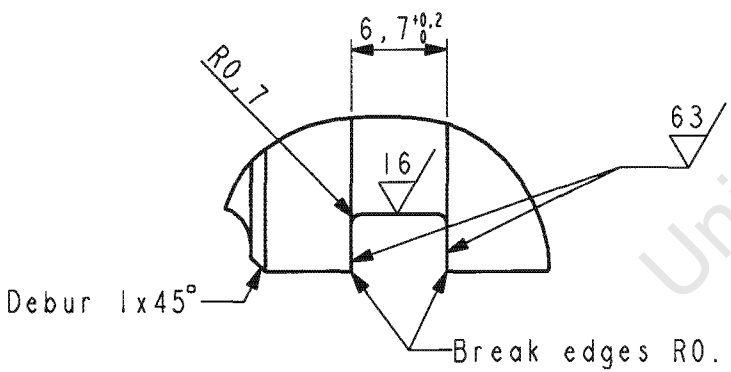

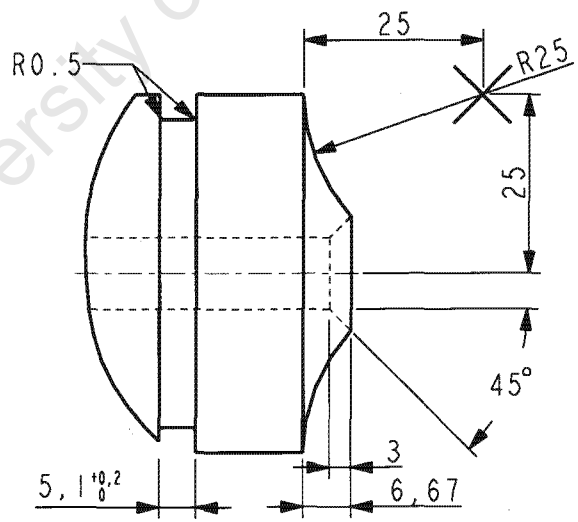

DETAIL A: O ring groove
SCALE 2,000
Note: Surf fin and break edges also apply to groove in detail B

DETAIL B
SCALE 1,000

Item	Material	Qty	Remarks
1	Mild steel	1	

University of Cape Town
Department of Mechanical Engineering

Title: shaft

Dimensions in mm Tolerance U.O.S.	Scale	Date	Sheet	of
0.1	0,500	30.10.2008	2	45
	Drawn By: Michael Downey		Drawing Number: STP001	

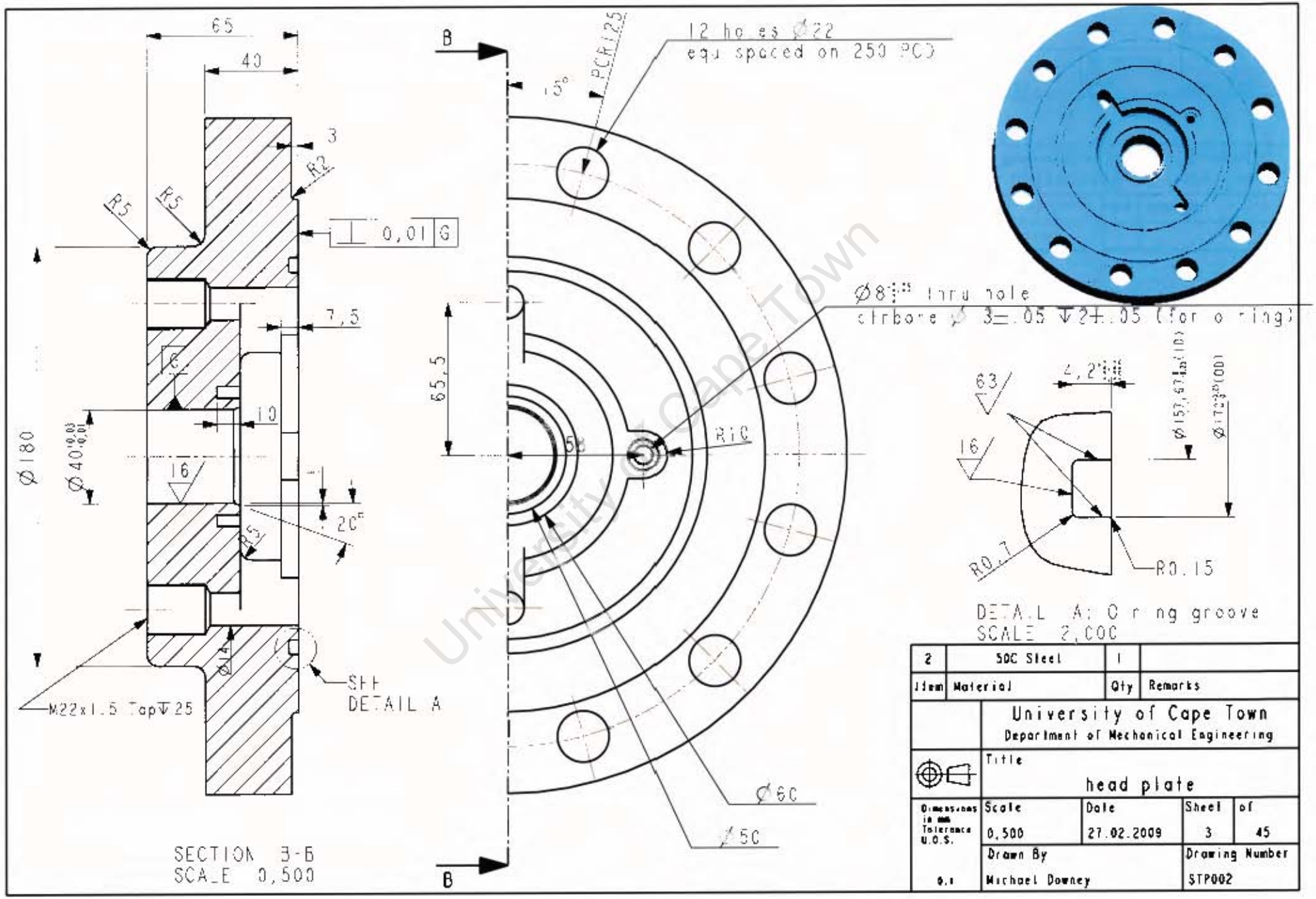

2	SDC Steel	1	
Item	Material	Qty	Remarks

University of Cape Town
Department of Mechanical Engineering

Title: head plate

Dimensions in mm Tolerance U.O.S.	Scale	Date	Sheet	of
	0,500	27.02.2009	3	45
	Drawn By		Drawing Number	
0,1	Michael Downey		STP002	

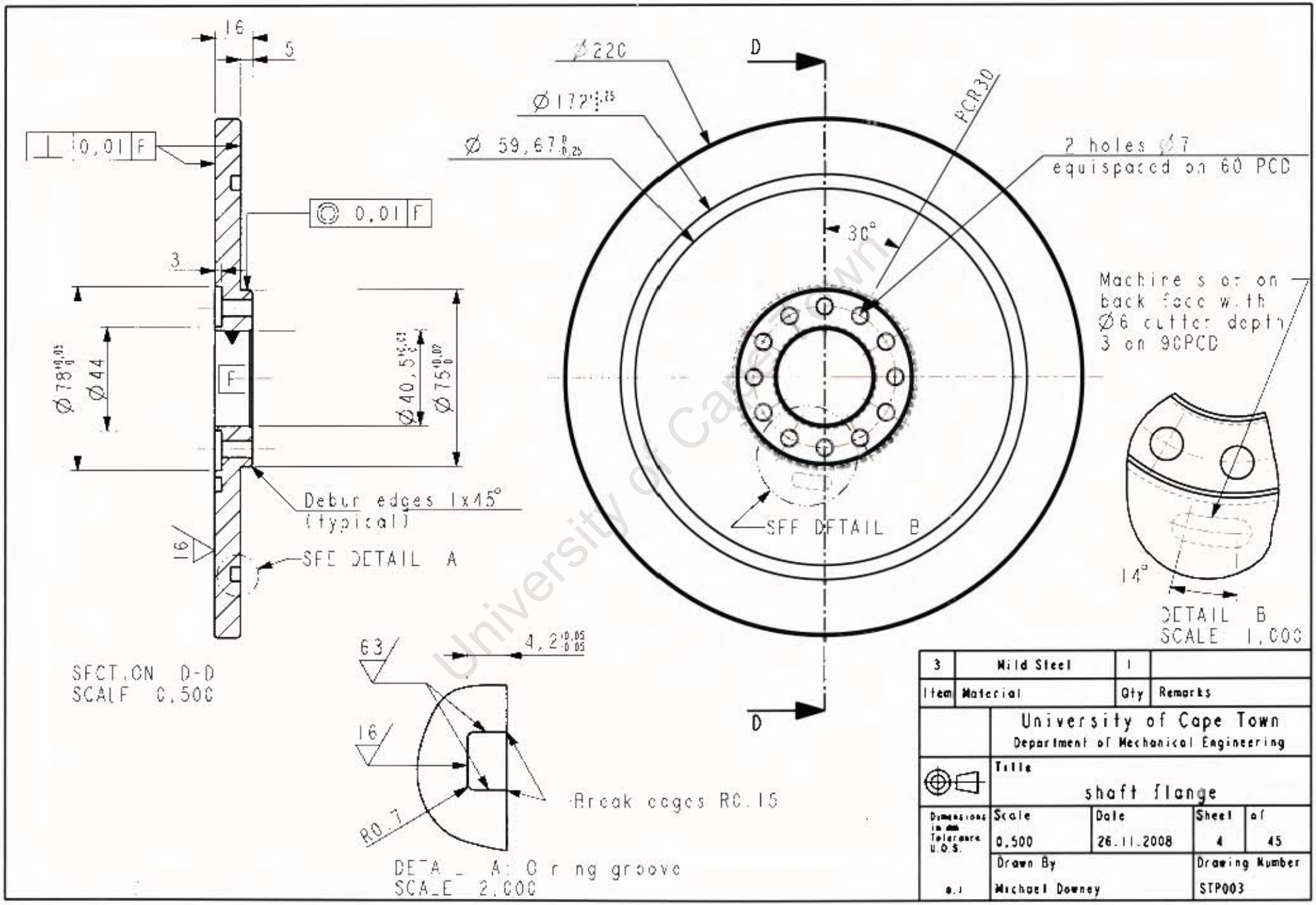

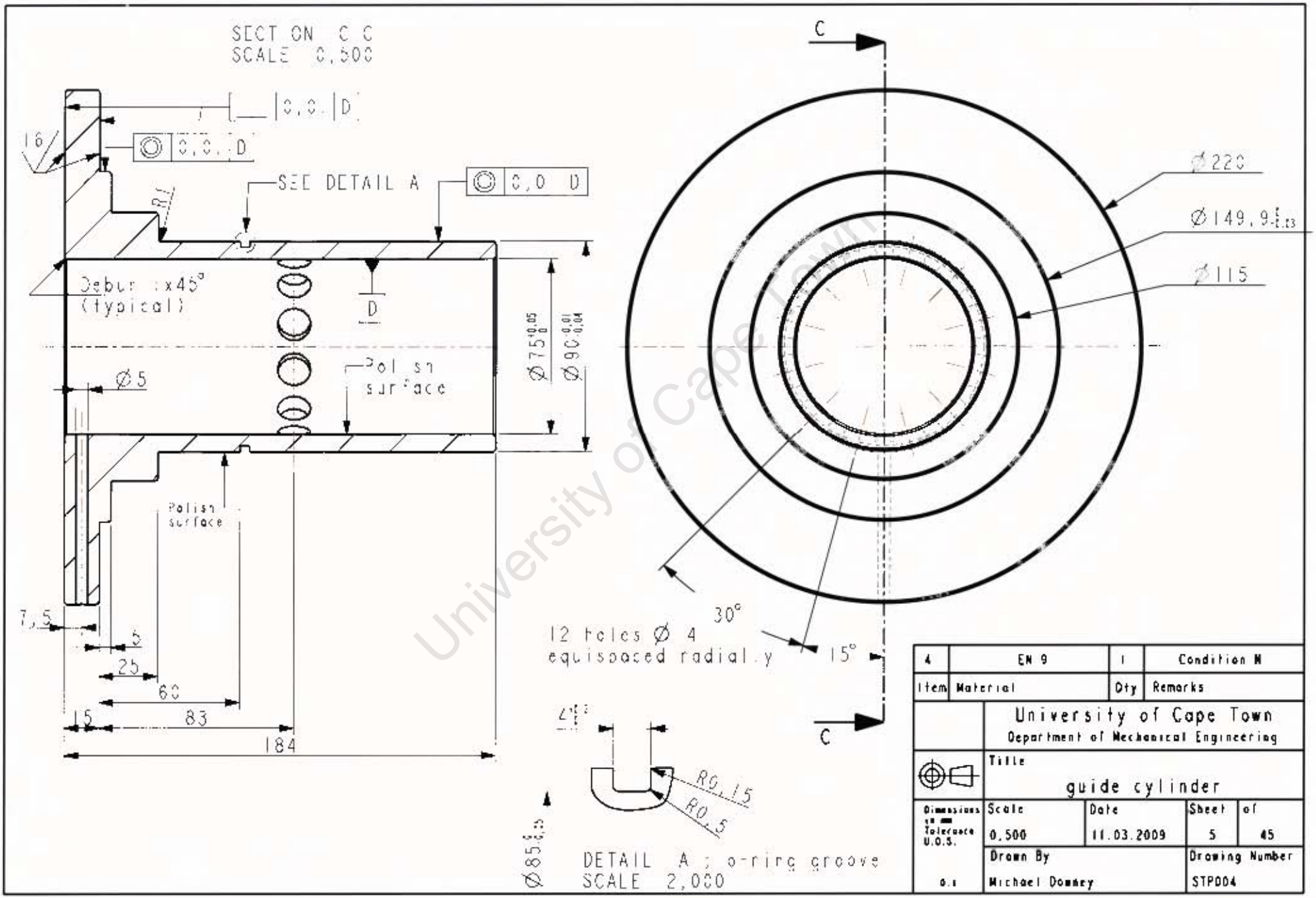

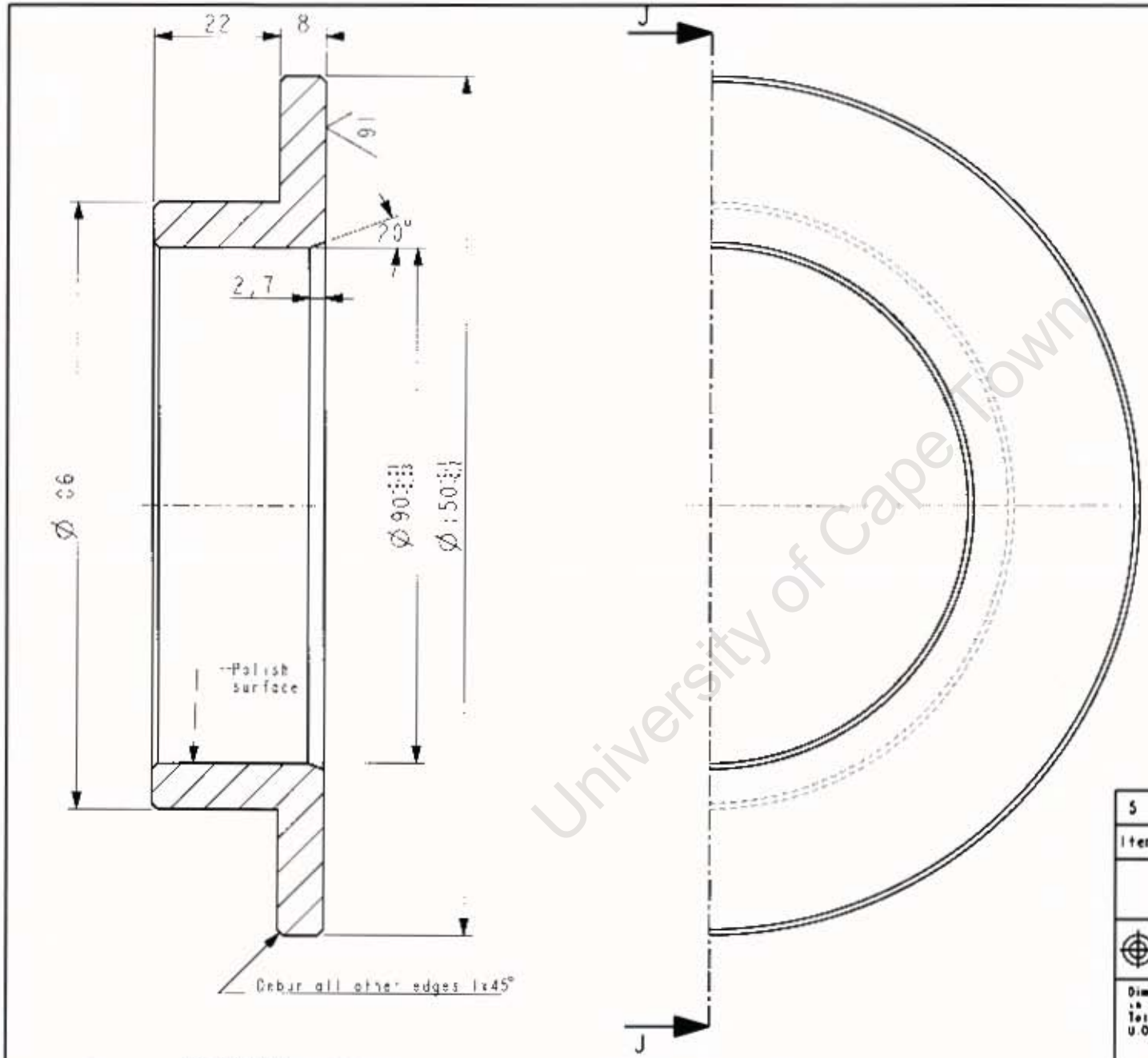

5	Bronze	1	
Item	Material	Qty	Remarks

University of Cape Town
Department of Mechanical Engineering

Title: ring piston

Dimensions in mm Tolerance ±0.5	Scale	Date	Sheet	of
	1.000	6.03.2009	6	45
	Drawn By		Drawing Number	
0.1	Michael Downey		STP005	

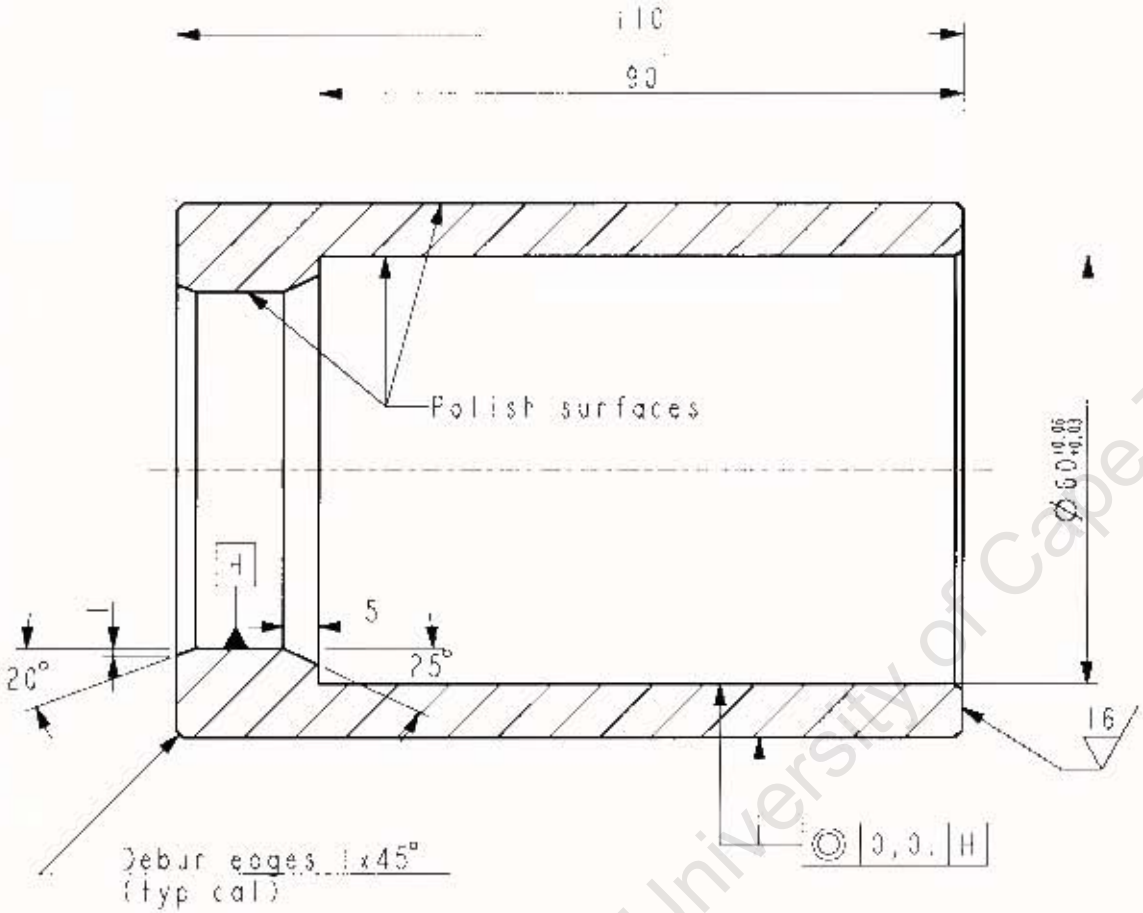

SECTION H-H
SCALE 1,000

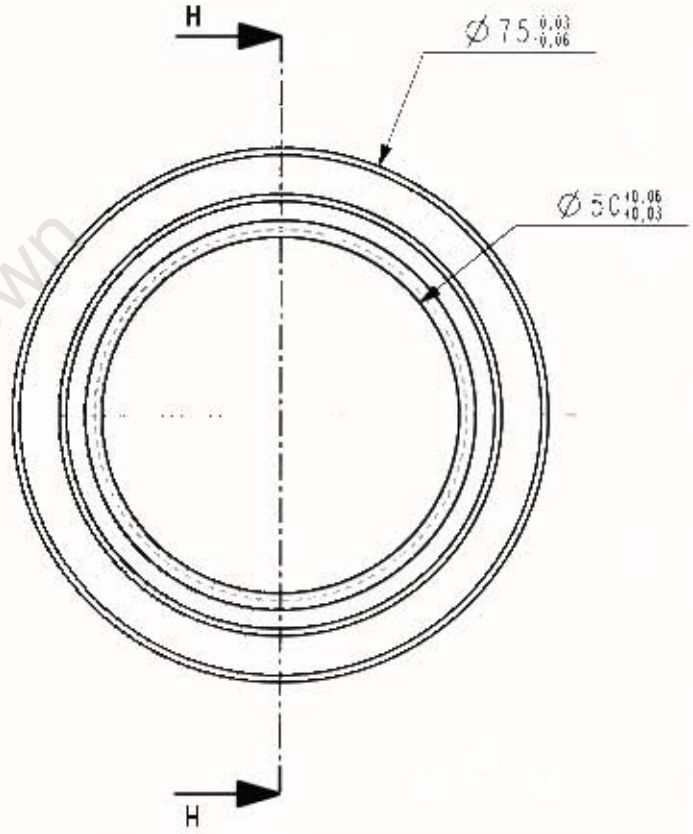

6	Aluminium 7075	1	Condition T6
Item	Material	Qty	Remarks

University of Cape Town
Department of Mechanical Engineering

Title: sliding sleeve

Dimensions in mm Tolerance u.o.s.	Scale	Date	Sheet	of
0.1	1,000	2.02.2009	7	45
	Drawn By: Michael Downey		Drawing Number: STP006	

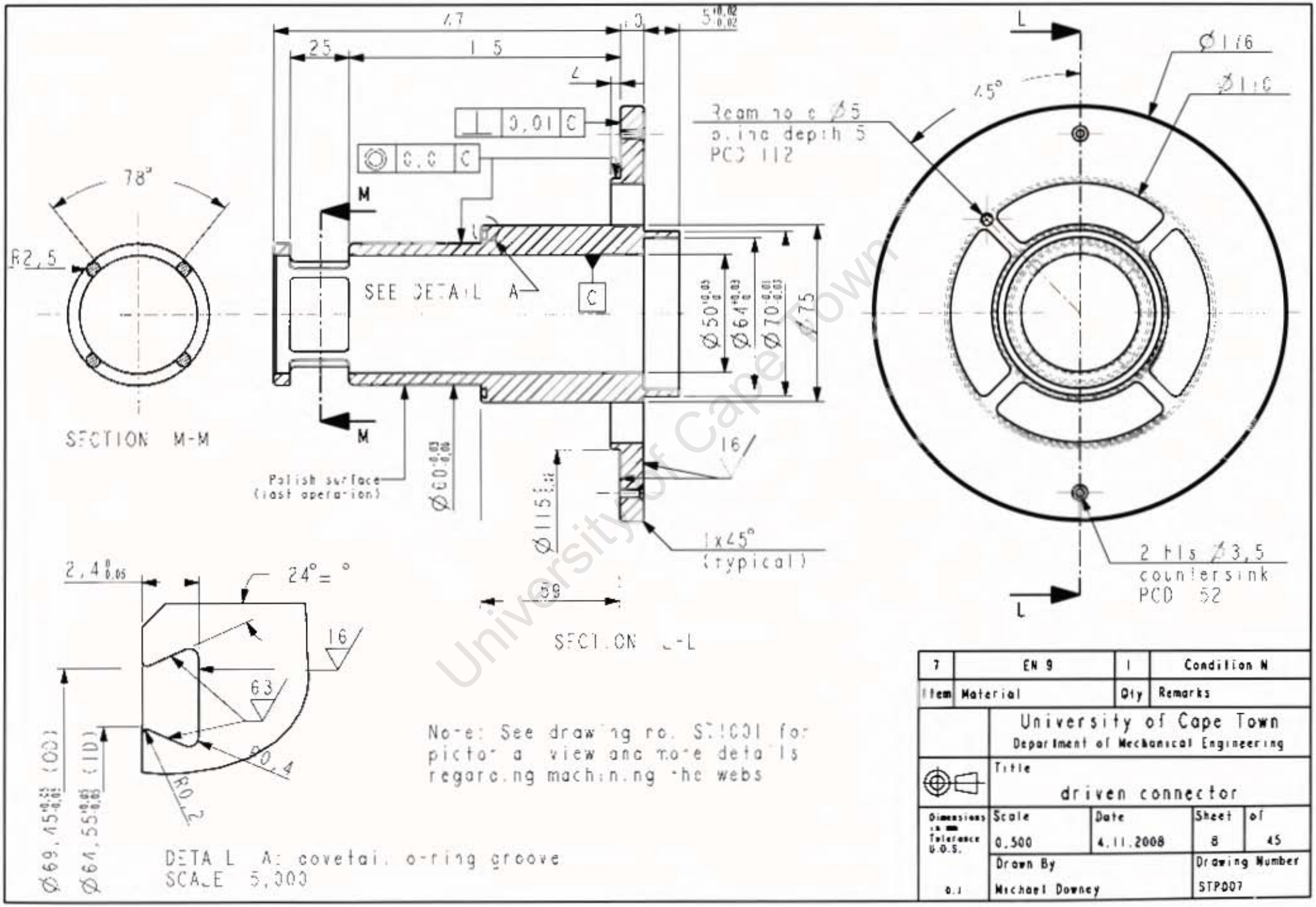

7	EN 9	1	Condition N
Item	Material	Qty	Remarks

University of Cape Town
Department of Mechanical Engineering

Title: driven connector

Dimensions in mm Tolerance U.O.S.	Scale	Date	Sheet	of
	0,500	4.11.2008	8	45
	Drawn By		Drawing Number	
0.1	Michael Downey		STP007	

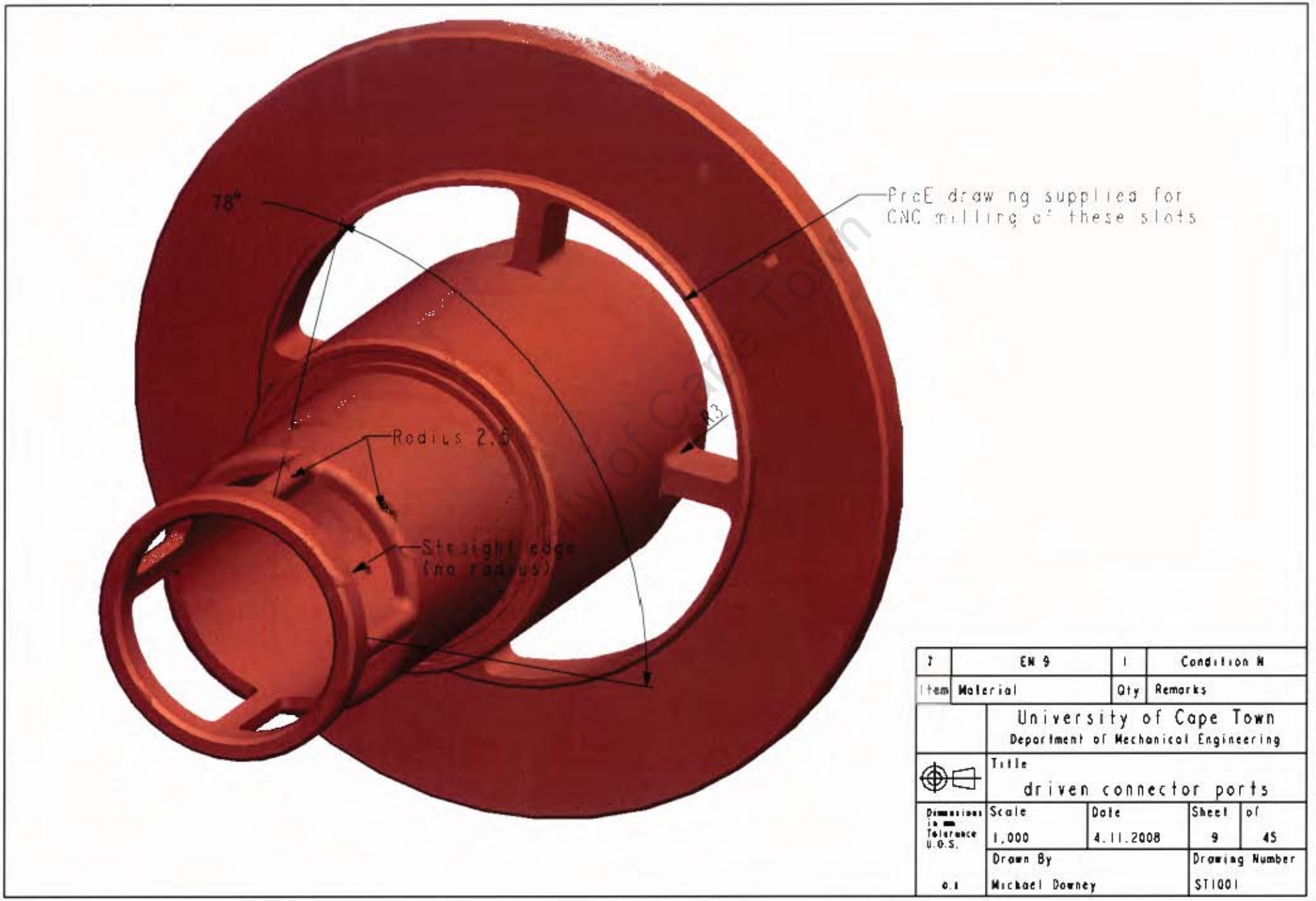

7	EN 9	1	Condition N
Item	Material	Qty	Remarks

University of Cape Town
Department of Mechanical Engineering

Title
driven connector ports

Dimensions in mm Tolerance U.O.S.	Scale	Date	Sheet	of
	1,000	4.11.2008	9	45
	Drawn By		Drawing Number	
0.1	Michael Downey		ST1001	

SECTION N-N

N

Blind hl M4x0.7 tapV 15
recm Ø5 V 5 cn 120°C)

1x45°
(typ cal)

45°

Ø176

Ø1.3

15°

Ø160
Ø124

Ø75
Ø70
Ø64

SEE DETAIL A

SEE DETAIL B

2 hls: ari l to groove
& tap M10x 1.5

Note: ProE arawings
supplied for CNC
mi l.ng of these s.o-s

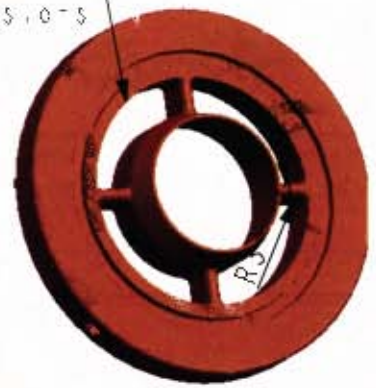

Note: no radius
on this surface

Reverse view

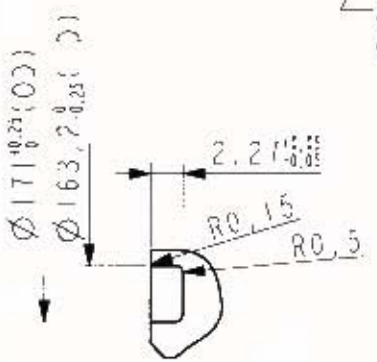

DETAIL B: sm. o-ring groove
SCALE 2,000

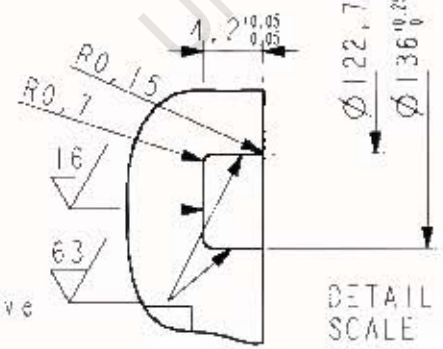

DETAIL A: ge o-ring grooves
SCALE 2,000 (typ su[illegible] in)

8	EN 9	1	Condition N
Item	Material	Qty	Remarks

University of Cape Town
Department of Mechanical Engineering

Title: sliding coupler

Dimensions in mm Tolerance U.O.S.	Scale 0,500	Date 4.11.2008	Sheet ID	of 45
	Drawn By Michael Downey		Drawing Number STP008	
9.1				

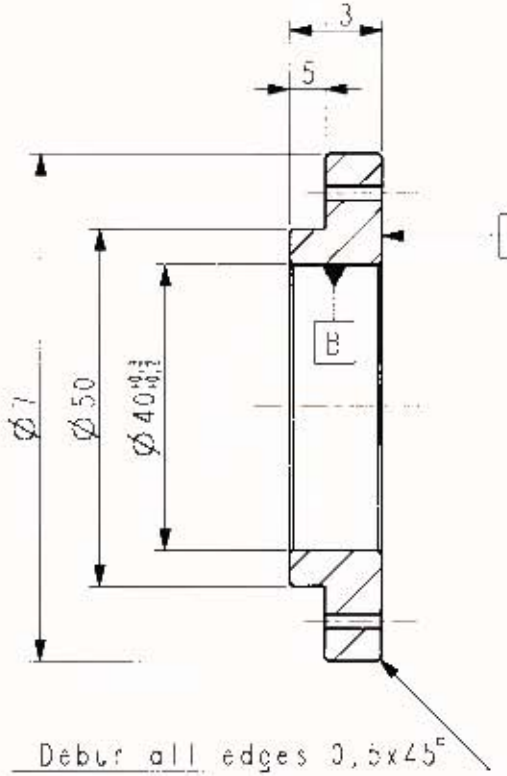

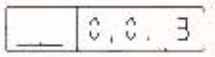

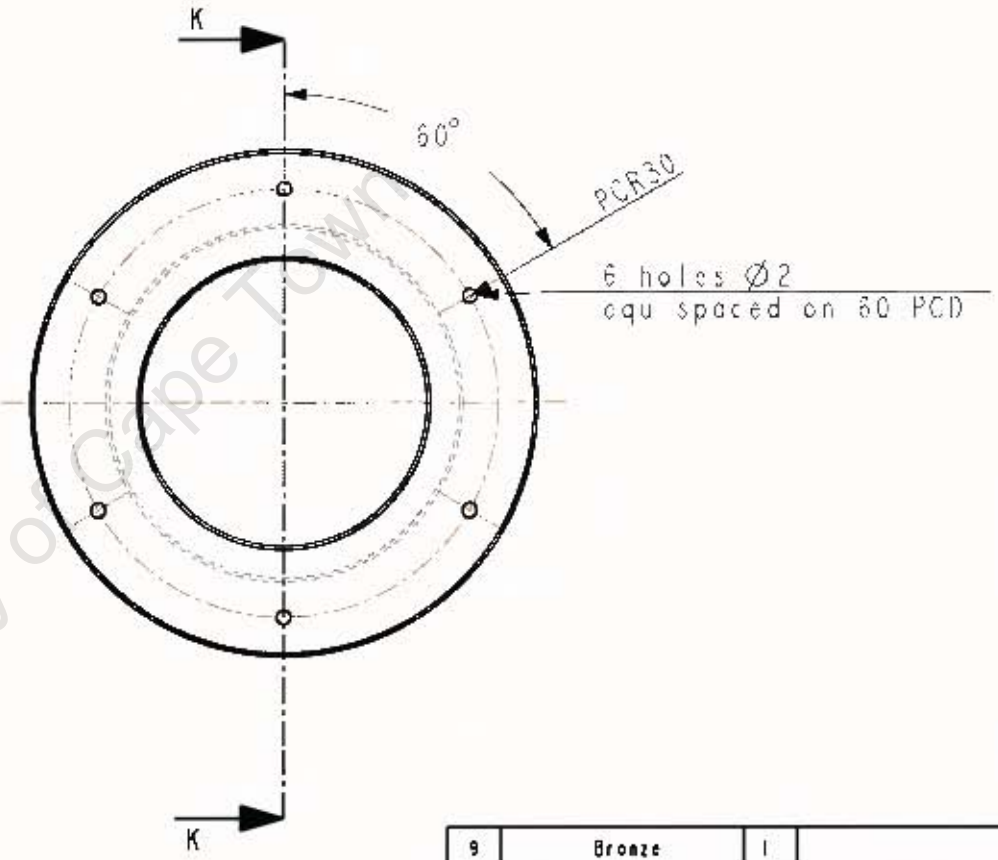

SECTION K K

9	Bronze	1	
Item	Material	Qty	Remarks

University of Cape Town
Department of Mechanical Engineering

Title: oneway ring

Dimensions in mm Tolerance to B.S.	Scale	Date	Sheet	of
	1,000	3.11.2008	11	45
	Drawn By		Drawing Number	
0.1	Michael Dommy		STP009	

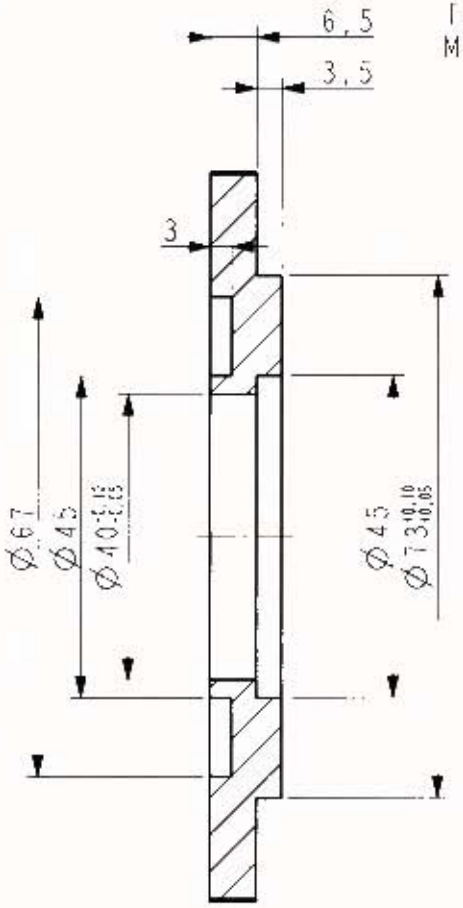

SECTION AB AB

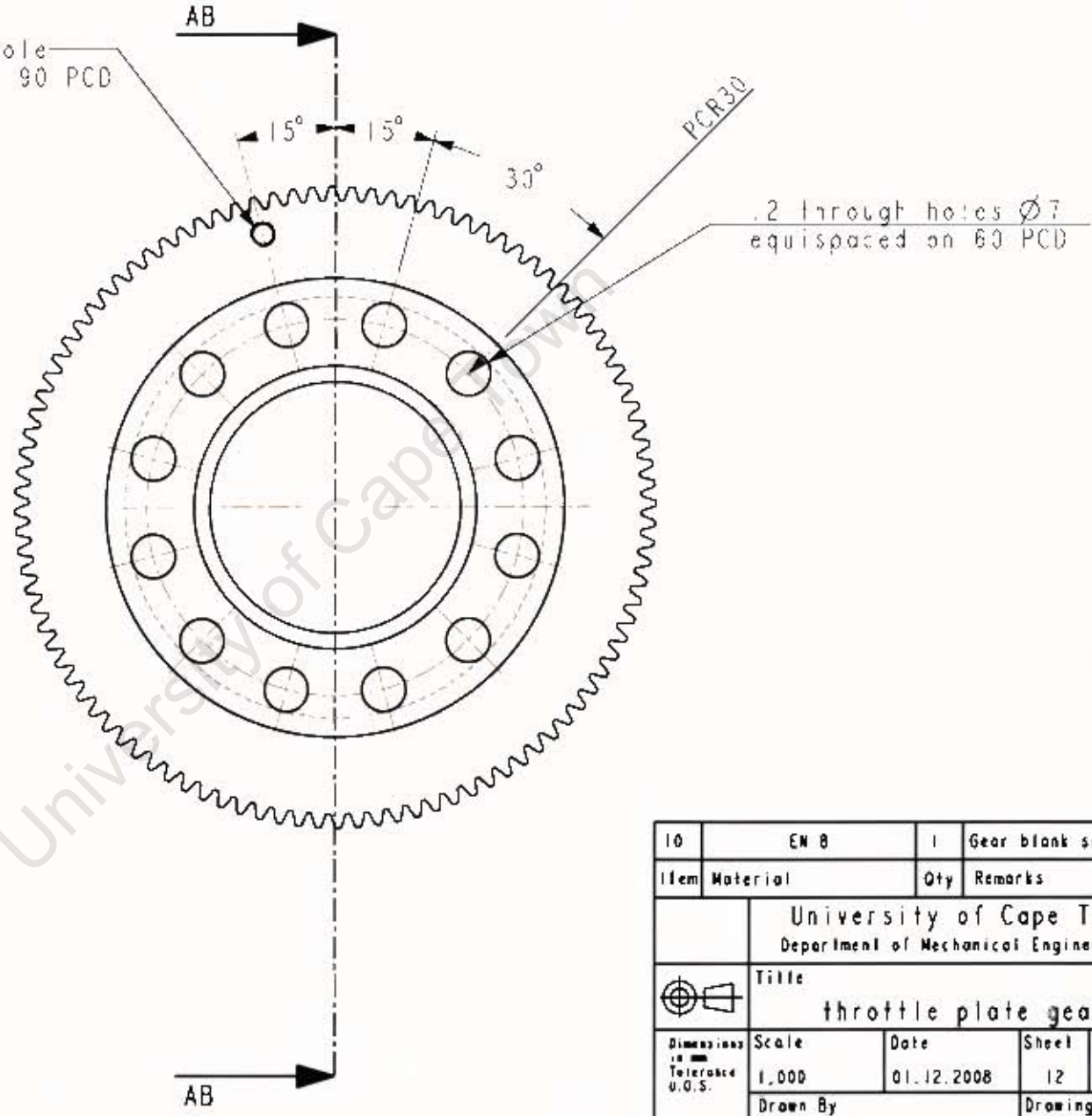

10	EN 8	1	Gear blank supplied
Item	Material	Qty	Remarks

University of Cape Town
Department of Mechanical Engineering

Title: throttle plate gear

Dimensions in mm Tolerance U.O.S.	Scale	Date	Sheet	of
0.1	1.000	01.12.2008	12	45
	Drawn By: Michael Downey		Drawing Number: STP010	

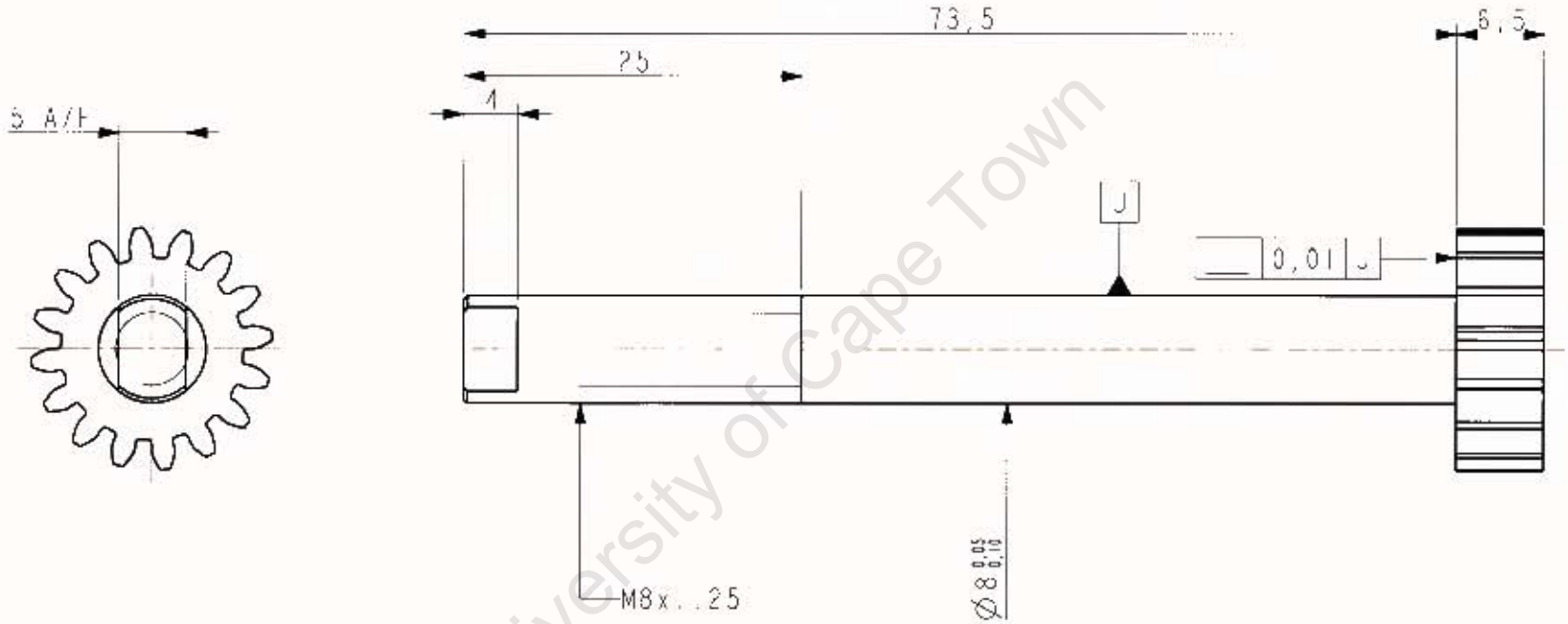

11	Mild Steel	1	Gear blank supplied
Item	Material	Qty	Remarks

University of Cape Town
Department of Mechanical Engineering

Title: gear pinion

Dimensions in mm Tolerance U.O.S.	Scale	Date	Sheet	of
0.1	2.000	01.12.2008	13	45

Drawn By	Drawing Number
Michael Downey	STP011

Note: weld rod into hole in gear then finish machine

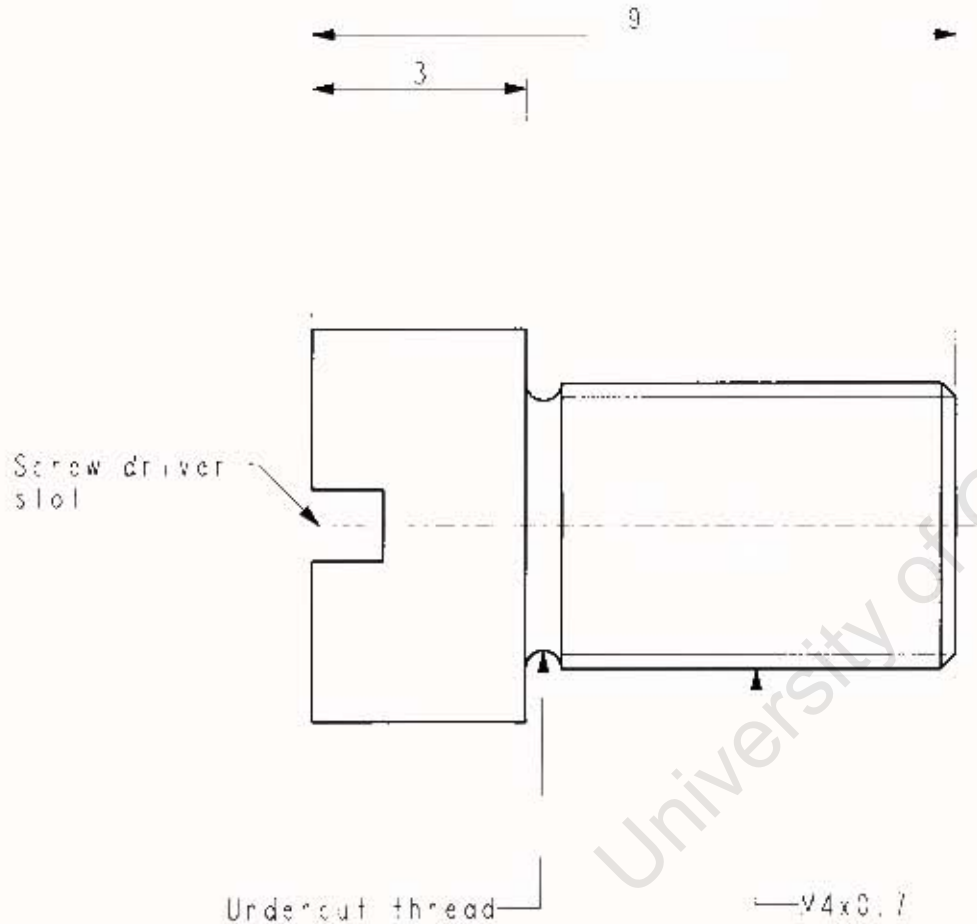

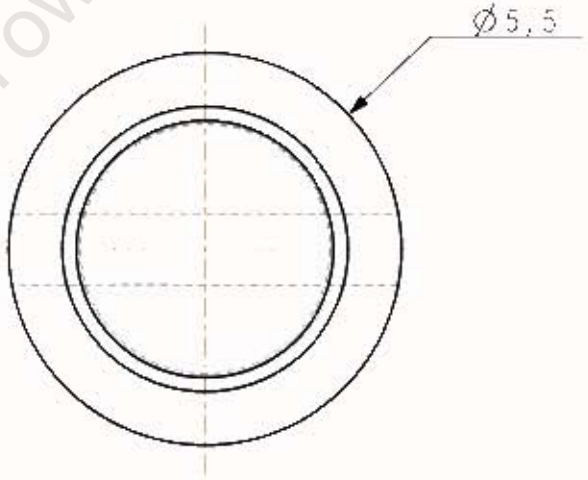

12	Mild Steel	1	
Item	Material	Qty	Remarks

University of Cape Town
Department of Mechanical Engineering

Title: gear align pin

Dimensions in mm, Tolerance U.O.S.	Scale	Date	Sheet	of
	4.000	01.12.2008	14	45
	Drawn By		Drawing Number	
0.1	Michael Downey		STP012	

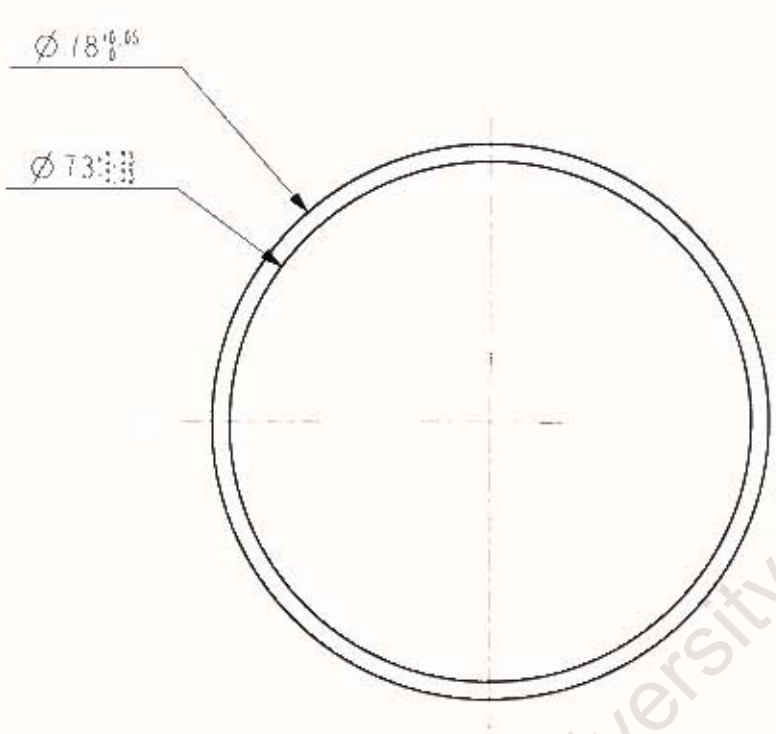

Note: Suggest first machine bore, then press onto part "GEAR_100T", then finish O.D.

13	Teflon	1	
Item	Material	Qty	Remarks

University of Cape Town
Department of Mechanical Engineering

Title: teflon bush

Dimensions in mm Tolerance U.O.S.	Scale	Date	Sheet	of
0.1	1.000	17.02.2009	15	45
	Drawn By: Michael Downey		Drawing Number: STP013	

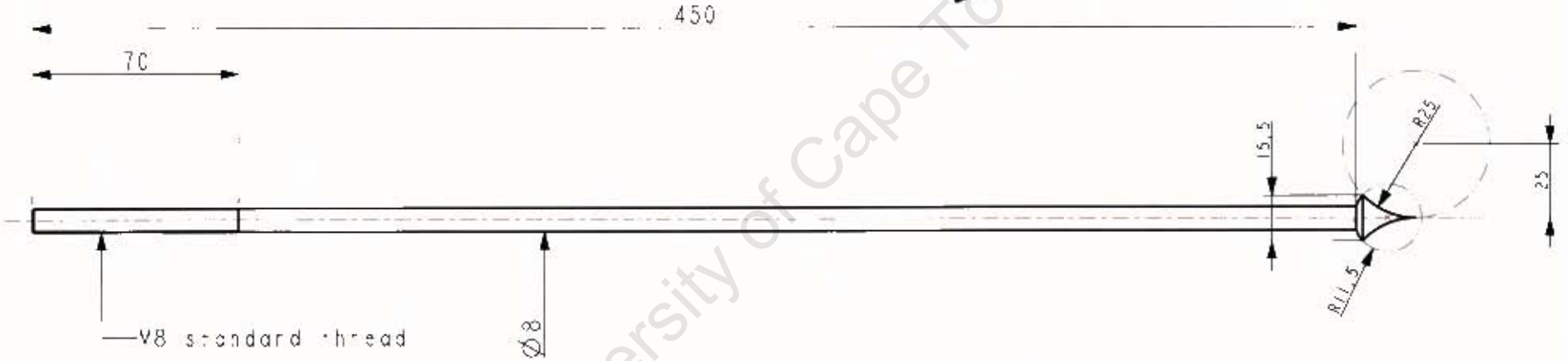

14	Mild Steel	1	Ball seat in cone
Item	Material	Qty	Remarks

University of Cape Town
Department of Mechanical Engineering

Title: inlet rod

Dimensions in mm Tolerance U.O.S.	Scale	Date	Sheet	of
0.1	0,500	03.02.2009	16	45
	Drawn By: Michael Downey		Drawing Number: STP014	

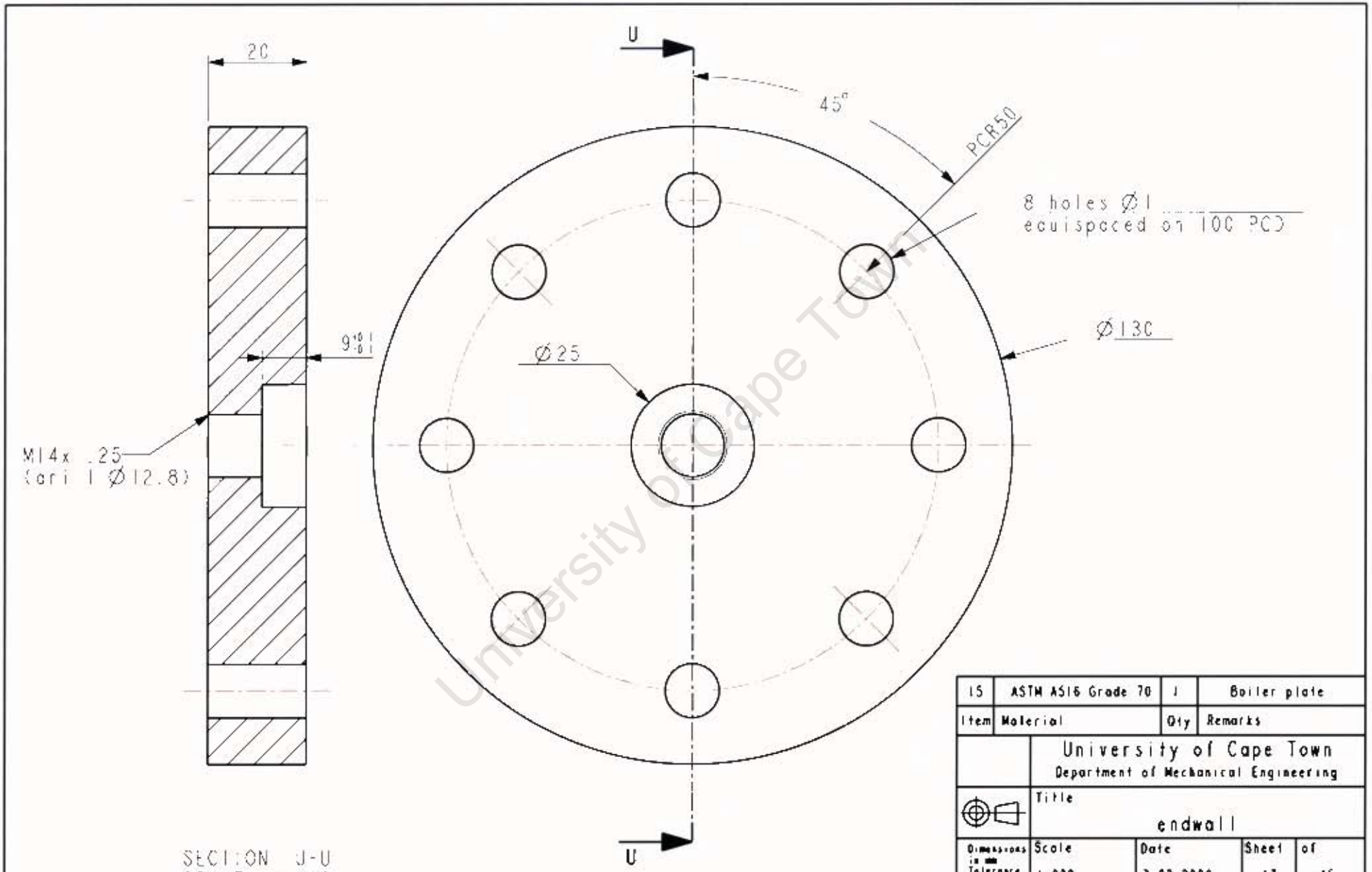

15	ASTM A516 Grade 70	1	Boiler plate
Item	Material	Qty	Remarks

University of Cape Town
Department of Mechanical Engineering

Title: endwall

Dimensions in mm Tolerance U.O.S.	Scale	Date	Sheet	of
	1,000	3.02.2009	17	45
	Drawn By		Drawing Number	
0.1	Michael Downey		STP015	

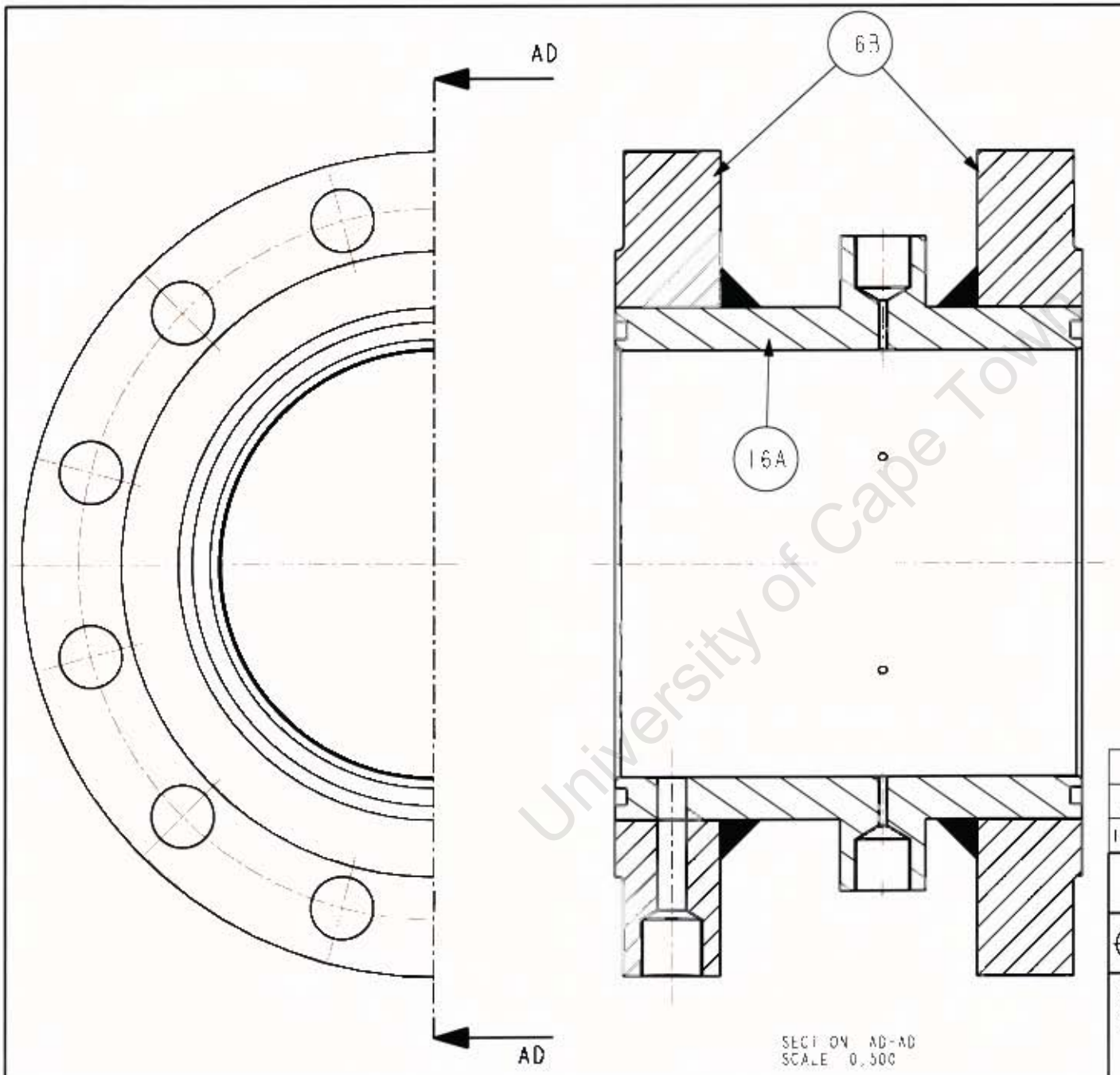

SECTION AD-AD
SCALE 0.500

Item	Material	Qty	Remarks
6B	ASTM A5 3 Gr 70	2	
16A	Hydraulic cylinder	1	

University of Cape Town
Department of Mechanical Engineering

Title
valve cylinder weld assembly

Dimensions in mm Tolerance U.O.S.	Scale	Date	Sheet	of
0.1	0.500	30.03.2009	18	45
	Drawn By: Michael Downey		Drawing Number: STA002	

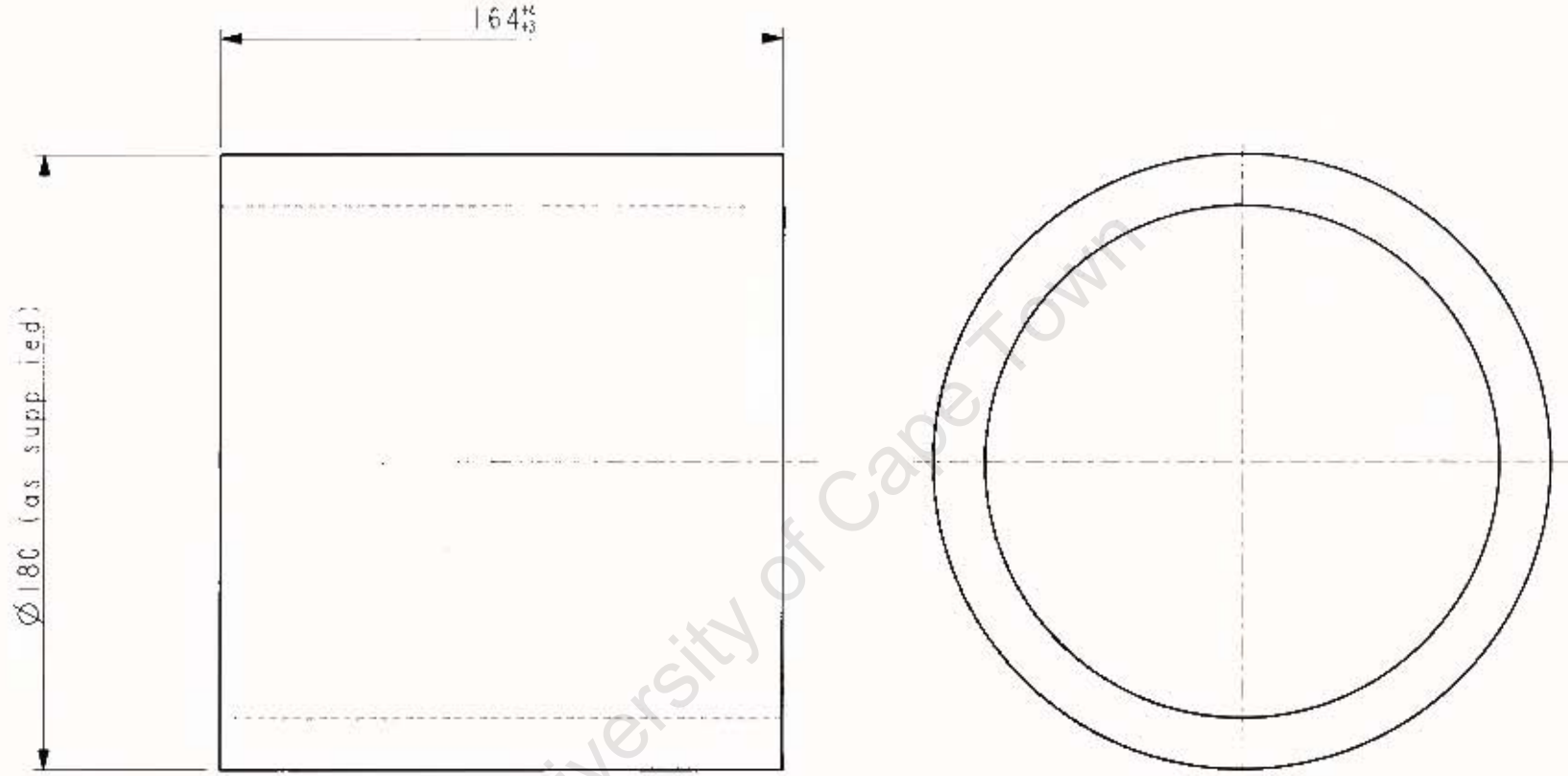

Note: Cut tube to length (note the oversize to ercrce), then press ora weld on flanges accora:ng to arawing # STW002, ther firish machine accora ng to arawing # S[illegible]002

16A	Hydraulic cylinder	1	As supplied
Item	Material	Qty	Remarks

University of Cape Town
Department of Mechanical Engineering

Title
valve cylinder basic

Dimensions in mm Tolerance U.O.S.	Scale	Date	Sheet	of
	0,500	03.11.2008	19	45
	Drawn By		Drawing Number	
0,1	Michael Downey		STP016A	

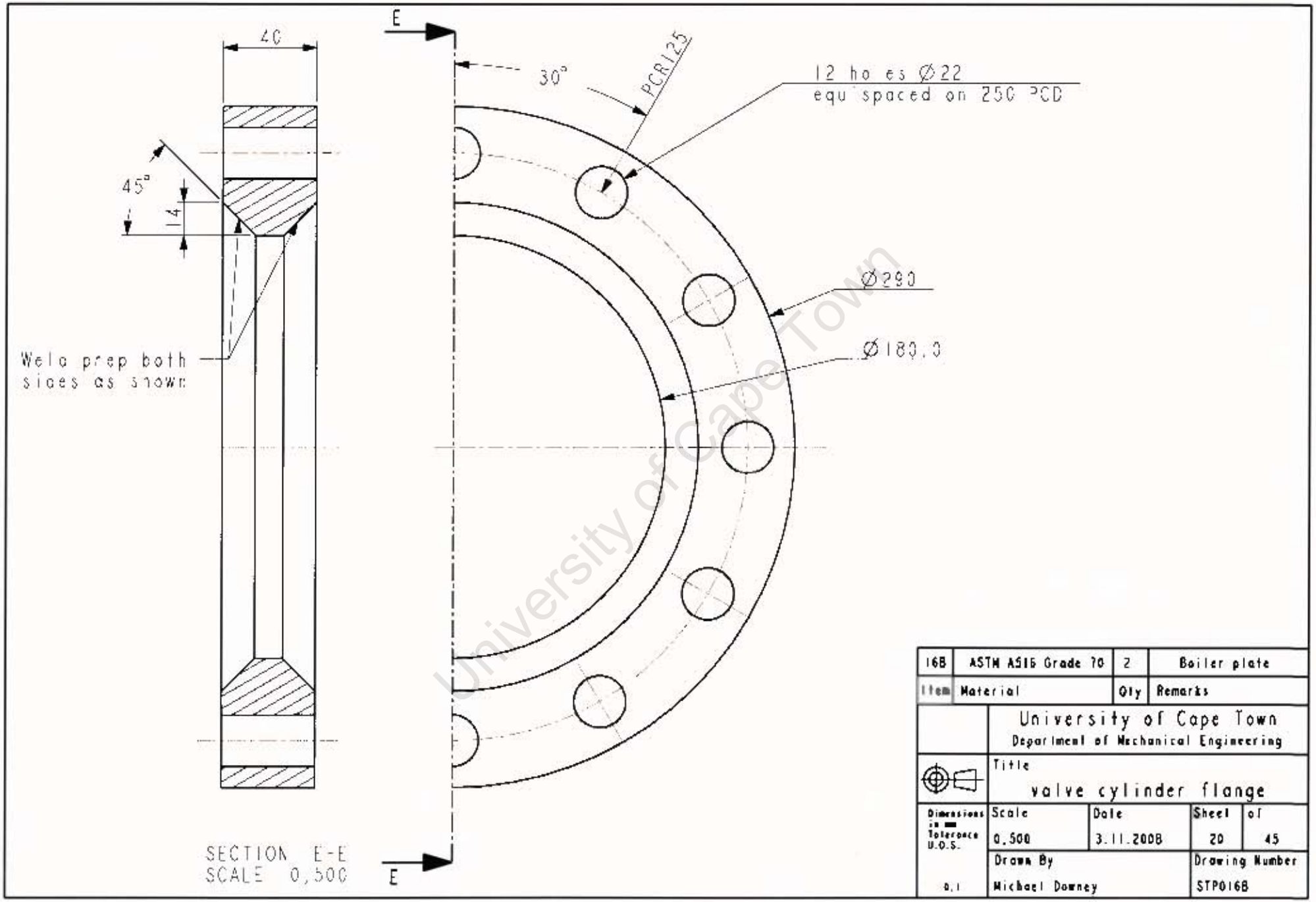

Item	Material	Qty	Remarks
16B	ASTM A516 Grade 70	2	Boiler plate

University of Cape Town
Department of Mechanical Engineering

Title: valve cylinder flange

Dimensions in mm, Tolerance U.O.S.	Scale	Date	Sheet	of
0,1	0,500	3.11.2008	20	45

Drawn By	Drawing Number
Michael Downey	STP016B

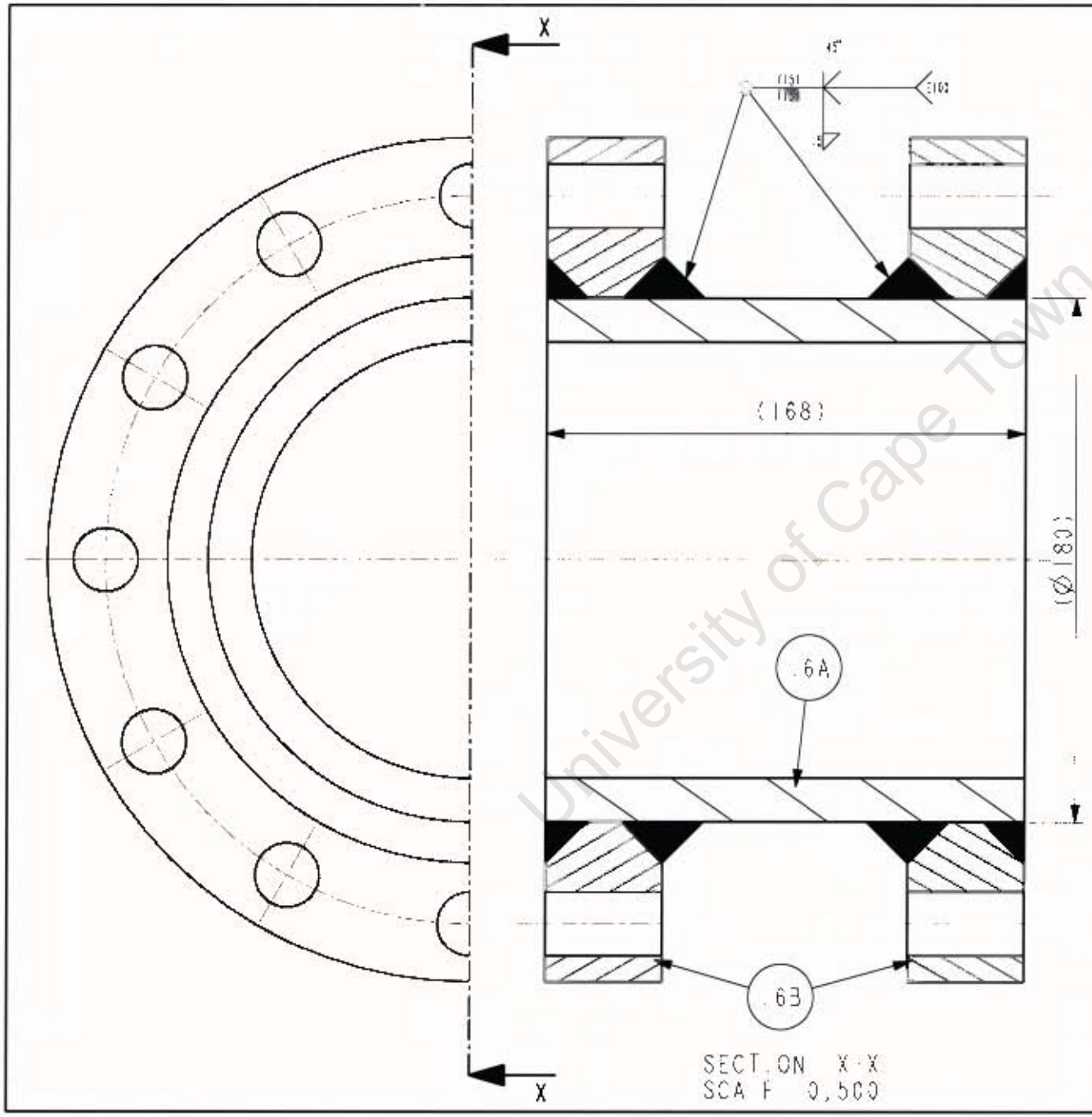

SECTION X-X
SCALE 0,500

Note: Flanges to be positioned flush with tube ends. Face side reinforcements will be machined off after welding. Minimum electrode yield strength is 500MPa. Flange holes to be aligned. Stress relieve welds. Finish machine according to drawing # STF002

Item	Material	Qty	Remarks
168	ASTM A516 Gr 70	2	od290 by id180 flange
6A	Hydraulic cylinder	1	precut to 168

University of Cape Town
Department of Mechanical Engineering

Title: valve cylinder welding

Dimensions in mm Tolerance U.O.S.	Scale	Date	Sheet	of
0,1	0,500	18.02.2009	21	45
	Drawn By: Michael Downey		Drawing Number: STW002	

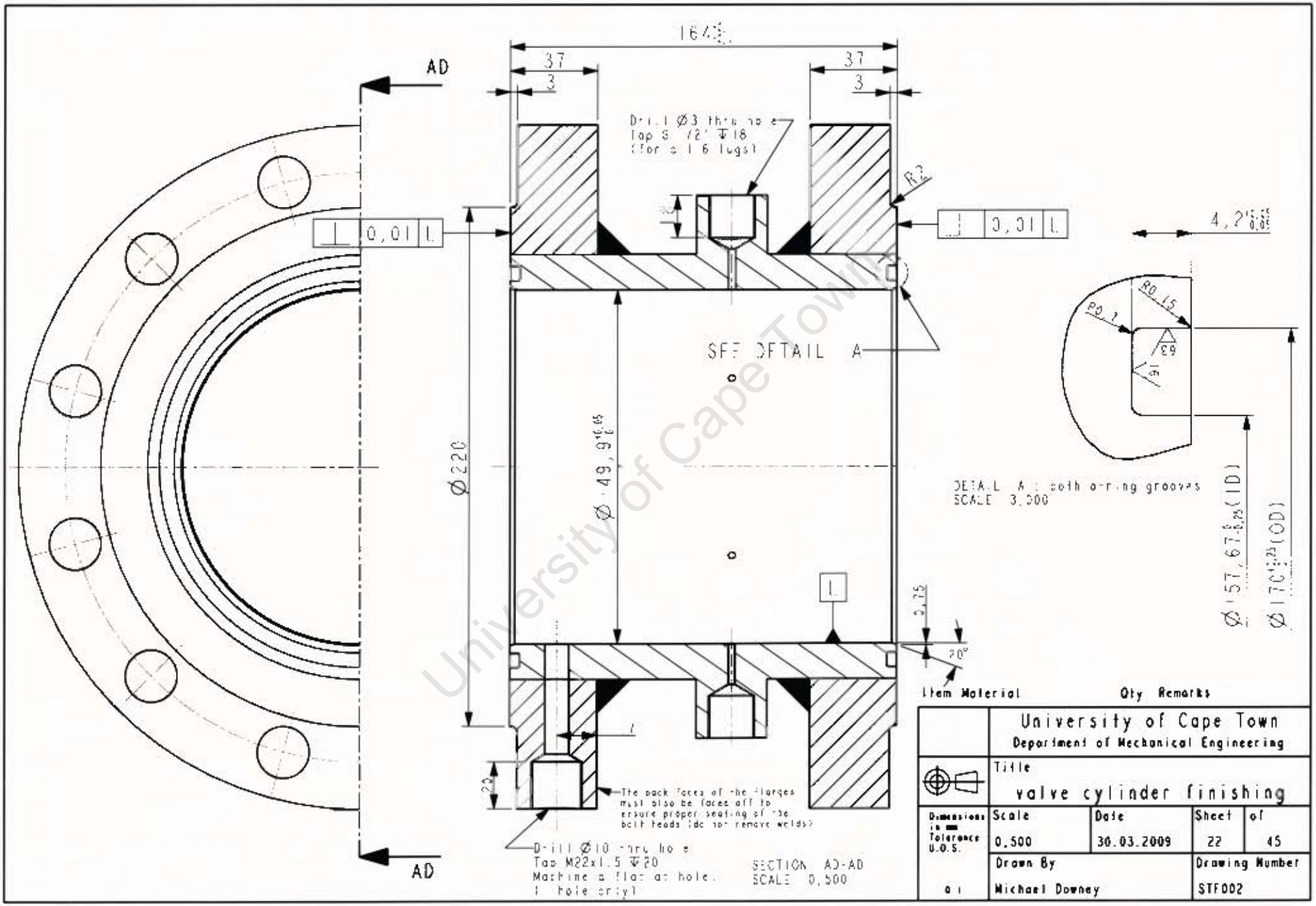

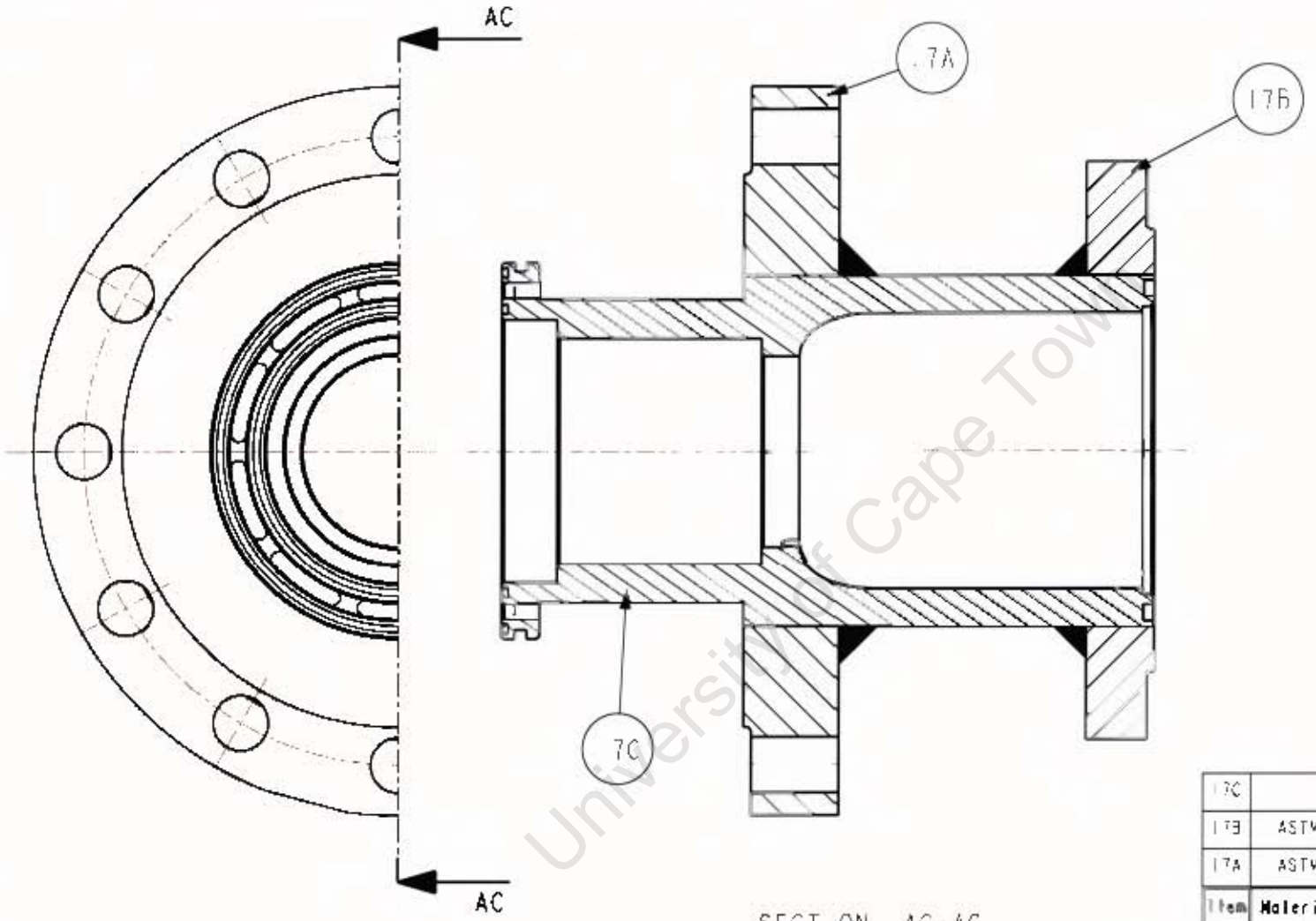

SECTION AC-AC
SCALE 0,400

Item	Material	Qty	Remarks
17C	EN9		
17B	ASTM A516 Gr 70		
17A	ASTM A516 Gr 70		

University of Cape Town
Department of Mechanical Engineering

Title: driver connector weld assembly

Dimensions in mm Tolerance U.O.S.	Scale	Date	Sheet	of
0.1	0,400	11.03.2009	23	45
	Drawn By: Michael Downey		Drawing Number: STA001	

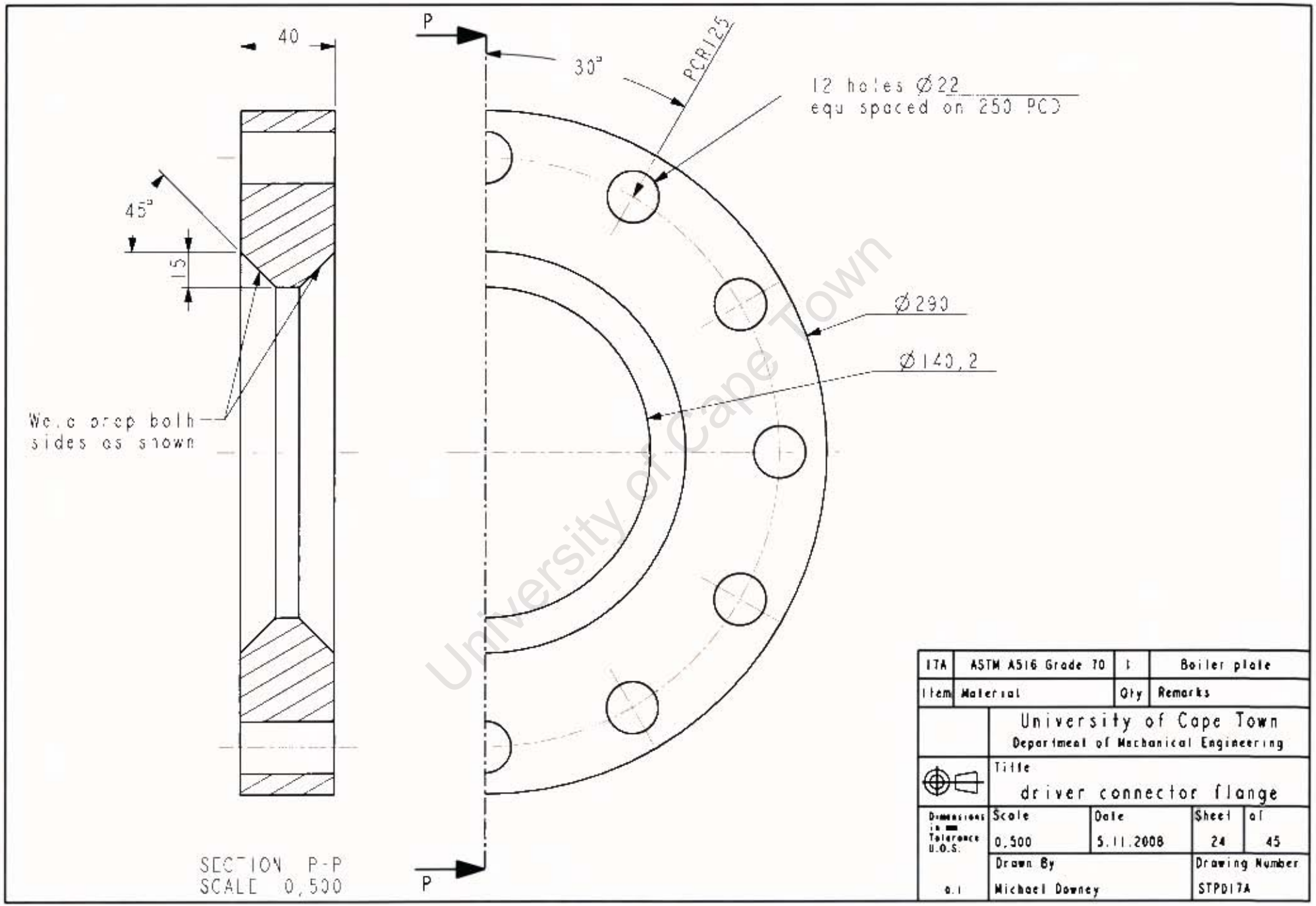

ITA	ASTM A516 Grade 70	1	Boiler plate
Item	Material	Qty	Remarks

University of Cape Town
Department of Mechanical Engineering

Title: driver connector flange

Dimensions in mm Tolerance U.O.S.	Scale	Date	Sheet	of
0.1	0,500	5.11.2008	24	45
	Drawn By: Michael Downey		Drawing Number: STPD17A	

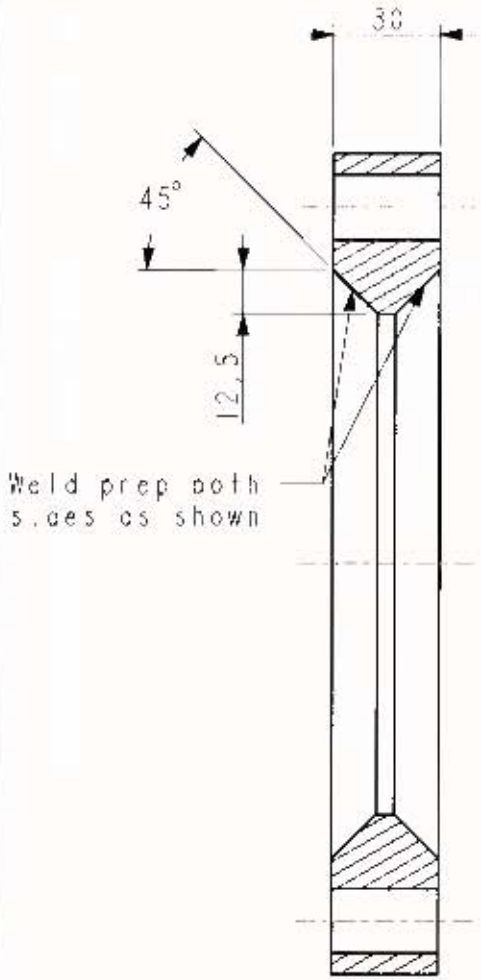

SECTION Q-Q
SCALE 0,500

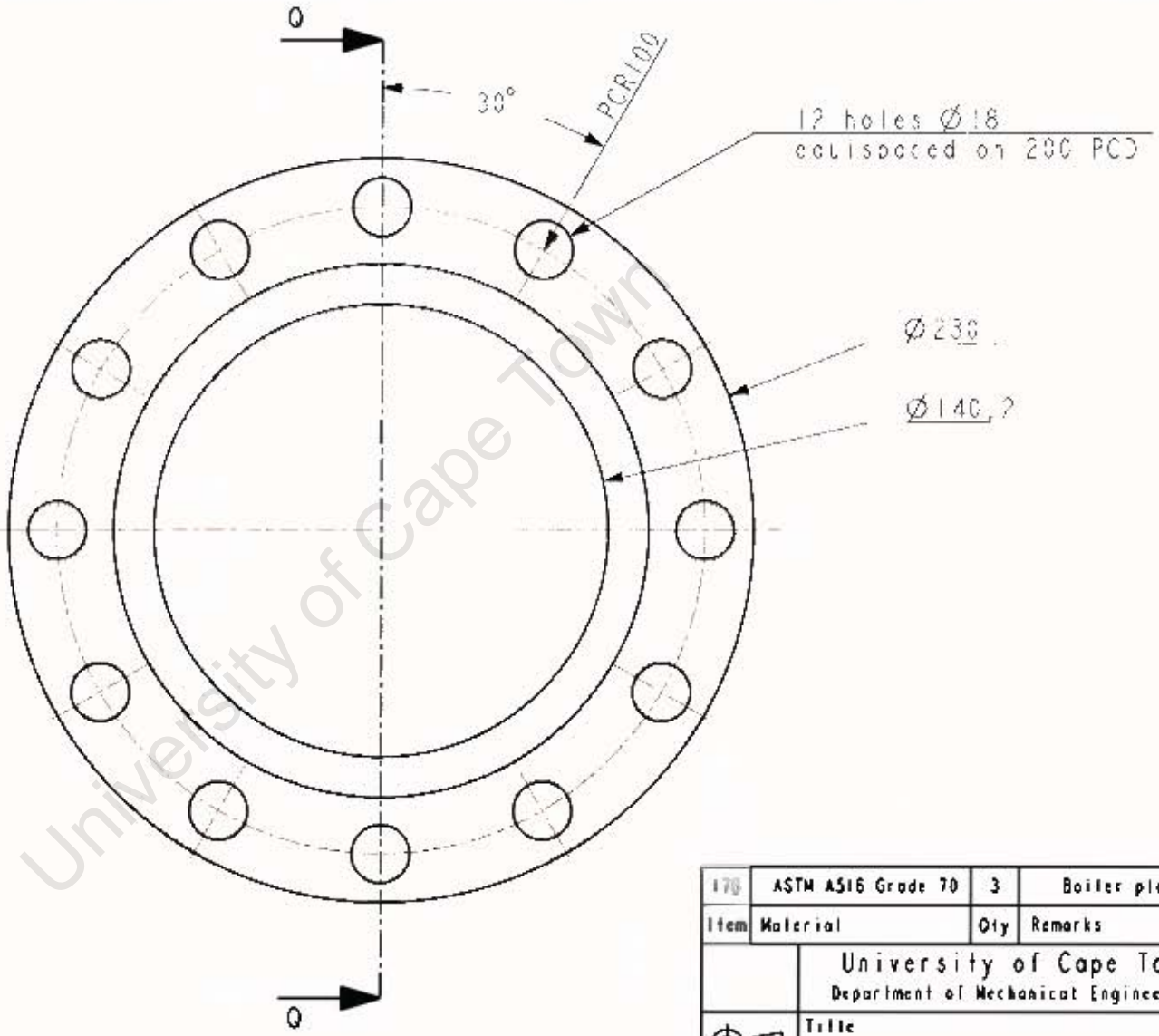

170	ASTM A516 Grade 70	3	Boiler plate
Item	Material	Qty	Remarks

University of Cape Town
Department of Mechanical Engineering

Title: driver tube flange

Dimensions in mm, Tolerance U.O.S.	Scale	Date	Sheet	of
0.1	0,500	5.11.2008	25	45
	Drawn By: Michael Downey		Drawing Number: STPD178	

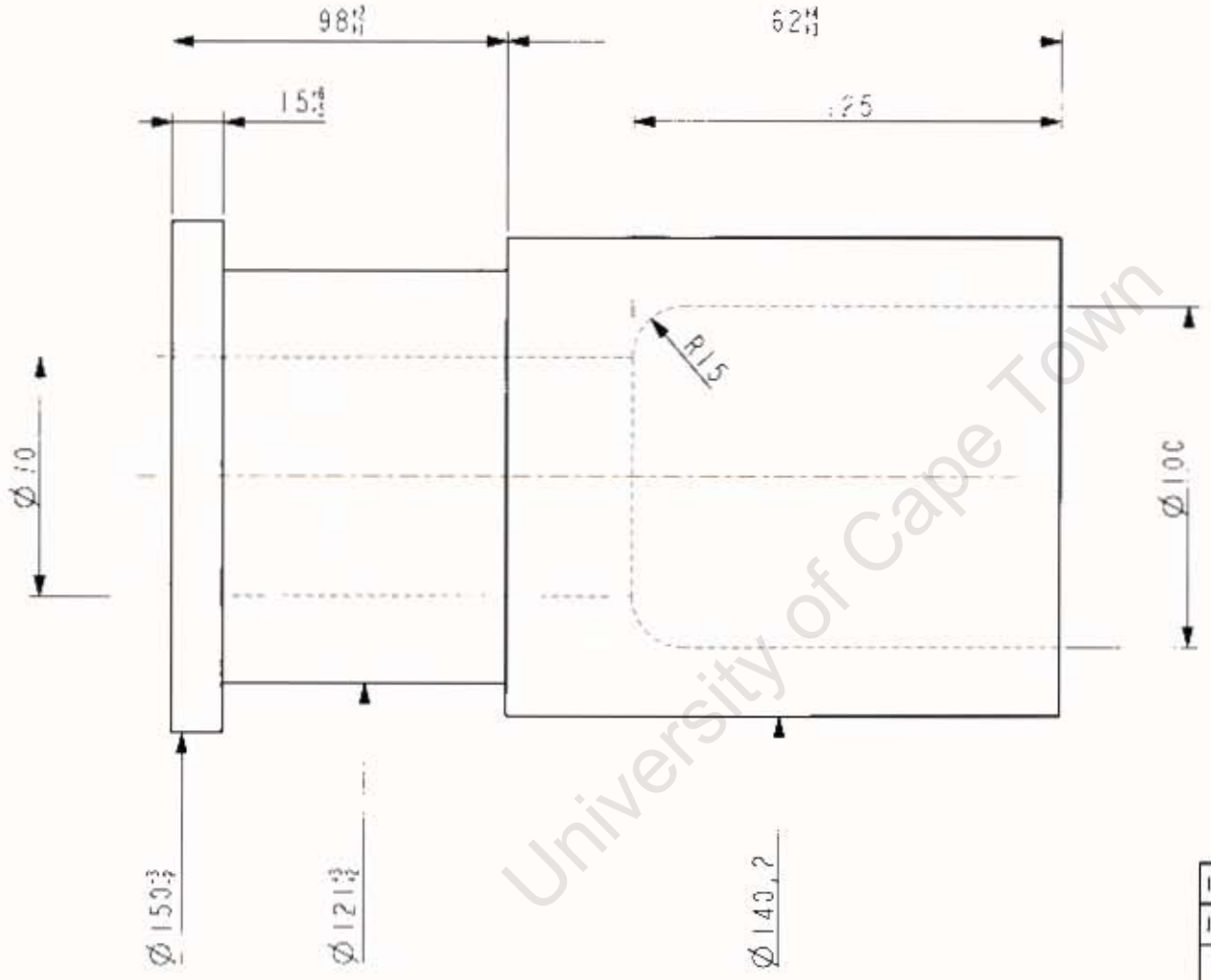

Note: Rough part out to the oversize dimensions shown, then press arc weld on the flanges according to drawing # STW001, then finish machine according to drawing # STF001

17C	EN 9	1	Condition N
Item	Material	Qty	Remarks

University of Cape Town
Department of Mechanical Engineering

Title: driver connector roughing

Dimensions in mm Tolerance U.O.S.	Scale	Date	Sheet	of
	0.500	27.11.2008	26	45
	Drawn By		Drawing Number	
0 1	Michael Downey		STP017C	

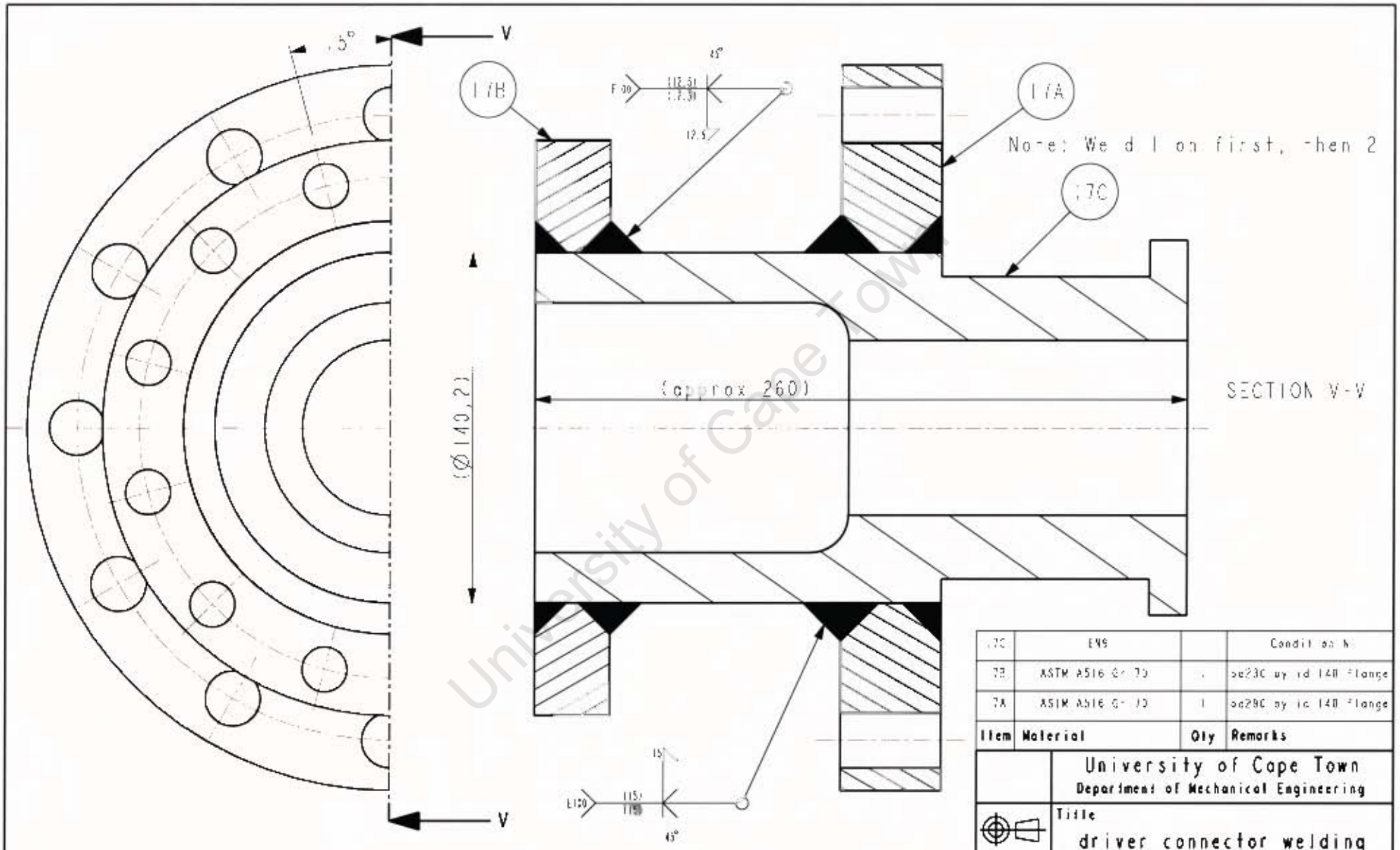

.1C	EN9		Condit on N
1B	ASTM A516 Gr 70	1	pe230 ay id 140 Flange
1A	ASTM A516 Gr 70	1	pe290 ay ic 140 Flange
Item	Material	Qty	Remarks

	University of Cape Town Department of Mechanical Engineering			
	Title driver connector welding			
Dimensions in mm Tolerance U.O.S. 0,1	Scale 0,500	Date 18.02.2009	Sheet 27	of 45
	Drawn By Michael Downey		Drawing Number STW001	

Note: Flanges to be posi-ioned flush wi-h edges. No-e the f ange no-e a ignment. Face side reinforcement wi l be mach.ned off after welding. M nimum electrode yield strength is 60CMPa. S-ress re e.ve welds. F nish machine according to drawing # S-F0C

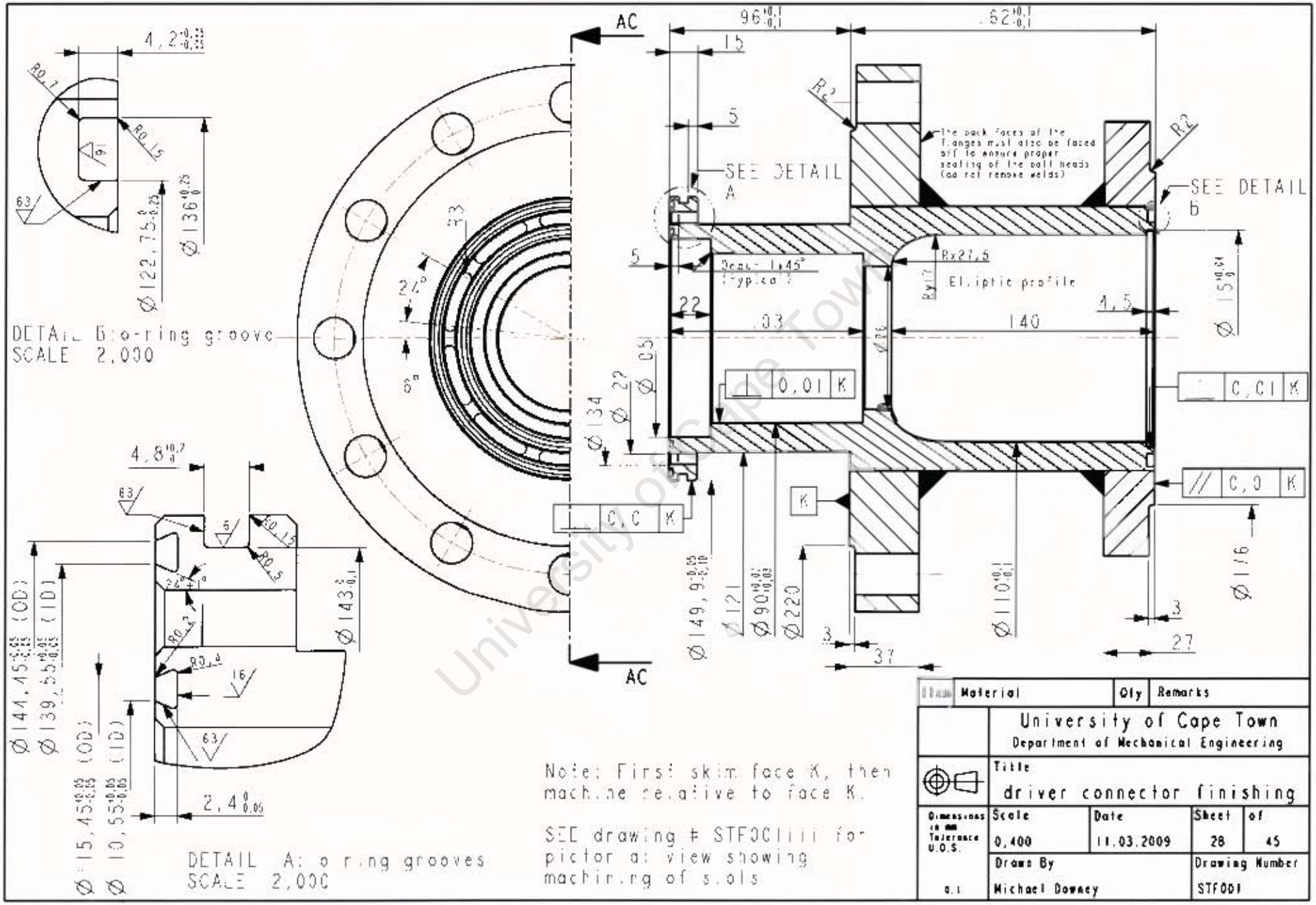

Item	Material	Qty	Remarks

University of Cape Town
Department of Mechanical Engineering

Title: driver connector finishing

Dimensions in mm Tolerance U.O.S.	Scale	Date	Sheet	of
0.1	0,400	11.03.2009	28	45
	Drawn By: Michael Downey		Drawing Number: STF001	

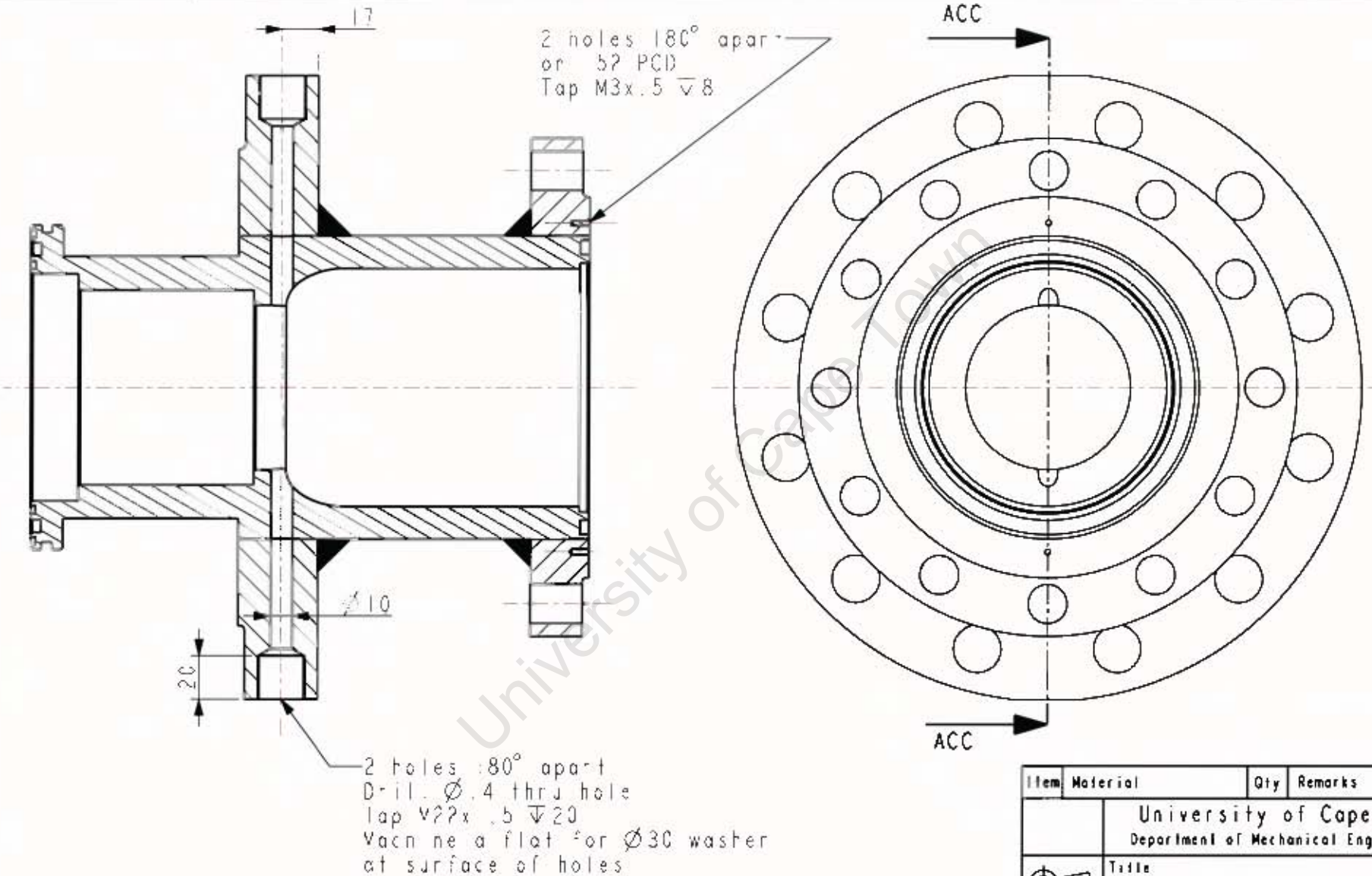

SECTION ACC-ACC
SCALE 0,400

Item	Material	Qty	Remarks
	University of Cape Town Department of Mechanical Engineering		
	Title driver connector finishing II		
Dimensions in mm Tolerance U.D.S. 0.1	Scale 0.400	Date 31.03.2009	Sheet 29 of 45
	Drawn By Michael Downey		Drawing Number STF001xx

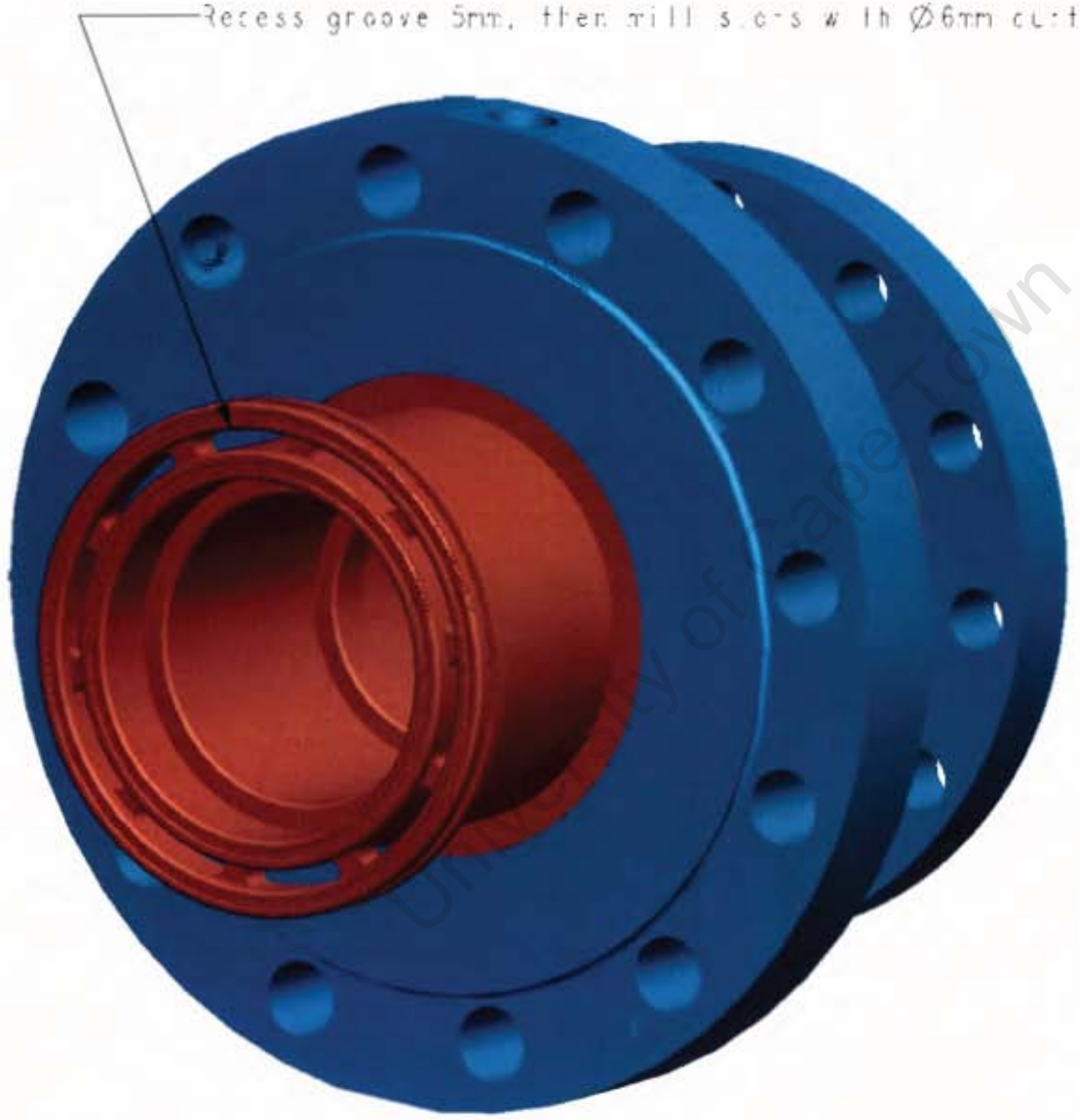

SCALE 0,500

Item	Material	Qty	Remarks

	University of Cape Town Department of Mechanical Engineering			
	Title driver connector finishing III			
Dimensions in mm Tolerance U.O.S. 0.1	Scale 0.500	Date 24.03.2009	Sheet 30	of 45
	Drawn By Michael Downey		Drawing Number STF001iii	

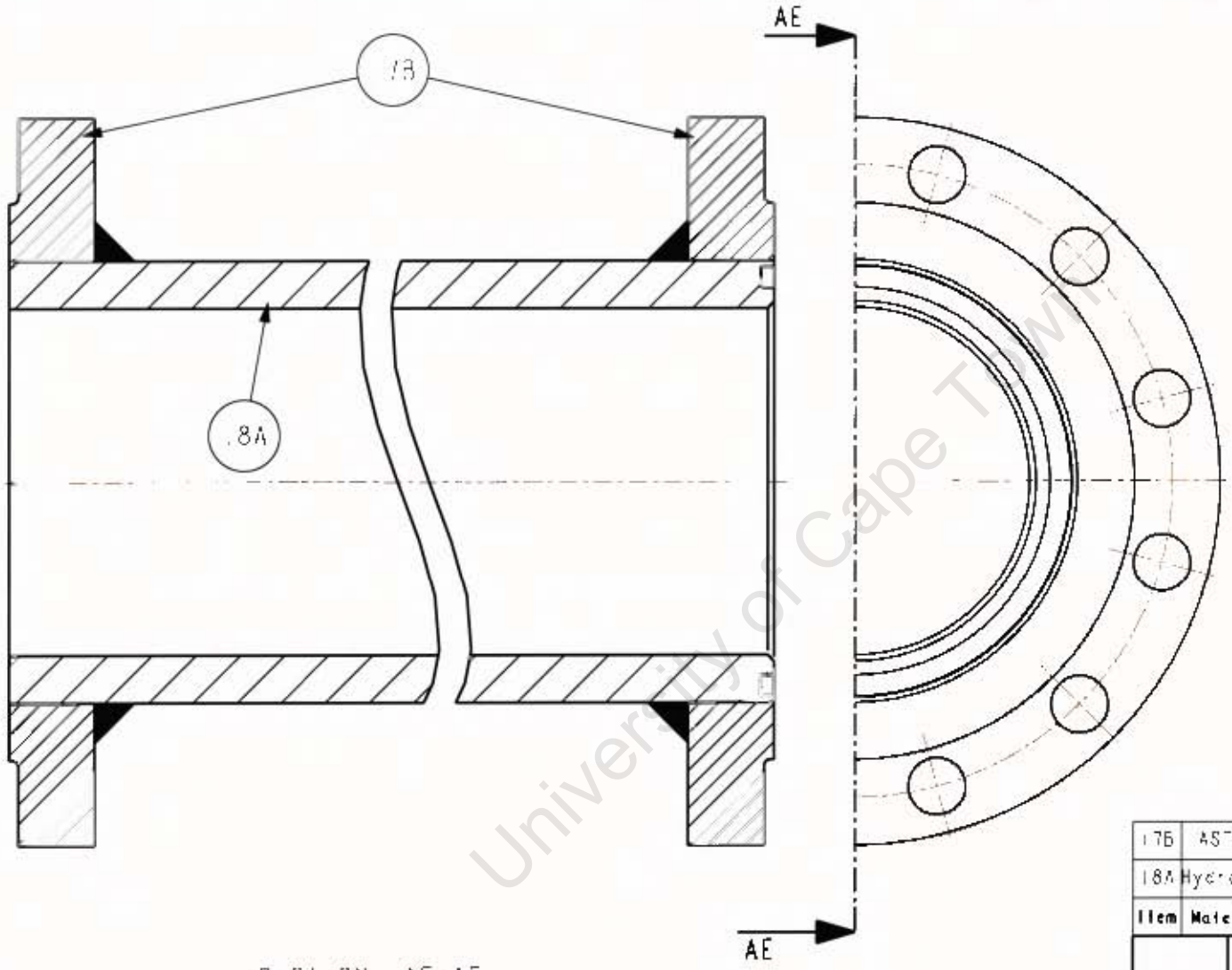

SECTION AE-AE

Item	Material	Qty	Remarks
18B	ASTM A516 Gr 70	2	
18A	Hydraulic cylinder	1	

University of Cape Town
Department of Mechanical Engineering

Title: driver tube weld assembly

Dimensions in mm Tolerance U.D.S.	Scale	Date	Sheet	of
	0.500	18.02.2009	31	45
	Drawn By		Drawing Number	
a.1	Michael Downey		STA005	

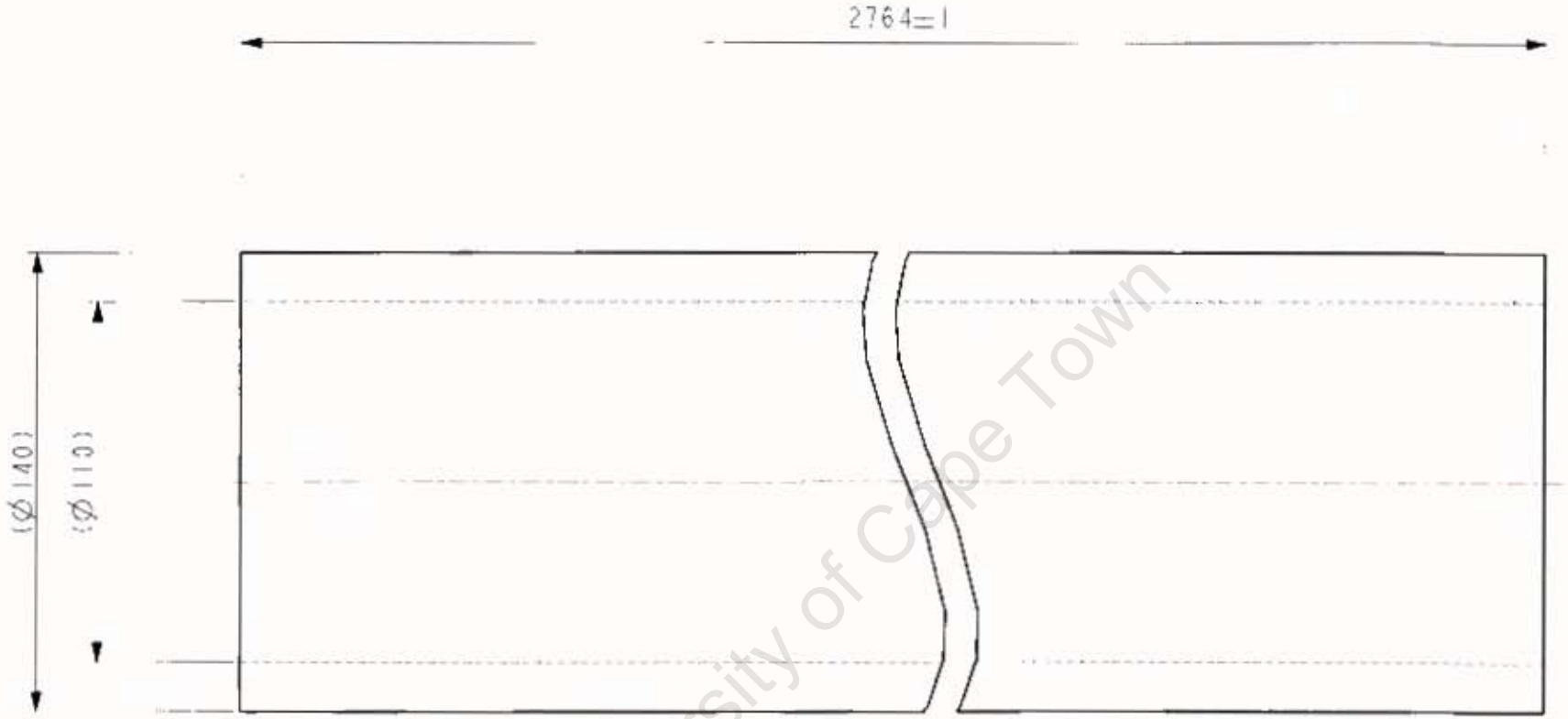

SCALE 0.500

Cut tube to length, then weld according to drawing # STW005, then finish according to drawing # STF005

Note: Tube to be clamped and machine cut, not hand cut.

JBA	Hydraulic cylinder	1	un-honed
Item	Material	Qty	Remarks
	University of Cape Town Department of Mechanical Engineering		
	Title driver tube basic		
Dimensions in mm Tolerance ± 0.5	Scale 0.500	Date 18.02.2009	Sheet 32 of 45
	Drawn By Michael Downey		Drawing Number STP018A
0.1			

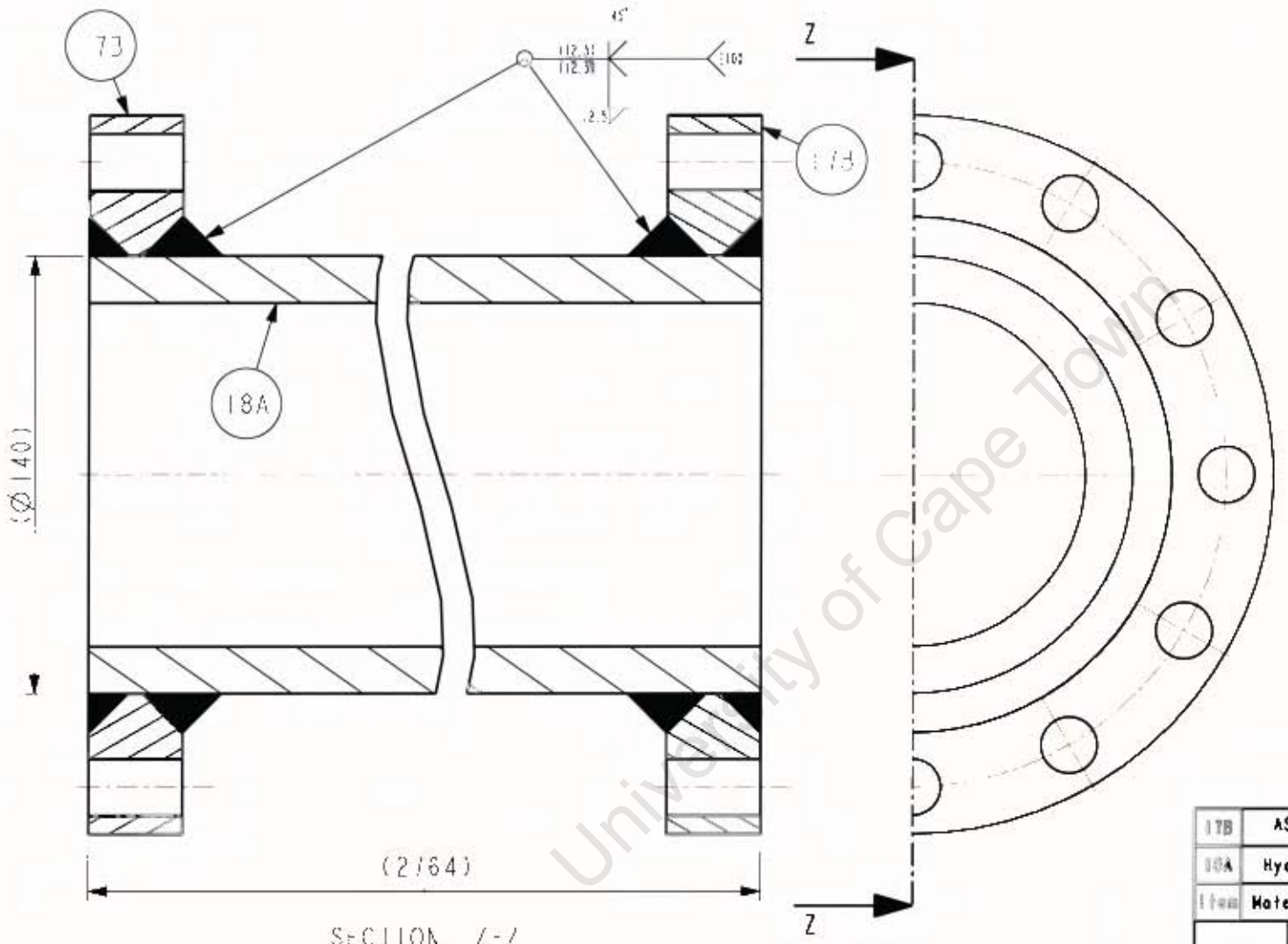

SECTION Z-Z
SCALE 0,500

Item	Material	Qty	Remarks
18B	ASTM A516 Gr 70	1	od230 by id140 flange
18A	Hydraulic cylinder	1	Precut to 2764

University of Cape Town
Department of Mechanical Engineering

Title: driver tube welding

Dimensions in mm Tolerance U.D.S.	Scale	Date	Sheet	of
0.1	0,500	18.02.2009	33	45
	Drawn By: Michael Dowsey		Drawing Number: STWD05	

Note: Weld flanges flush with tube ends. Face side reinforcements will be machined off after welding. Minimum elec-trode yield strength is 600MPa. Stress relieve welds. Flange to e alignment not critical. Finish machine according to drawing # SIF005

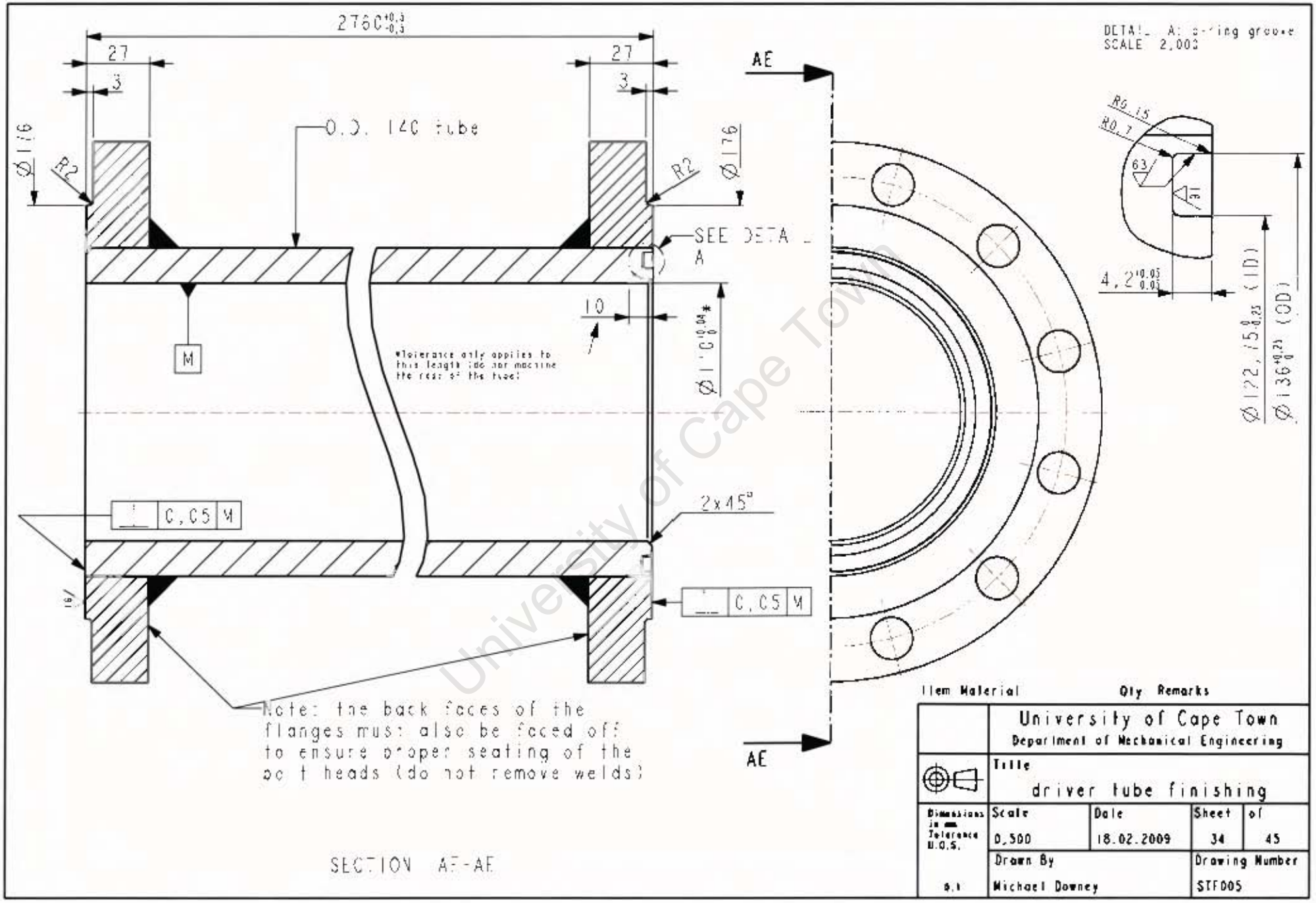

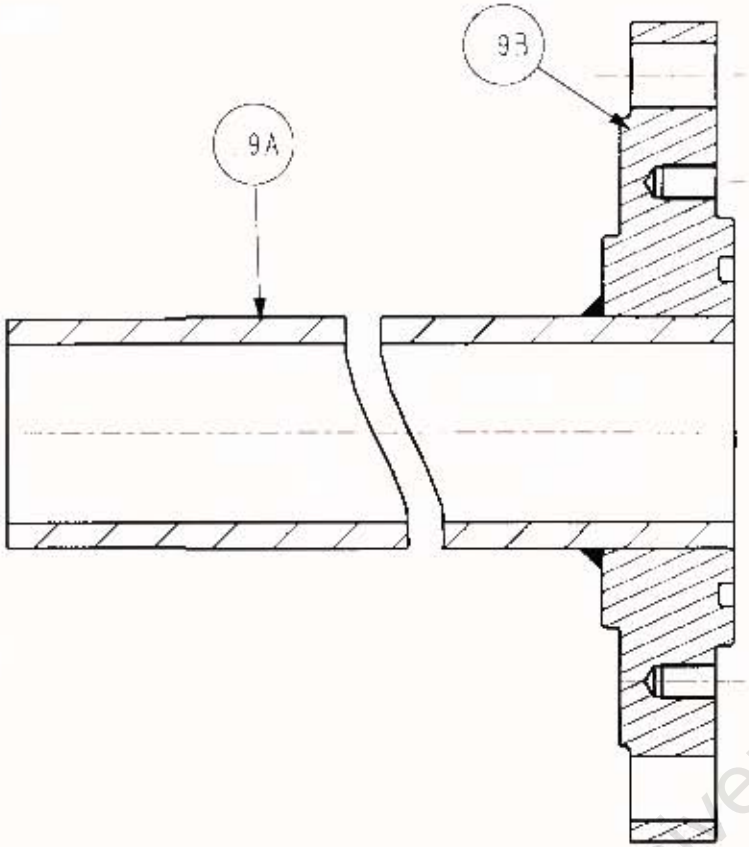

SECTION AG-AG

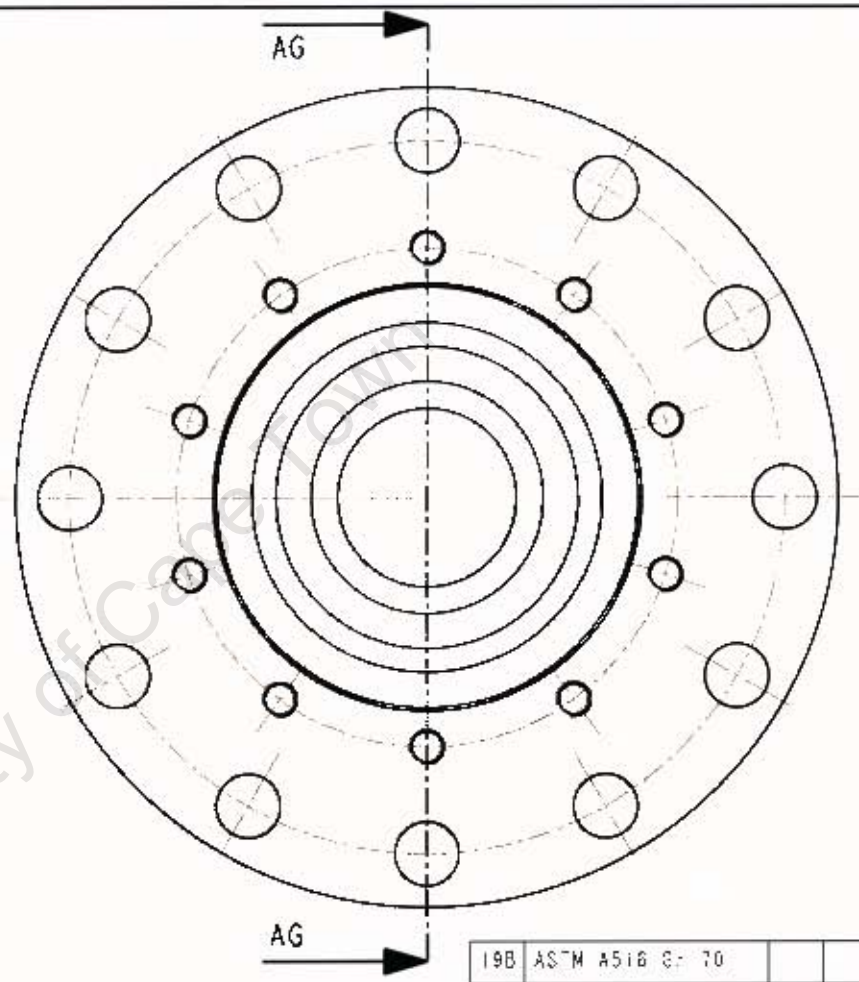

Item	Material	Qty	Remarks
19B	ASTM A516 Gr 70		
19A	Hydraulic cylinder		

University of Cape Town
Department of Mechanical Engineering

Title
driven tube inn weld assembly

Dimensions in mm Tolerance U.O.S.	Scale	Date	Sheet	of
	0,500	23.04.2009	35	45
	Drawn By: Michael Downey		Drawing Number: STA004	

0.1

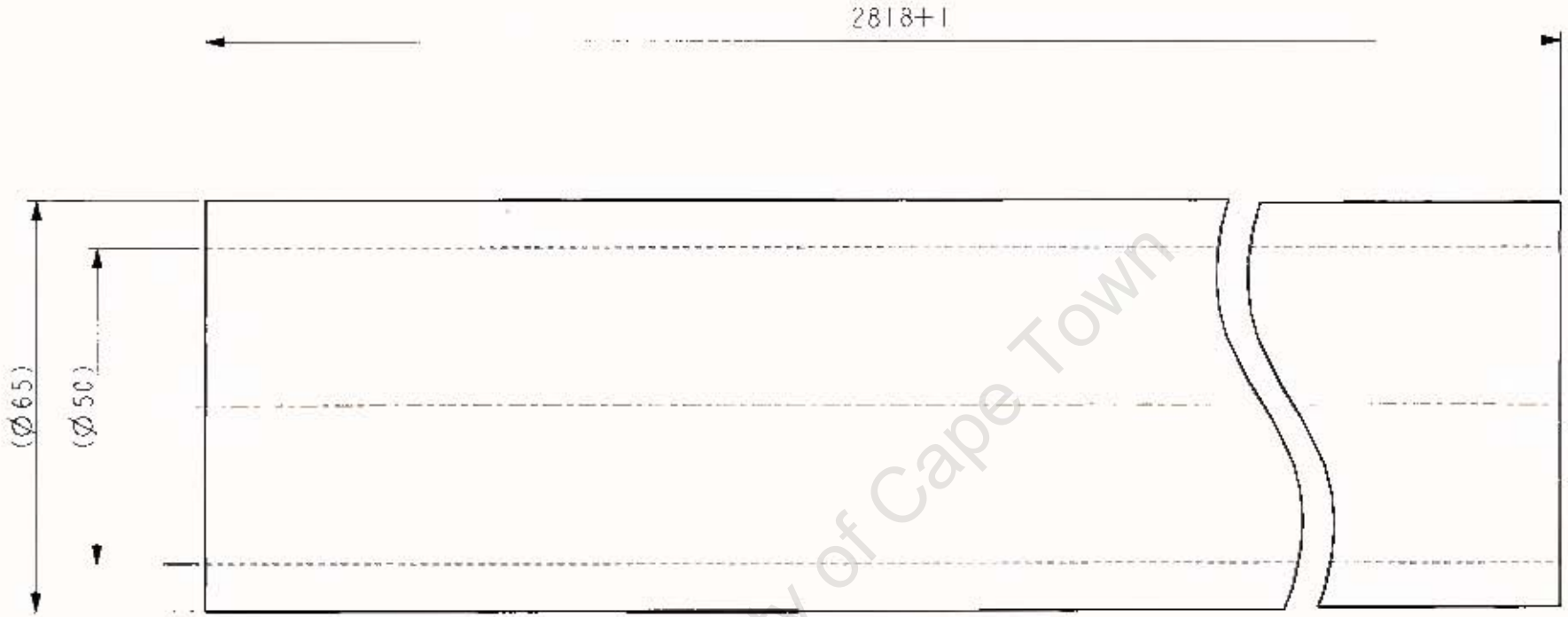

SCALE 1,000

Cut tube to length, then weld according to drawing # STWC04, then finish according to drawing # STFC04

Note: Tube to be clamped and machine cut, not hand cut.

19A	Hydraulic cylinder	1	Un-honed
Item	Material	Qty	Remarks

University of Cape Town
Department of Mechanical Engineering

Title: driven tube inn basic

Dimensions in mm Tolerance U.O.S.	Scale	Date	Sheet	of
0.1	1,000	18.02.2009	36	45
	Drawn By: Michael Downey		Drawing Number: STP019A	

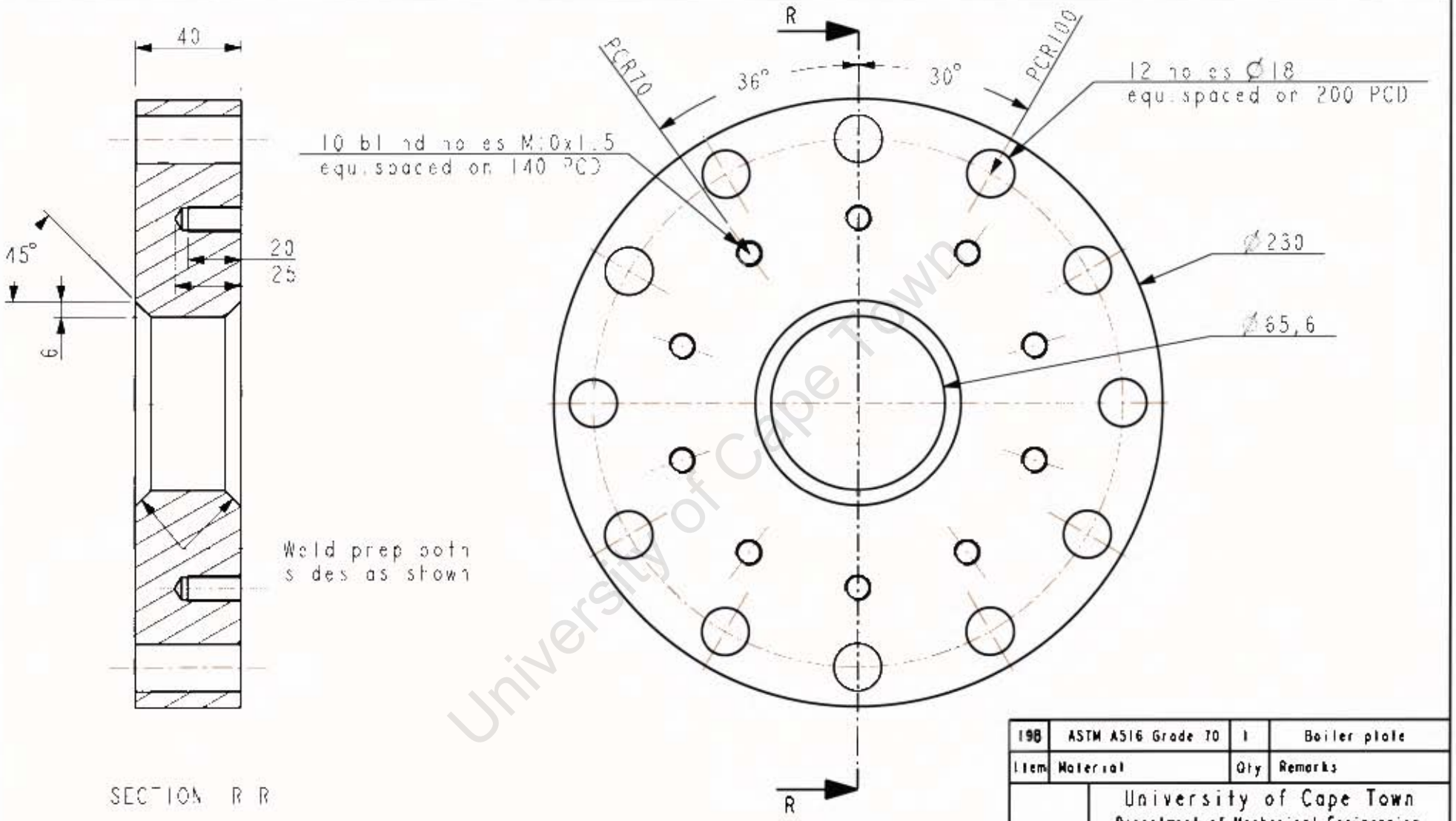

SECTION R R

198	ASTM A516 Grade 70	1	Boiler plate
Item	Material	Qty	Remarks

University of Cape Town
Department of Mechanical Engineering

Title: driver tube inn flange

Dimensions in mm Tolerance U.O.S.	Scale	Date	Sheet	of
0.1	0.500	5.11.2008	37	45
	Drawn By: Michael Downey		Drawing Number: STP0198	

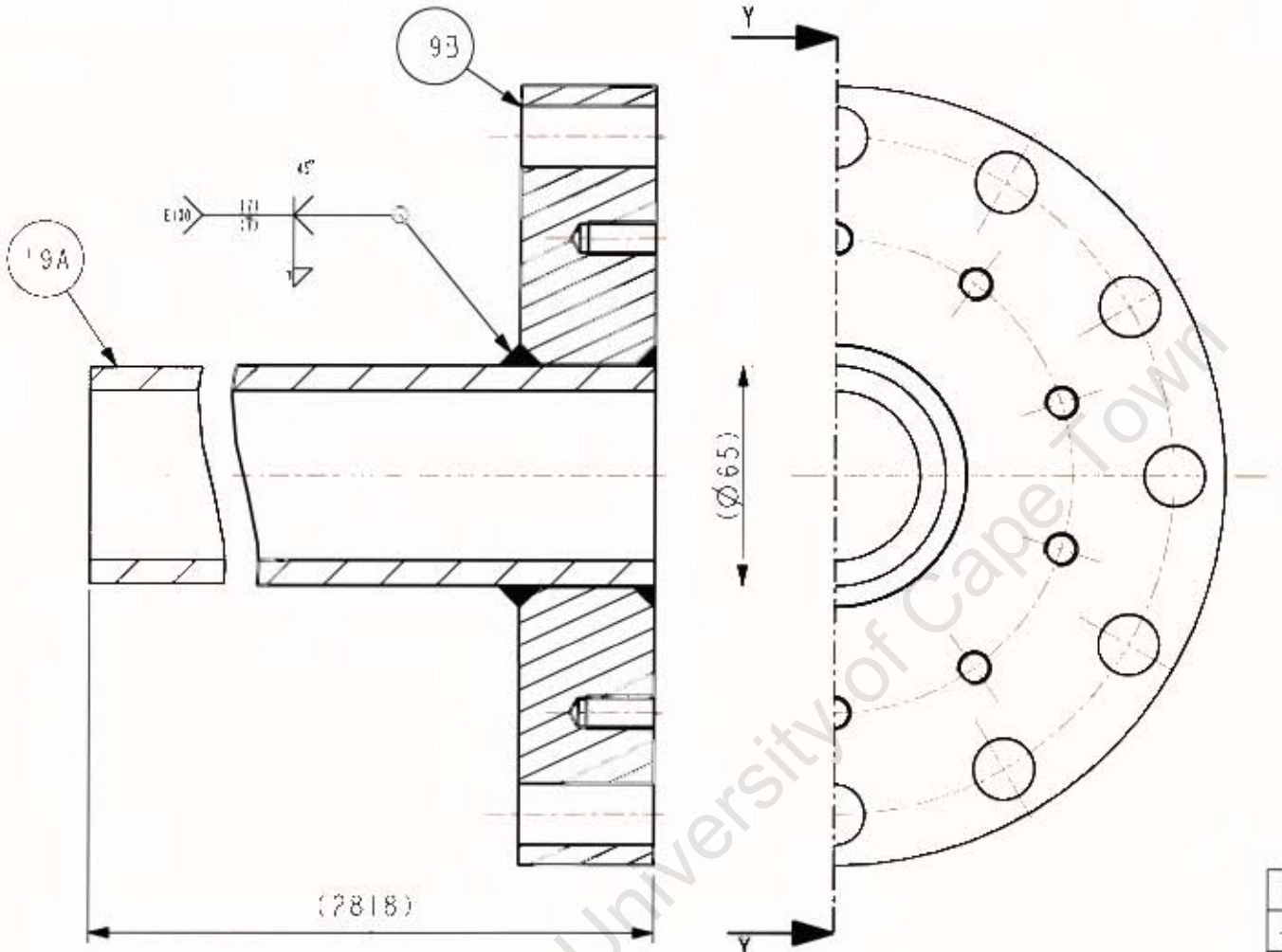

SECTION Y Y
SCALE 0,500

Note: Weld flange flush with tube edge. Face side reinforcements will be machined off after welding. Minimum electrode yield strength is 600MPa. Stress relieve welds. Finish machine according to drawing # ST-004

Item	Material	Qty	Remarks
9B	ASTM A5 6 Gr 70	1	od230 by id65 flange
9A	Hydraulic cylinder	1	procur to 2818

University of Cape Town
Department of Mechanical Engineering

Title: driven tube inn welding

Dimensions in mm Tolerance U.O.S.	Scale	Date	Sheet	of
0.1	0,500	18.02.2009	38	45
	Drawn By: Michael Downey		Drawing Number: STW004	

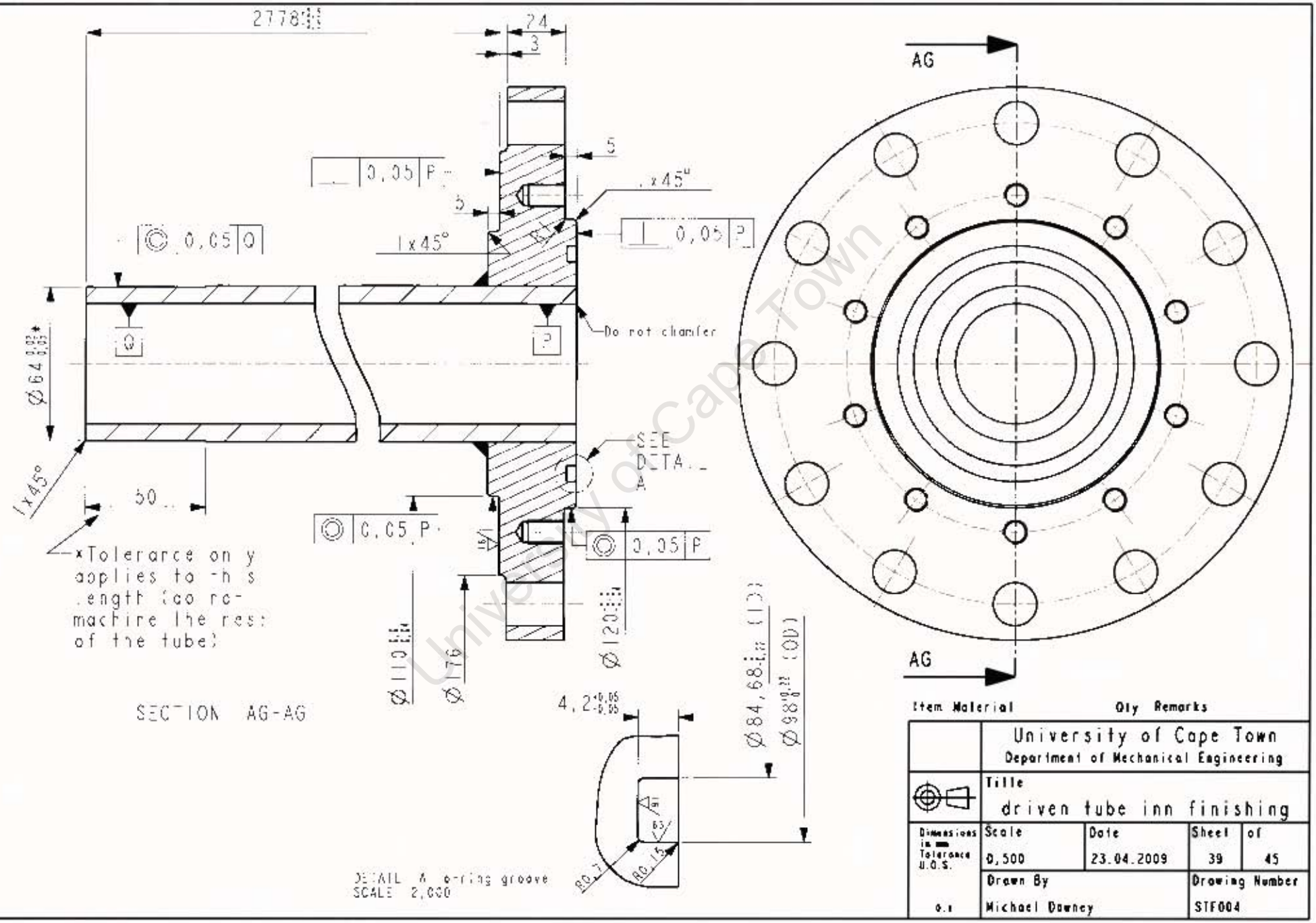

x Tolerance on y applies to this length (do not machine the rest of the tube)

Item	Material	Qty	Remarks

	University of Cape Town Department of Mechanical Engineering			
	Title driven tube inn finishing			
Dimensions in mm Tolerance U.O.S.	Scale 0,500	Date 23.04.2009	Sheet 39	of 45
0.1	Drawn By Michael Downey		Drawing Number STF004	

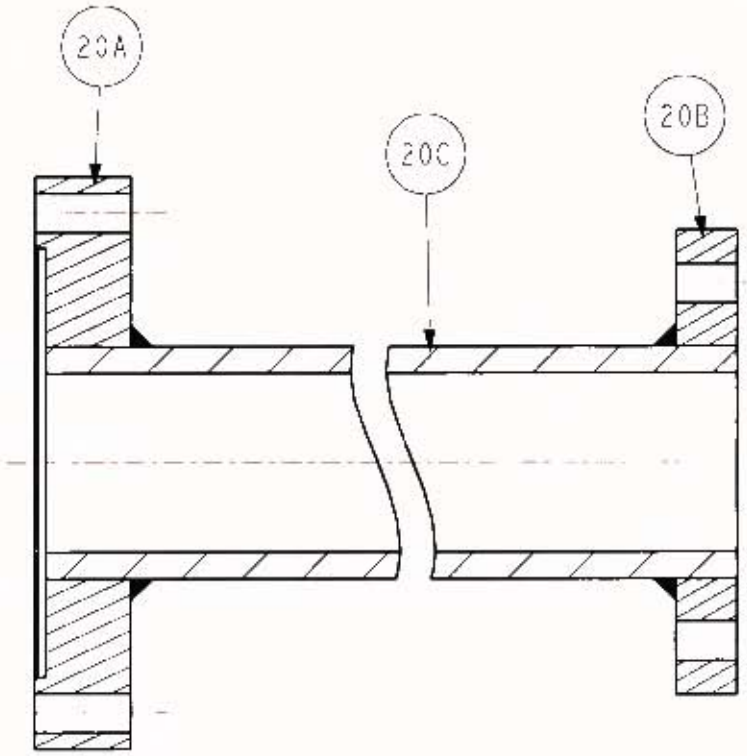

SECTION AF-AF
SCALE 0,500

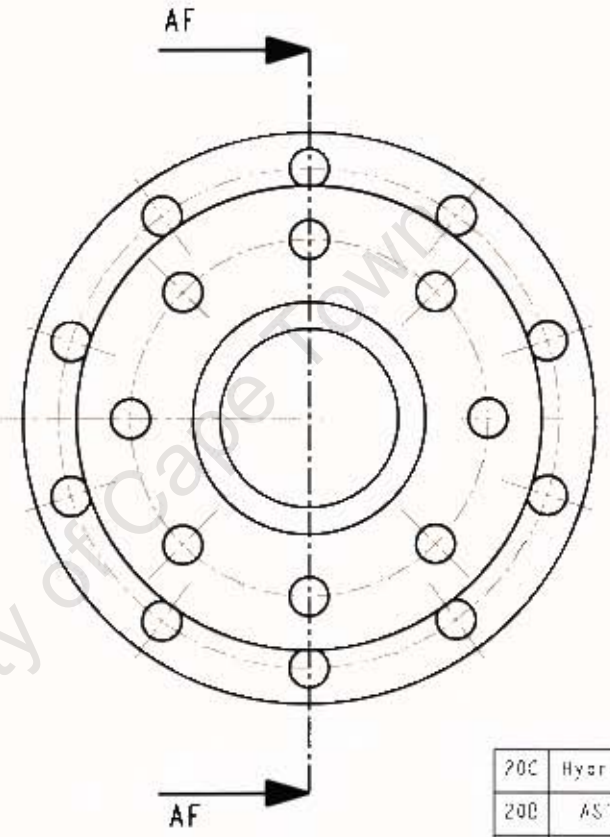

Item	Material	Qty	Remarks
20C	Hydraulic cylinder	1	
20B	ASTM A516 Gr 70	1	
20A	50B Mild Steel	1	

University of Cape Town
Department of Mechanical Engineering

Title: driven tube ext weld assembly

Dimensions in mm Tolerance U.O.S.	Scale	Date	Sheet	of
0.1	0,500	18.02.2009	40	45
	Drawn By: Michael Downey		Drawing Number: STA003	

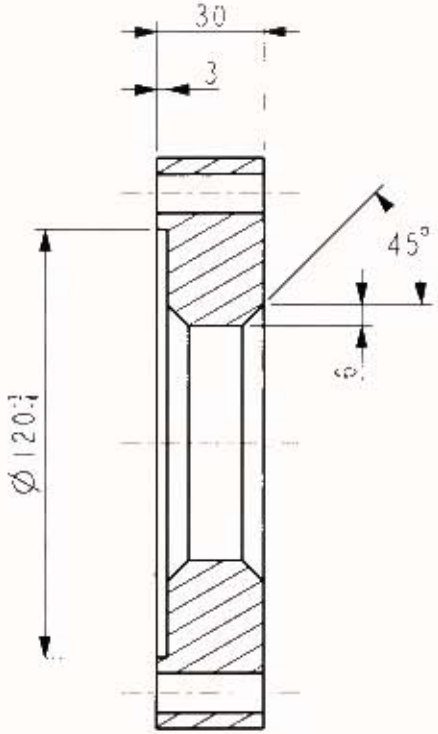

SECTION S-S
SCALE 0,500

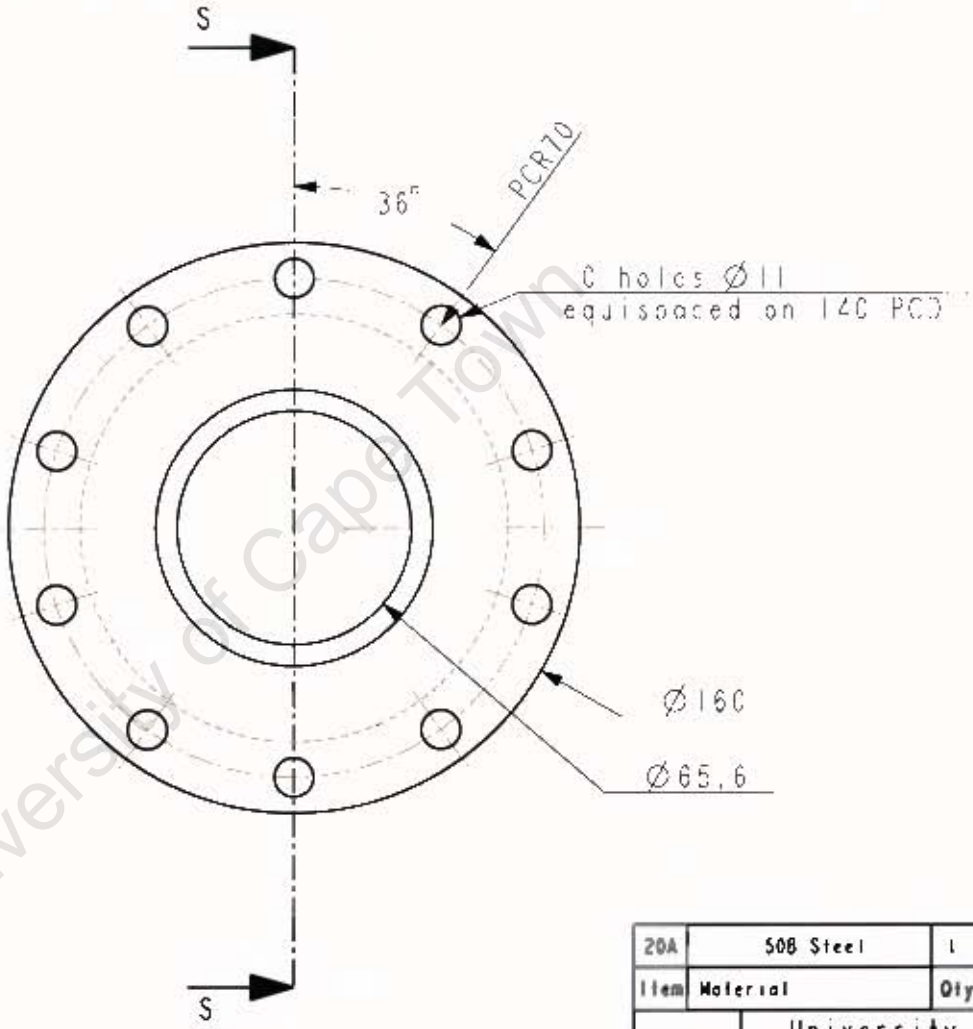

20A	508 Steel	1	
Item	Material	Qty	Remarks

University of Cape Town
Department of Mechanical Engineering

Title: driven tube exf join flange

Dimensions in mm Tolerance U.O.S.	Scale	Date	Sheet	of
0.1	0,500	20.02.2009	41	45
	Drawn By: Michael Downey		Drawing Number: STP020A	

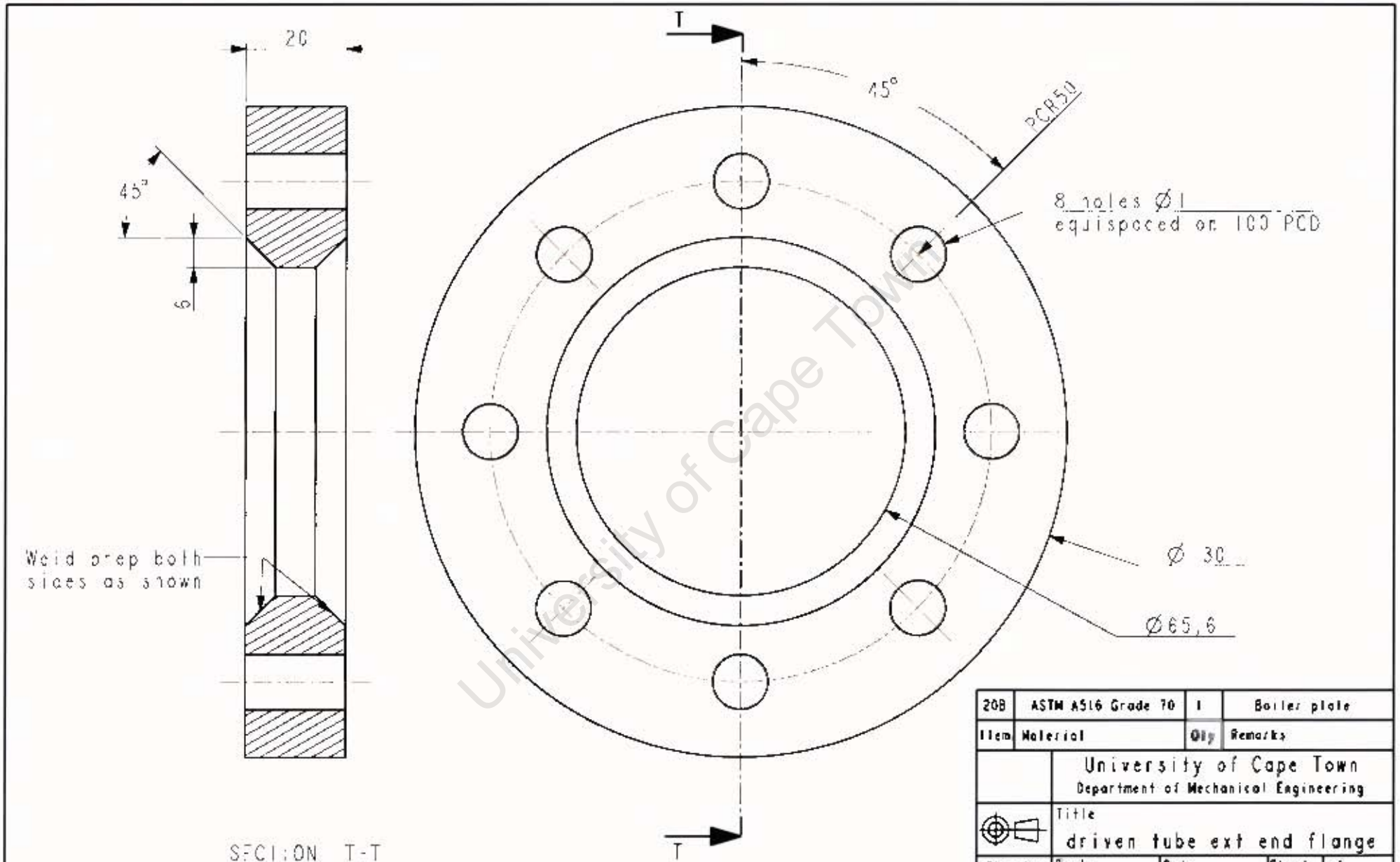

208	ASTM A516 Grade 70	1	Boiler plate
Item	Material	Qty	Remarks

University of Cape Town
Department of Mechanical Engineering

Title
driven tube ext end flange

Dimensions in mm Tolerance U.O.S.	Scale	Date	Sheet	of
	1,000	5.11.2008	42	45
0.1	Drawn By: Michael Downey		Drawing Number: STP0208	

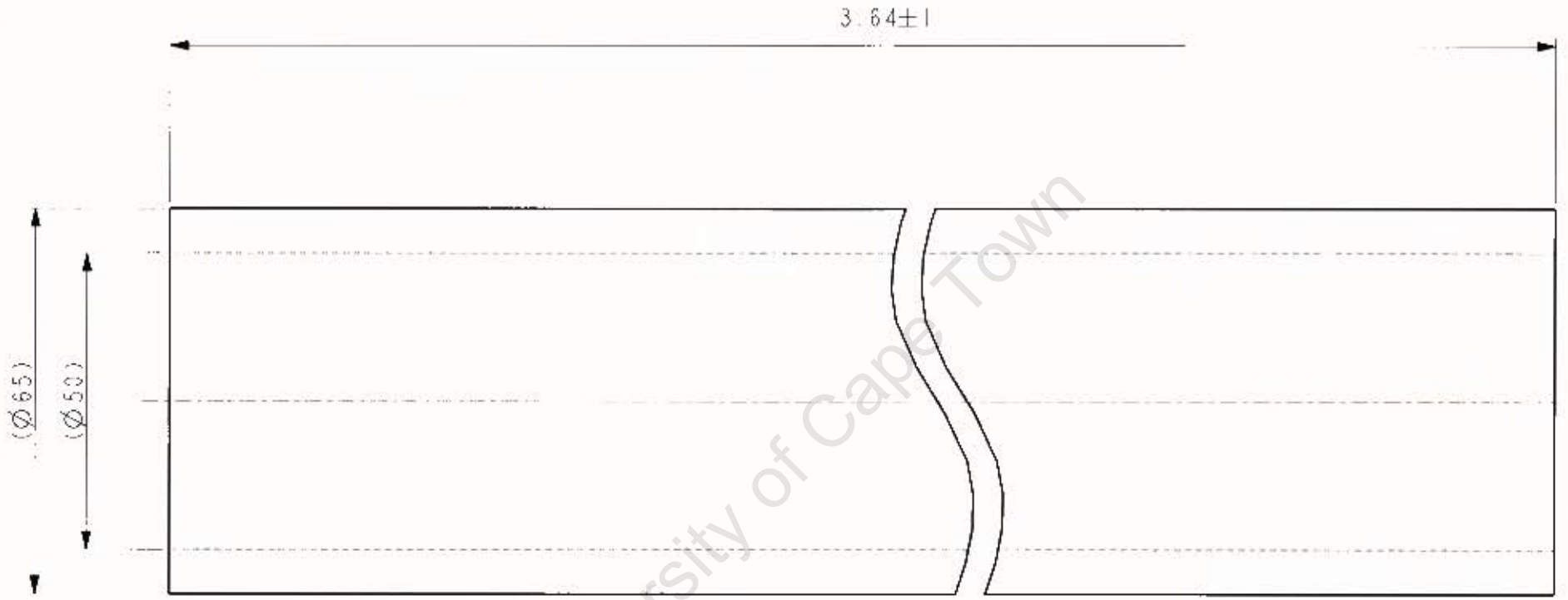

SCALE 1,000

Cut tube to length, then weld according to drawing # STW003, then finish according to drawing # STF003

Note: Tube to be ordered and machine cut, not hand cut.

20C	Hydraulic cylinder	1	Un-honed
Item	Material	Qty	Remarks
	University of Cape Town Department of Mechanical Engineering		
	Title driven tube ext basic		
Dimensions in mm Tolerance U.O.S. 0.1	Scale 1,000	Date 18.02.2009	Sheet 43 of 45
	Drawn By Michael Downey		Drawing Number STP020C

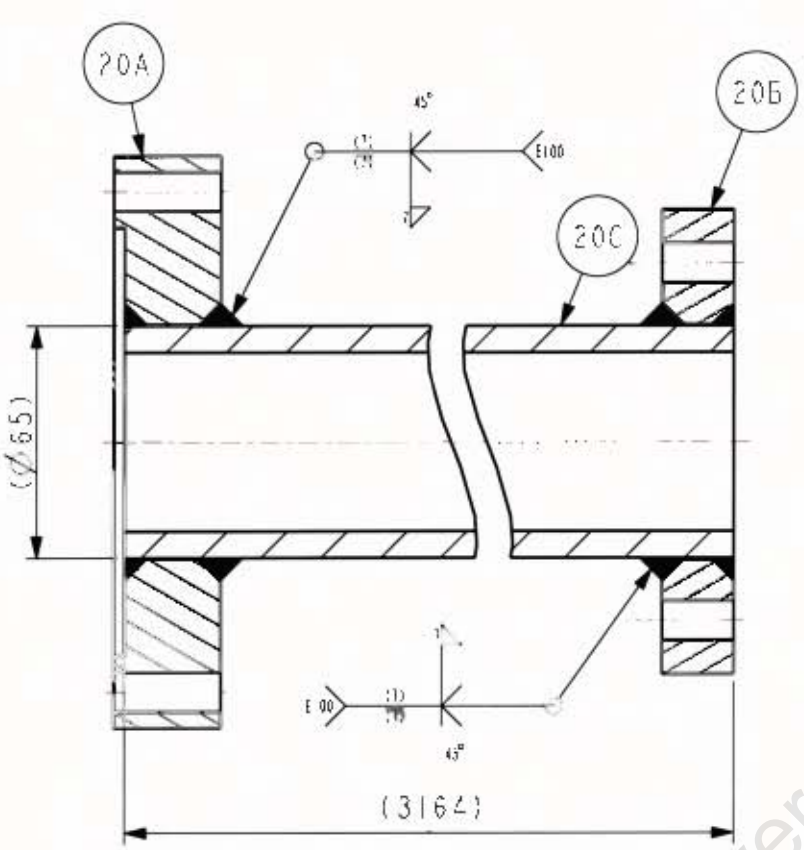

SECTION W-W
SCALE 0,500

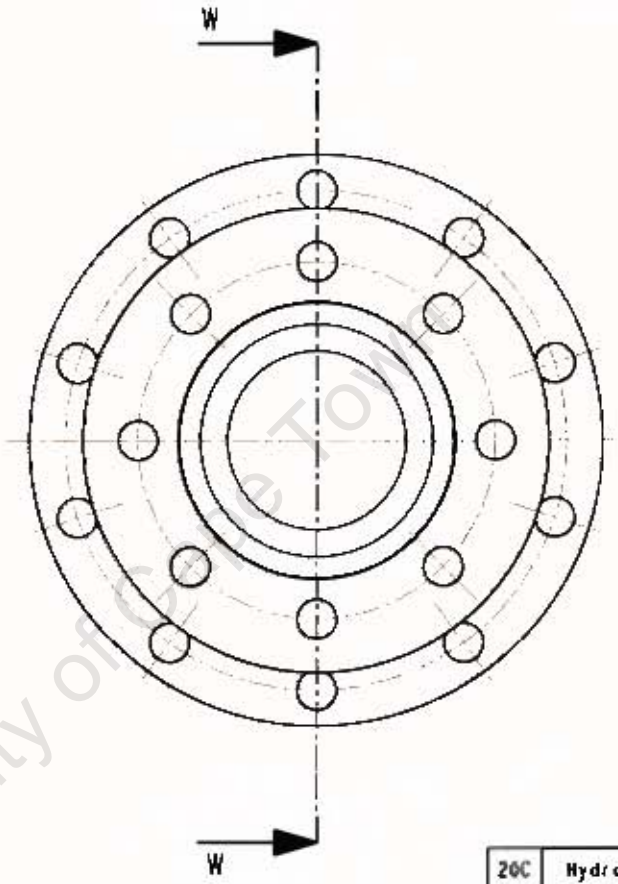

Item	Material	Qty	Remarks
20C	Hydraulic cylinder	1	precut to 3164
20B	ASTM A516 Gr 70	1	od130 by id65 flange
20A	50B Mild Steel	1	od160 by id65 flange

University of Cape Town
Department of Mechanical Engineering

Title: driven tube ext welding

Dimensions in mm Tolerance U.O.S.	Scale	Date	Sheet	of
	0,500	18.02.2009	44	45
	Drawn By		Drawing Number	
0.1	Michael Downey		STW003	

Note: Weld flanges flush with tube ends. Face surface reinforcements will be machined off after welding. Minimum electrode yield strength is 600MPa. Stress relieve welds. Flange hole alignment not critical. Finish machine according to drawing # ST-003

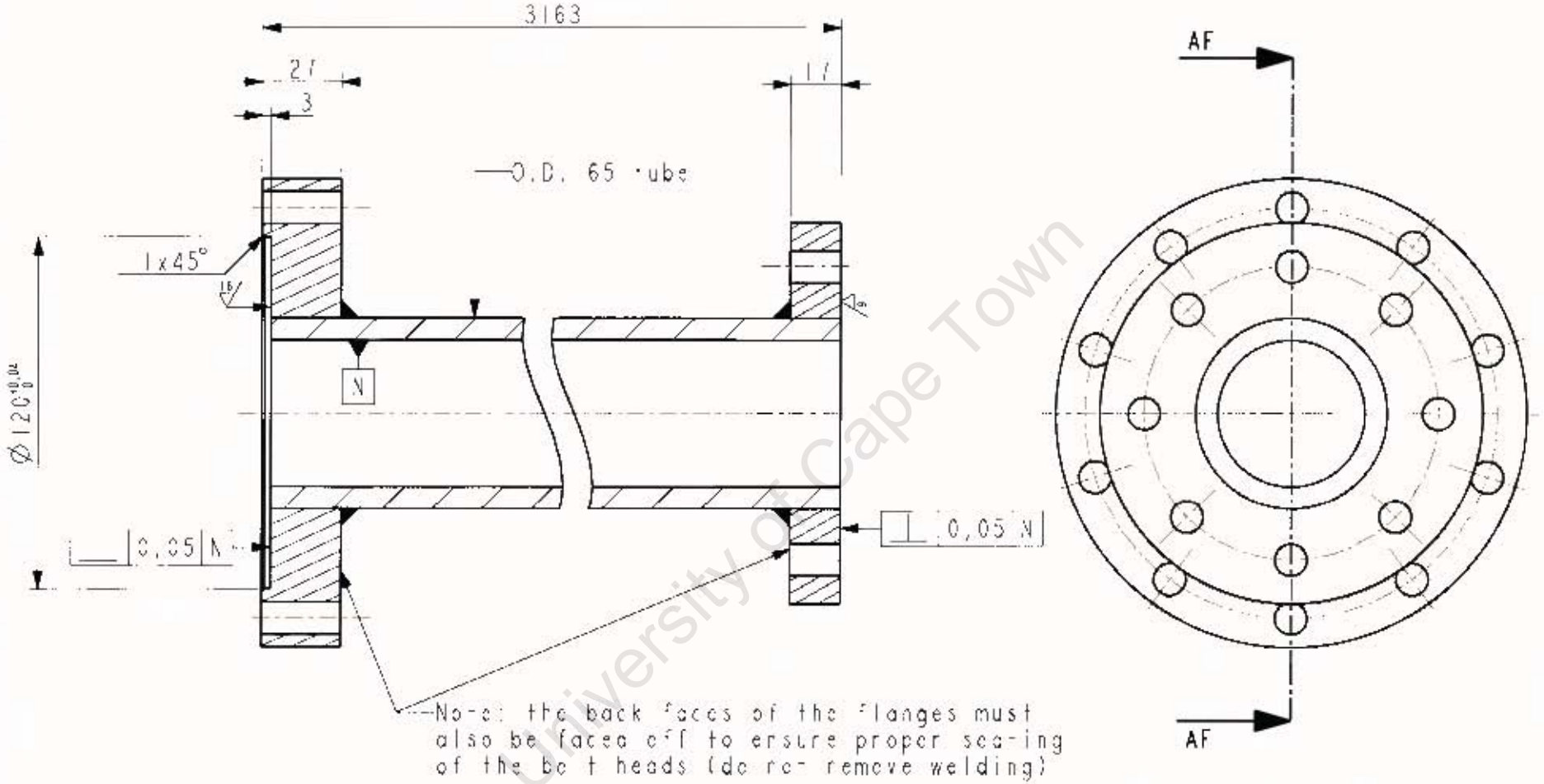

SECTION AF-AF
SCALE 0,500

Item	Material	Qty	Remarks

	University of Cape Town Department of Mechanical Engineering			
	Title driven tube ext finishing			
Dimensions in mm Tolerance U.O.S. 0.1	Scale 0,500	Date 18.02.2009	Sheet 45	of 45
	Drawn By Michael Downey		Drawing Number STF003	